THE BIOLOGICAL MECHANISM BEHIND EARLY AND LATE APPLE SPORTS

By

Alexander J. Engelsma

A THESIS

Submitted to
Michigan State University
in partial fulfillment of the requirements
for the degree of

Horticulture – Master of Science

2024

ABSTRACT

Somatic mutations in apple commonly develop into viable bud sports that can be propagated clonally. When the apple bud sport has a desirable attribute such as improved color, size, shape, flavor, firmness, sweetness, or harvest timing, it has potential to be introduced as a new cultivar that growers utilize, and consumers enjoy. The genetic mutations and related mechanisms associated with early or delayed maturation (respectively resulting in early or late harvest date) in apple sports are not known despite their value to the industry. By acquiring knowledge about genetic mutations affecting harvest date and their respective molecular mechanisms, breeders can identify markers to conduct more informed crosses to select for early or late maturing apple lines. In this study, the late maturing 'Gala' sport 'Autumn Gala', the early maturing 'Fuji' sport 'September Wonder Fuji', and the early maturing 'Cripps Pink' ('Pink Lady®') sport 'Maslin Cripps Pink', were compared to the controls for each cultivar (i.e., those possessing standard harvest times). We found that in each comparison, fruit growth rate of the early variant was significantly greater early in fruit development, during the cell division phase. The early emergence of phenotypic differences in growth rate between the bud sport and the control lines suggests the physiological processes leading to an early or late harvest date may also emerge very early in fruit development. If so, the early or delayed maturation date is very likely not strictly a function of ripening-related processes, but rather is derived from a season-long shift in metabolic activity. Genomic analyses were also done to identify genetic differences between early and late apple sports. Collectively, hundreds of genetic variants were identified. Our phenological studies reduced the developmental window for these transcriptomic investigations.

To Grace and Raine

ACKNOWLEDGEMENTS

On my wedding day I thought I would acknowledge all the people that led my wife Grace and I to that moment. Likewise, I originally planned to here acknowledge all the shoulders upon whom I relied through this unique part of my life in graduate school. After just a few moments in thought, I knew I would fail to mention everyone. As in life, it is impossible to sufficiently thank everyone or repay the debt of mentorship and love. Here I acknowledge a few select individuals and their unique contribution to my mindset and worldview that tremendously assisted me in graduate school.

To my wife, Grace, who has loved and supported me through the past ~3 years of marriage. She gave me so much inspiration from her work ethic, love for family, love for our daughter Raine, and insurmountable intelligence.

To my parents, both mine and Grace's. My Dad taught me many things, due likely to his appreciation for learning. Specifically, he taught me to work one piece at a time and persevere. Ma taught me contentment and joy in all things. My father- and mother-in-law taught me to think critically and conscientiously, respectively.

To my Uncle Jim, who taught me a great deal of life lessons while working on his apple farm. He instilled in me how to balance self-worth and self-sacrifice, wealth and honor. Hard work on the farm taught me that I could do anything if I set my mind to it. He was the first to recommend that I pursue graduate school.

To Courtney and Randy, who inspire me in so many ways to be the best researcher I can be.

To Jesus Christ, my savior. "Nothing in my hands I bring, simply to the cross I cling."

TABLE OF CONTENTS

LIST OF ABBREVIATIONS

A: photosynthetic rate (μmol CO_2 m^{-2} s^{-1})

Apple bud sport: cultivars originating not from cross pollination and seed, but from mutated meristematic tissue in the bud of its parent progenitor

Cultivar: specific genotype (e.g., 'Gale Gala', 'Imperial Gala', 'Royal Red Honeycrisp', 'Premier Honeycrisp', 'September Wonder Fuji', 'Yataka Fuji', 'Aztec Fuji')

DAFB: days after full bloom

DEGS: differentially expressed genes

Development: the span of growth, differentiation of tissue, and physiological behavior from fertilization of apple flower until harvest

GDH: growing degree hours

LG: linkage groups

Maturation: stage when the fruit is mature and ready to ripen, and envelops starch degradation, the beginning of pre-climacteric and climacteric ripening postharvest

Maturity: indicator of harvest date

Ripening: ethylene induced developmental stage when the fruit prepares itself for the consumer

Variety: a collection of specific genotypes (cultivars) marketed uniformly as one name to the consumer (e.g. 'Gala', 'Honeycrisp', 'Fuji', 'Red Delicious')

CHAPTER 1. Literature Review

1.1. INTRODUCTION

New varieties and cultivars of apples often originate through genetic mutations in meristematic tissues. These natural phenomena result in something called a bud sport, which can be vegetatively propagated. Apple bud sports may develop apple fruit with a phenotype that differs from that of the progenitor. Phenotypic differences in apple fruit may become apparent at any time during development and can impact apple fruit quality (e.g., skin color, flesh color, development rate, maturation date). Developing early- and late-harvesting apple sports is important not only for economic value, saving grower return on investment and dominating an earlier fresh apple market, but also feeding the world.

Consumer preference has required apple growers to plant and produce fruit with desirable visual and eating characteristics while maintaining marketability. As a result, apple growers continually plant new cultivars to remain competitive in their markets. Therefore, when a new apple bud sport develops and is commercially available, growers often have the incentive to grow that unique cultivar if it fits into their marketing program. It has been shown in a comprehensive study that consumer preference is primarily driven by firmness in the apple fruit and fruit firmness interplay with soluble solid content (SSC) and titratable acidity (TA) (Harker et al., 2008). Growers, however, prioritize color and storability over flavor and texture. Successful cultivars generally contain several of these qualities. Successful apple bud sports typically retain all or most of the traits of the progenitor with additional qualities, such as enhanced color, extended shelf life (may imply higher fruit firmness) and altered maturation.

On an apple grower's orchard, there are many things to consider throughout the growing season, such as cultural practices of protection, nutrition, fruit quality, the harvest process, and its

timeline. The timeline of harvest is critical for growers. If a grower has a primarily ‘Gala’ and ‘Honeycrisp’ farm, those two varieties have a standard harvest window at nearly the same time, the first/second week of September in the Grand Rapids, Michigan area (Shane & Lavely, 2023). It is difficult for a grower to hire enough help or harvest fruit fast enough in this timeframe depending on the acreage, so spreading out the harvest window is the best option to obtain full yield potential. Currently, growers utilize plant growth regulators (PGRs) to delay ripening and maintain apples on the tree for a longer period (AgroFresh, n.d.; Argenta et al., 2022; Bramlage et al., 1980). In the apple industry to date, the use of PGR’s is economically and logistically one of the best strategies to broaden this harvest window, as most growers in the Michigan area utilize these products. Although these products are effective, their cost is substantial, amounting to several hundred dollars per acre (J. Engelsma & E. Ott, personal communication, 2024) with apple prices at 751 bushels per acre amounting to about $14.40 per bushel, $10,816 gross per acre. Investigations into the physiological and genetic background of apple development can lead to discoveries that help growers improve control over the harvest window and protect their investments by reducing overall harvest costs. Future discoveries in the genetic background of apple development and maturation may provide more tools for growers to manipulate their own harvest.

Apples that are late harvesting may be impacted by freezing temperatures, which can significantly injure the crop (Chassagne-Berces et al., 2009). This is a primary reason why growers in the Michigan area planted early harvesting sport ‘Maslin Cripps Pink’ (~2 weeks early) instead of its progenitor ‘Cripps Pink’ which harvests in the first week of November, a week with high probability of freezing temperatures in Michigan (Isard & Schaetz, 1998). In addition, Michigan growers must focus on storage, shipping and managing postharvest issues in

the late fall. Early harvesting cultivars also present a positive trait of shorter growing season, thus less cost, sprays, water resources, and less cumulative risk due to pest or weather-related issues. All these positive traits make early harvesting cultivars attractive to grow for reasons other than return on investment. Further, the greater control over harvest window may be of benefit in a warming climate. Positive cropping traits that combat our changing climate would benefit the entire apple industry.

1.2. APPLE BUD SPORTS

1.2.1. Background

A 'bud sport' is a lateral shoot, inflorescence or single flower/fruit with a visibly different phenotype from the rest of the plant; it develops in response to a mutation within the somatic cells of the meristematic tissue (Foster & Aranzana, 2018). These genetic events are found frequently in apple (*Malus* ξ *domestica*), in some varieties more commonly than in others. There are bud sports for select traits such as early harvesting sports (e.g., 'Premier Honeycrisp', 'Yataka Fuji', 'Wildfire Gala'), late harvesting sports (e.g., 'Autumn Gala'), and enhanced color sports (e.g., 'Firestorm Honeycrisp', 'Royal Red Honeycrisp', 'Aztec Fuji', 'Gale Gala', 'RubyMac'). Successful bud sports most often contain all desirable characteristics of the progenitor with one, rarely two or more, additional desirable traits exceeding the quality of the progenitor.

1.2.2. History

The first known instance of an apple bud sport observation was made by Peter Collinson in 1741 (Linné et al., 1821). He wrote to a friend of his, mentioning he had found russet apples growing on two thirds of what originally was a green apple tree. Charles Darwin observed similar spontaneous mutations in many plant species and mentions them in his book, *The Variation of*

Plants and Animals Under Domestication (Darwin, 1868). Apple bud sports grew in popularity during the early 1900's, according to a review by Shamel and Pomeroy (1936). They reported numerous findings in which hundreds of apple bud sports were found. After news of growers patenting their bud sports, there was a race to find anomalies in the orchard. Most valuable apple bud sports were red sports, having more red color than the progenitor (Zotta, 2015). The value of red apple sports was driven by consumer preference of a red apple. There were also many cases in which apple bud sports differed in maturity. Early maturing bud sports were often preferred because of their rapid entry into the markets. Shamel and Pomeroy (1936) informed growers how to look for bud sports and discussed the importance and value of bud mutations in horticultural crops.

1.3. APPLE FRUIT DEVELOPMENT

1.3.1. Pre-harvest Fruit Development

Apple fruit development is a complex process involving several stages that take place from floral bud break until the apples are harvested. Before fruit fertilization, flower bud induction and initiation take place during the previous year of fruit development. After a period of dormancy during the winter, flower buds resume growth (break) in the early spring of the following season, progressing through the following stages: silver tip, green tip, quarter-inch green, half-inch green, tight cluster, (first) pink, full pink, king bloom, full bloom, petal fall, 8-mm fruitlet, and 10-mm fruitlet, as described by Michigan State University Extension (MSUE, 2014).

Apple fruit development is commonly divided into 3 stages, cell division, cell expansion, and maturation. Following the latter stage, the apple ripens, and this can happen on or off the tree. Once fruit development initiates after fertilization, early fruitlet cortex growth is primarily due only to cell division for about the first 7-10 days after bloom, although it continues until about

35-40 days after bloom (Goffinet et al., 1995). Cell division and cell expansion overlap a few weeks after bloom, and cell expansion, primarily of the cortex, continues until harvest (A. N. Lakso, 2011). Cell division is very important to final fruit set and fruit growth, which is highly regulated by temperature and photosynthetically active solar radiation (A. N. Lakso, 2022). Goffinet et al. (1995) found that cell division during the first 3 weeks after bloom controls the maximum final fruit size. Apple fruit growth is highly sensitive to temperature in the first 42 days (Bergh, 1990). Effects of solar radiation on fruitlet abscission are primarily controlled by the demand of carbon by the fruit and that is markedly influenced by temperature (A. N. Lakso et al., 2001). At lower temperatures, low solar radiation isn't as inhibitory to fruit growth as it is at high temperatures (A. N. Lakso, 2022). Fruit may thin easily during high rates of cell division due to strong carbon demand, and under high temperatures and cloudy conditions thinning may be further promoted. Cell expansion begins roughly 7-10 days after bloom (Goffinet et al., 1995) and continues until harvest. The phase of cell expansion overlaps both cell division and maturation/ripening phases. Expansion of cells is less correlated with whole fruit growth, as Goffinet et al. (1995) found that fruit size was positively correlated with cell number, not cell size or proportion of intercellular space (Goffinet et al., 1995). After cell division ceases at ~40 days after bloom, cell expansion continues until harvest.

1.3.2. Ripening

Ripening is another complex process which involves many different reactions and substrates. Ripening in apple is driven by the gaseous plant hormone ethylene. In postharvest physiology, ethylene production displays itself through two different systems during fruit ripening (Biale, 1964; Pratt & Goeschl, 1969). Apples are climacteric, meaning that apples continue to ripen after harvest, involving a burst in respiration. The ethylene production system (system II) associated

with ripening is autocatalytic, in that the reaction product, ethylene, is perceived and stimulates more ethylene production. The other system of ethylene production is in all fruits, climacteric and non-climacteric. This latter system (system I) does not result in a burst of ethylene, but a steady perception and limits ethylene production to small quantities because it is self-inhibitory. As ethylene accumulates within the apple fruit via system II, the apple rapidly ripens, and its qualities (e.g. firmness, color, flavor, starch degradation, simple sugar accumulation) develop for a desirable eating experience. Another popular method for tracking maturation and ripening of apples is by assessing starch degradation, which occurs before higher ethylene production (system II) (Blanpied & Silsby, 1992; Brookfield et al., 1997; Thammawong & Arakawa, 2007), by staining the inner cortex and core with an iodine solution. This solution stains the starches in the fruit and, as the fruit ripens, the starch declines and converts to simple sugars that cannot be stained by the iodine solution.

1.3.3. Ripening Comparisons

The nature of behavioral differences in ripening between apple varieties is well-studied (Giné-Bordonaba et al., 2019; Gussman et al., 1993; Song et al., 1997; Tong et al., 1999). The sensitivity of apple fruit to ethylene has been analyzed across varieties with differing harvest dates (Singh et al., 2017). Singh et al. (2017) found that early-maturing apple variety ‘Anna’, developed in Israel, produces higher amounts of ethylene, and has higher respiration rates in comparison to later harvesting varieties ‘Galaxy’ and ‘Golden Delicious’. Not only are the levels of ethylene and respiration higher, but the ‘Anna’ cultivar exhibits properties of system II ethylene production (auto stimulatory) throughout fruit development (Singh et al., 2017). Cultivar ‘Anna’ responded to exogenous ethylene treatments during the early stages of fruit development, while the late harvesting cultivars did not. Loss of postharvest quality and early

maturation in ‘Anna’ may be a result of higher ethylene production earlier in fruit development. Comparisons of early and late sports of the same apple variety have also been made (Dong et al., 2011; Iglesias et al., 2012; Kim et al., 2023; Wang et al., 2009). In the case of Wang et al. (2009), they compared mutant cultivar ‘Hirosaki Fuji’ to the progenitor, ‘Fuji’. In their study, they find different expression levels of several ethylene biosynthesis and perception genes, and a heat shock protein coding gene. Although the data is unpublished, Wang et al. (2009) mention that fruit diameter data indicate a faster rate of growth in the early sport as opposed to the standard harvesting ‘Fuji’. They describe the implication of the data by mentioning that the mutation responsible for the early maturation in ‘Hirosaki Fuji’ is unrelated to the difference in expression of genes involved in ripening processes (Wang et al., 2009).

1.4. PHOTOSYNTHESIS AS A DRIVER OF FRUIT DEVELOPMENTAL RATE

1.4.1. Background

Photosynthesis has been extensively studied in apple, primarily in relation to stress or field environment of apple trees (Bhusal et al., 2019; DeJong, 2022; Grappadelli et al., 1994; A. N. Lakso, 1983; Schneider & Childers, 1941; X. Sun et al., 2018; Tartachnyk & Blanke, 2004; Z. Wang et al., 2018). Much of the past and current research on photosynthesis in apple trees relates to response during different light conditions, seasonal conditions, stress or environmental conditions, and low or high nutrition conditions.

1.4.2. Photosynthesis Methodology in Apple

The method of measuring photosynthesis in apple trees is important to review and understand due to the complexity of the photosynthetic mechanism and the biology of an entire tree organism. Infrared gas analyzers have been utilized for quite some time (Fastie & Pfund, 1947). In apple tree fruit photosynthesis, primarily two different infrared gas analyzer systems are used:

open and closed systems (Flore & Lakso, 1989). In an open system, air is continuously flowing through the chamber, allowing steady-state to be reached between the chamber headspace and the leaf. In a closed chamber system, the leaf is put into the chamber and the measurements are immediately read as the CO_2 is taken up by the leaf, creating a CO_2 deficit that is measured by the instrument. Both systems are viable for measuring leaf photosynthesis, but the open chamber is preferred due to the ability to control temperature, humidity, and CO_2 concentrations (Trimble, 2020).

1.4.3. Units

A very important element of measuring photosynthesis to consider is what is being measured. Interpretation of photosynthesis data relies on what plant part is used in the photosynthetic rate measurements (Flore & Lakso, 1989). In peach, Kappel and Flore (1983) measured photosynthetic assimilation (*A*) rate in 4 ways: *A* per leaf area, *A* per whole leaf, *A* per mg chlorophyll, and *A* per unit dry weight (Kappel & Flore, 1983). Flore and Lakso recalculated Kappel and Flore's work to update units (mass to mol). They found that, based upon light levels described as photosynthetic photon flux (*PPF*), measurements based on dry weight decreased with an increase in *PPF*, while *A* expressed per unit chlorophyll increased with increasing *PPF* (Fig. 1). Thus, research questions for a project may heavily depend upon which measure of *A* is considered. Measuring *A* of CO_2 as μmol m^{-2} s^{-1} is an appropriate method to capture total carbon assimilated by leaf area for an entire day.

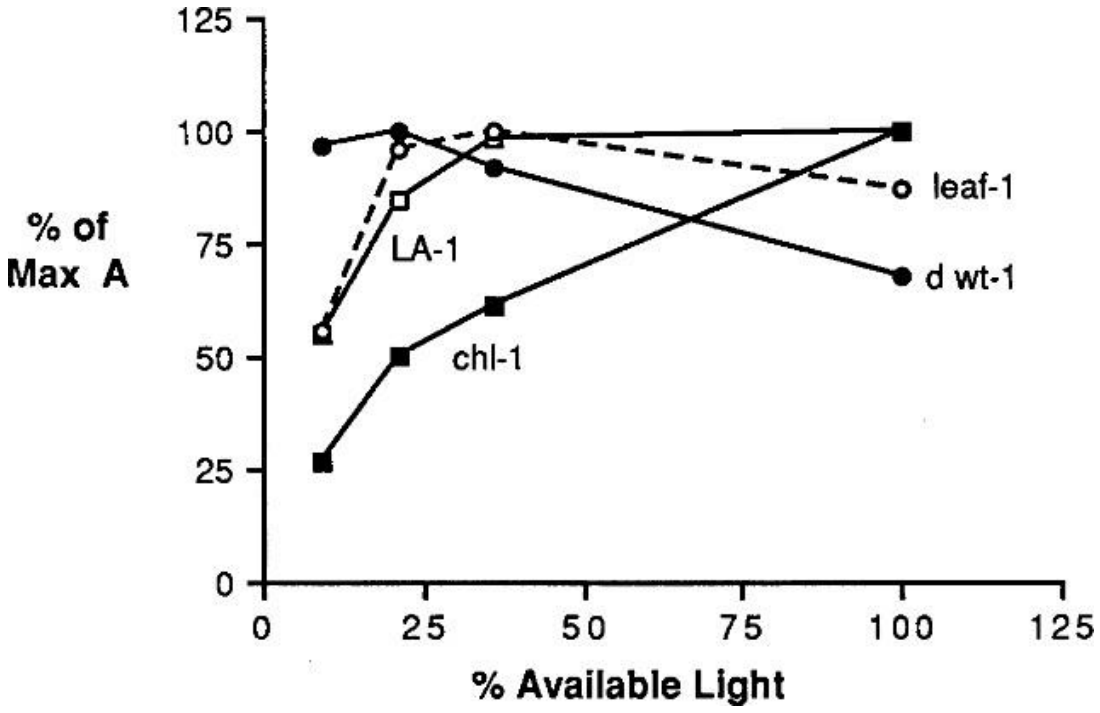

Figure 1. Relative photosynthetic carbon assimilation of peach leaves grown under different levels of PPF, expressed as A per leaf area (LA-1), A per whole leaf (leaf^{-1}), A per mg chlorophyll (chl^{-1}) and A per unit dry wt^{-1}(d wt-1). (Recalculated from Kappel and Flore 1983). Figure taken from Lakso and Flore, 1989.

1.4.3. Diurnal and Seasonal Photosynthetic Activity

Diurnal measurements are an important method of analysis in determining peak *A*, decreases in *A*, and *A* throughout a day at specific times. There is added benefit by capturing diurnal measurements due to potential trends throughout the day that the apple tree is exhibiting, not detectable by just one measurement. Diurnal measurements also allow one to integrate total carbon fixed for the day. These trends of carbon fixation may vary throughout the day due to a few reasons, one reason being shifts in stomatal conductance. Stomatal conductance, a critical factor in photosynthesis, is the measurement of the ease of gas exchange through the stomatal aperture. Interplay between stomatal conductance, temperature, and humidity can play a large role in an increase or decrease of *A* (Flore & Lakso, 1989). Stomatal conductance and net photosynthesis are very linearly correlated (A. N. Lakso, 1979). Thus, increases or decreases in photosynthetic rate throughout the day may heavily rely on the environmental conditions of the day, such as vapor pressure gradient and temperature, and their effect on stomatal conductance. Seasonal changes result in a gradual decline in net photosynthesis approaching harvest, the highest rate of photosynthesis during the season averaging a net CO_2 flux of ~15-22 μmol m^{-2} s^{-1} (Flore & Lakso, 1989). A comprehensive study performed by Fujii and Kennedy (1984) revealed two periods of time during the growing season that photosynthetic rates differed from each other according to fruit load (Fujii & Kennedy, 1984). Photosynthetic rates first differed during bloom, exhibiting a 25% increase in photosynthetic rate on flowering shoots compared to vegetative shoots. Fujii and Kennedy (1984) found that at a later period in the growing season, from July to September, CO_2 assimilation rates were higher in fruiting trees than nonfruiting trees. From the findings of this study, it is important to note the importance of crop load on apple leaf or tree

photosynthesis because the crop load amount on the tree may determine and/or influence net photosynthetic rate.

There is little literature comparing one variety to another regarding carbon assimilation, stomatal conductance, and photosystem II efficiency. Most, if not all research in apple photosynthesis has revealed environmental, exogenous hormone application, nutrient level, and water effects on photosynthetic rate, photorespiration, photochemistry, dark respiration, and stomatal conductance. Furthermore, to the author's knowledge, there is no literature on photosynthesis analyses between apple cultivars within the same variety. Additionally, no known comparison has been conceived between early/late maturing sports and their progenitor/standard harvest time cultivar. Further knowledge and understanding of carbon assimilation rates amongst cultivars of the same apple variety may provide answers as to why there is a stark difference in maturity time between a progenitor and its early or late maturing bud sport. If development before harvest is compressed or extended, net photosynthesis data may provide an explanation for that advanced or delayed development. Photosynthesis may limit fruit development, or on the contrary, fruit growth may regulate net photosynthetic rates. A lower photosynthetic rate may delay fruit development or, conversely, lower rates of fruit development may result in lower demand on the leaves, leading to a decline in photosynthetic rate.

1.5. APPLE GENOMICS AND TRANSCRIPTOMICS

1.5.1. Background

Only a handful of select widely cultivated varieties of apple (*Malus domestica*) have been comprehensively sequenced (Daccord et al., 2017; Khan et al., 2022; X. Sun et al., 2020); however this number is likely to grow exponentially as prices decline and sequencing technologies advance. Primary reasons for sequencing the 'Honeycrisp' genome were because of

its high value to the apple industry and preference of the consumer, in addition to the major problems it presents after harvest (Khan et al., 2022) such as internal browning (Contreras et al., 2014) and bitter pit (Griffith, 2022). Sequencing apple cultivars has the potential to contribute to an expanded understanding of genetic heritage, evolution, predisposition to disease and physiological disorders, as well as breeding new cultivars for enhanced quality, resistance to disease, robust photosynthesis, enhanced storability and, in the case of the project discussed hereafter, harvest date manipulation.

1.5.2. Gene Mutation in Apple Fruit Qualities

There have been several studies regarding mutations causing phenotypic change in apple quality (ethylene production, color, volatile production, and overall ripening behavior) (Cho et al., 2020; Dong et al., 2011; Kim et al., 2023; H. Sun et al., 2023; Telias et al., 2011). Few studies (Ban et al., 2022; Kim et al., 2023; Wei et al., 2020) have analyzed mutations resulting in altered harvest dates in apple or other fruit crops, despite the value that the background knowledge of genetic predetermination of harvest date may bring. In the case of the red sport 'RubyMac' they identified altered candidate genes that may play a significant role in fruit coloration (Sun et al., 2023). Comparisons between bud sports of the same variety have been investigated with regard to several fruit qualities including ethylene (Dong et al., 2011), color and anthocyanin content (Cho et al., 2020; Telias et al., 2011), volatile compounds (Iglesias et al., 2012) and overall fruit maturation, ripening, and ripening gene expression (Kim et al., 2023). Dong et al. (2011) found that early maturing 'Fuji' cultivar 'Beni Shogun' displayed earlier and higher expression of key genes related to ethylene synthesis, signaling, and transduction than 'Fuji'. Cho et al. (2020) found genes whose expression was associated with the skin color of 'Fuji' cultivars at mature stages, as well as higher expression of *MdMYB10* and *MdGST* genes related to anthocyanin

production in ‘Beni Shogun’ cultivar compared to ‘Fuji’. Iglesias et al. (2012) found volatile compound concentration and profile differences among ‘Fuji’ cultivars. They found the lowest concentration in ‘Aztec Fuji’. They also show correlations through a full-data principal component analysis between consumer preference and volatile profiles in the different ‘Fuji’ cultivars. Study of mechanisms behind early and late bud sports is not limited only to apple. Other species such as grape, peach, and pear are also being evaluated for their maturity differences (X. Liu et al., 2014; Y. Liu et al., 2007; Wei et al., 2020; Wu et al., 2015)

1.5.3. Gene Expression in Grape Cultivars Differing in Harvest Date

In grape, Wei et al. (2020) discover candidate genes, differentially expressed between an early-ripening cultivar and its progenitor (Wei et al., 2020). Some of the differentially expressed genes (DEGS) are thought to be involved in berry ripening, implying possible mechanisms for the early ripening phenotype of the grape bud mutant. Another study compared two bud sports to their parent in a transcriptomic analysis with the intention of confirming the two bud sports as reliable cultivars for cultivation (Wu et al., 2015). They found a handful of genes associated with early ripening which were significantly up-regulated including the 1-aminocyclopropane-1-carboxylate synthase (ACC synthase) encoding gene in the bud sports in comparison to their parent.

1.5.4. Genomic Understanding of Harvest Date in Apple

Many studies have the genetic mechanisms linked to color change in apple bud sports (Cho et al., 2020; Iglesias et al., 2012; Y. Liu et al., 2022; H. Sun et al., 2023; Tian et al., 2022), but investigations into mutations resulting in altered harvest date have not been thoroughly explored. Regarding harvest date, several QTLs with a critical role in apple fruit maturation have been identified. The proposed fruit maturation date QTLs are numerous and complex, spread across

14 of the 17 chromosomes. The specific QTLs are found on linkage groups (LG) 3 (Migicovsky et al., 2016), 9 (Morimoto et al., 2013), 10, 15, and 16 (Kunihisa et al., 2014). Another finding suggests that there are 16 regions of the apple genome on 9 LGs linked to maturation date (Chagné et al., 2014). This leads to the idea that fruit developmental and/or maturation rate and the timing of apple harvest has very complex genetic underpinnings. For example, Morimoto et al. (2013) found correlations between fruit flesh anthocyanin content and harvest date. Also, fruit firmness and harvest date are thought to be tightly linked (Ban et al., 2022; Migicovsky et al., 2016). Growers find a tradeoff between early harvesting cultivars going to market earlier, but these cultivars do not store as long as later harvesting cultivars.

1.5.5. Gene Mutation Resulting in Altered Harvest Date

The complexity of harvest date is discussed in the recent study that identified a candidate gene/genetic event for the mutation responsible for the late maturing 'Autumn Gala' phenotype (Ban et al., 2022). They utilized genomic and RNA-seq analysis throughout the growing season to analyze genetic alterations and differing gene expression. A genetic event called a retrotransposon insertion was discovered in this study. A retrotransposon insertion is when a segment of DNA is transcribed into RNA, reverse-transcribed back into DNA, and then inserted elsewhere in the genome. Results from Ban et al. (2022) suggest that a large (2.8 Mb) genomic deletion on chromosome 6 was caused by a 10.7 kb retrotransposon insertion. Because of the deletion, the remaining intact chromosome 6 had only one copy of each gene it contained, so these genes were the sole source of proteins from this chromosomal segment. In the late maturing phenotype 'Autumn Gala', a 10.5-fold suppression of '*MdACT7*' resulted from a 2.5-kb insertion of a transposable element into that gene. Interestingly, both the parent and the mutant 'Gala' lines possessed the disrupted *Mdact7* and it was suggested loss of the 2.8-Mb

segment with its functional version of *MdACT7* resulted in the phenotype. The '*MdACT7*' gene is orthologous to the '*ACT7*' gene in *Arabidopsis*, an actin-related protein that plays a role in cell division, seed germination, root hair growth, and overall cell growth. Mutants of this gene display stunted growth and development phenotypes. However, apart from the rate of fruit development, the 'Autumn Gala' does not appear to differ phenotypically from the progenitor line. Since there is no other known phenotypic difference between 'Autumn Gala' and 'Kidd's D-8', their finding is noteworthy. Ban et al. (2022) may be one of, if not the first, to explore the unique change in harvest date. Finding genomic variants is a vital aspect of discovering why these valuable mutations occur and evaluating the biology and physiology of the growth of both the apple tree and fruit bolsters genetic findings.

CHAPTER 2. Apple bud sport comparisons to progenitor/standard harvest cultivar of fruit growth suggest physiological predetermination of maturation date early in fruit development

2.1. INTRODUCTION

2.1.1. Background

Apple bud sports contribute tremendous value to apple production. Bud sports originate from meristematic tissue in which a stable mutation has occurred. As the new genetic tissue arising from the mutated meristem continues to undergo cell division, differentiation, and expansion, new limb, leaf, and fruit phenotypes may emerge (Foster & Aranzana, 2018). Variable phenotypes in the fruit are most discoverable because of the distinct, visible difference in color, shape, or harvest date, as elaborated in the comprehensive review by Shamel and Pomeroy (Shamel and Pomeroy, 1936). Retold in LeAnn Zotta's *200 Years and Growing: The Story of Stark Bro's Nurseries & Orchards*, the Stark family from Louisiana, Missouri first realized the value of bud sports when they discovered the bud sport they named 'Starking® Delicious'. Their nursery began in the year 1816 and has continued producing nursery fruit trees ever since. 'Starking® Delicious' was originally discovered by New Jersey grower Lewis Mood, who noticed a limb producing red apples on the 'Delicious' (later marketed and known as the variety 'Red Delicious') tree while the rest were still green. Paul Stark Sr. rushed to pay $6,000 for this limb and now that limb has been grafted into millions of trees all over the world (Zotta, 2015). Ever since this event, apple bud sport numbers grew in value and popularity as a resourceful method of introducing and producing new apple cultivars. For example, within six years of the enacted Plant Patent Act (1930), over 1600 fruit tree bud sport patents were issued Shamel and Pomeroy, 1936). This means that there was at least one fruit tree patent issued every working day for six years.

Among the various classifications of bud sports in apple, ‘maturity sports’, sports that harvest at a different date than their progenitor, are of significant value. Early maturing sports bring more value than late sports, due primarily to their fruit’s early presence in the market, but also because of a shorter growing period and the potential for avoiding early autumnal frosts. The apple harvest window is an extremely important aspect of apple production. Each variety has a general harvest date window, varying year to year by plus or minus a couple of days, depending on environmental conditions (Shane et al., 2023). Growers spread their harvest window amongst different varieties to spread labor needs and diversify their crops. Growers also apply plant growth regulators days/weeks before harvest to slow ripening to delay harvest or retain fruit on the tree to prevent fruit drop (Bramlage et al., 1980). This practice is broadly utilized to improve labor efficiencies during harvest so field laborers can pick apples block by block in the orchard.

2.1.2. Fruit Development

Fruit growth is a complex process that involves many metabolites and processes. In evaluating fruit development over the season, fruit size may be readily measured. Morphology during the development of apple fruits has been well characterized for decades (Tukey & Young, 1942) (Fig. 3). In apple fruits, cell division is the primary force behind fruit size for 7-10 days after bloom. After this first phase of fruit growth, cell expansion occurs simultaneously with cell division until about 4-6 weeks after bloom when cell division ceases (Lakso & Goffinet, 2017). From this point on, cell expansion and growth in intercellular space are the main contributors to fruit growth. In Michigan, the cool season promotes a sigmoidal curve of fruit growth (Tukey & Young, 1942) (Fig. 2), as opposed to the expo-linear pattern of fruit growth (A. Lakso & Goffinet, 2017).

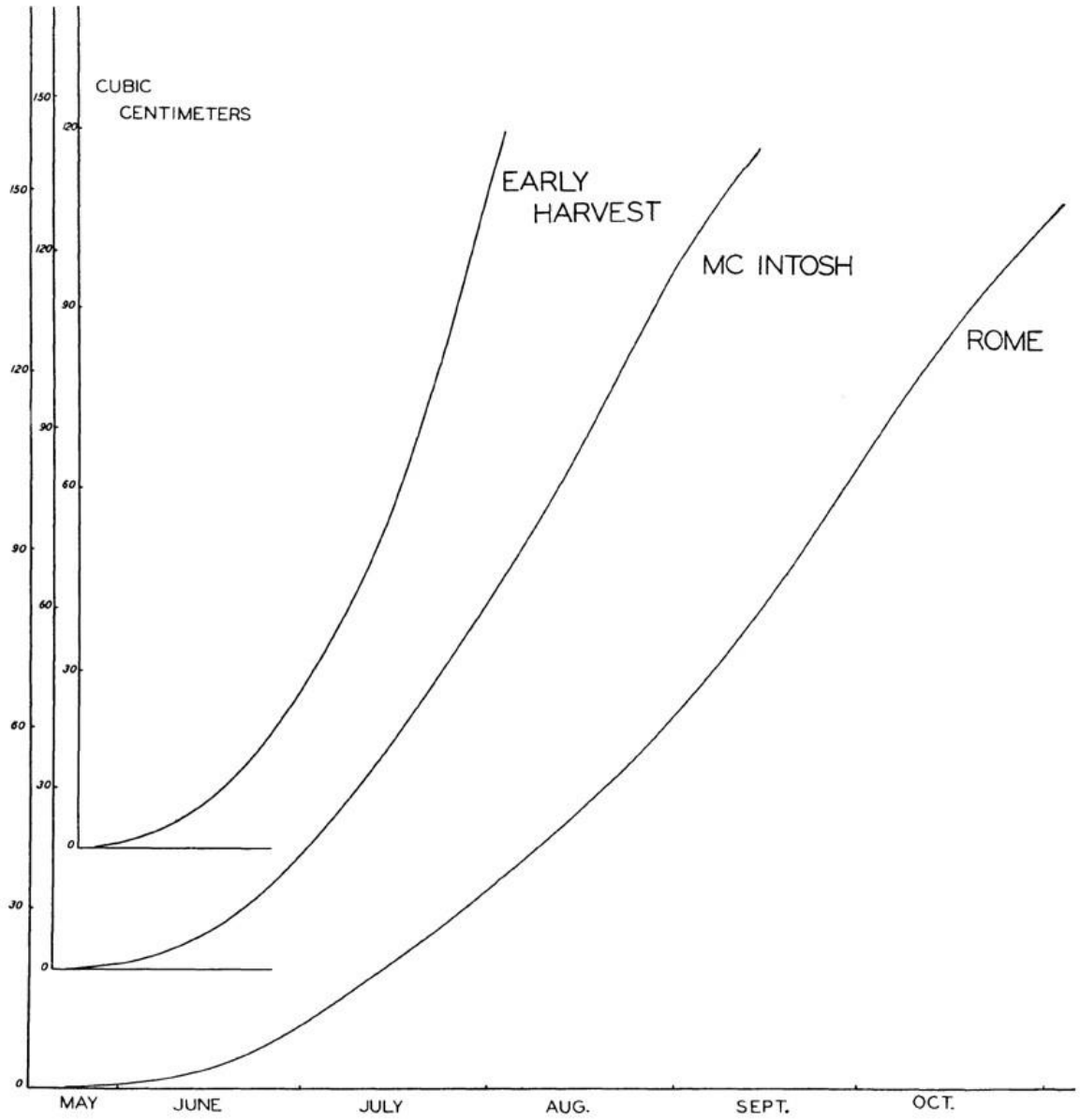

FIG. 4.—Increase in volume of fruit of Early Harvest, McIntosh, and Rome apples from full bloom to fruit ripening (water displacement method).

Figure 2. Expolinear and sigmoidal curves showing volume increase of 3 different apple cultivars during the growing season. 'Early Harvest' exhibits an expolinear behavior while 'Mcintosh' and 'Rome' have a sigmoidal growth behavior.

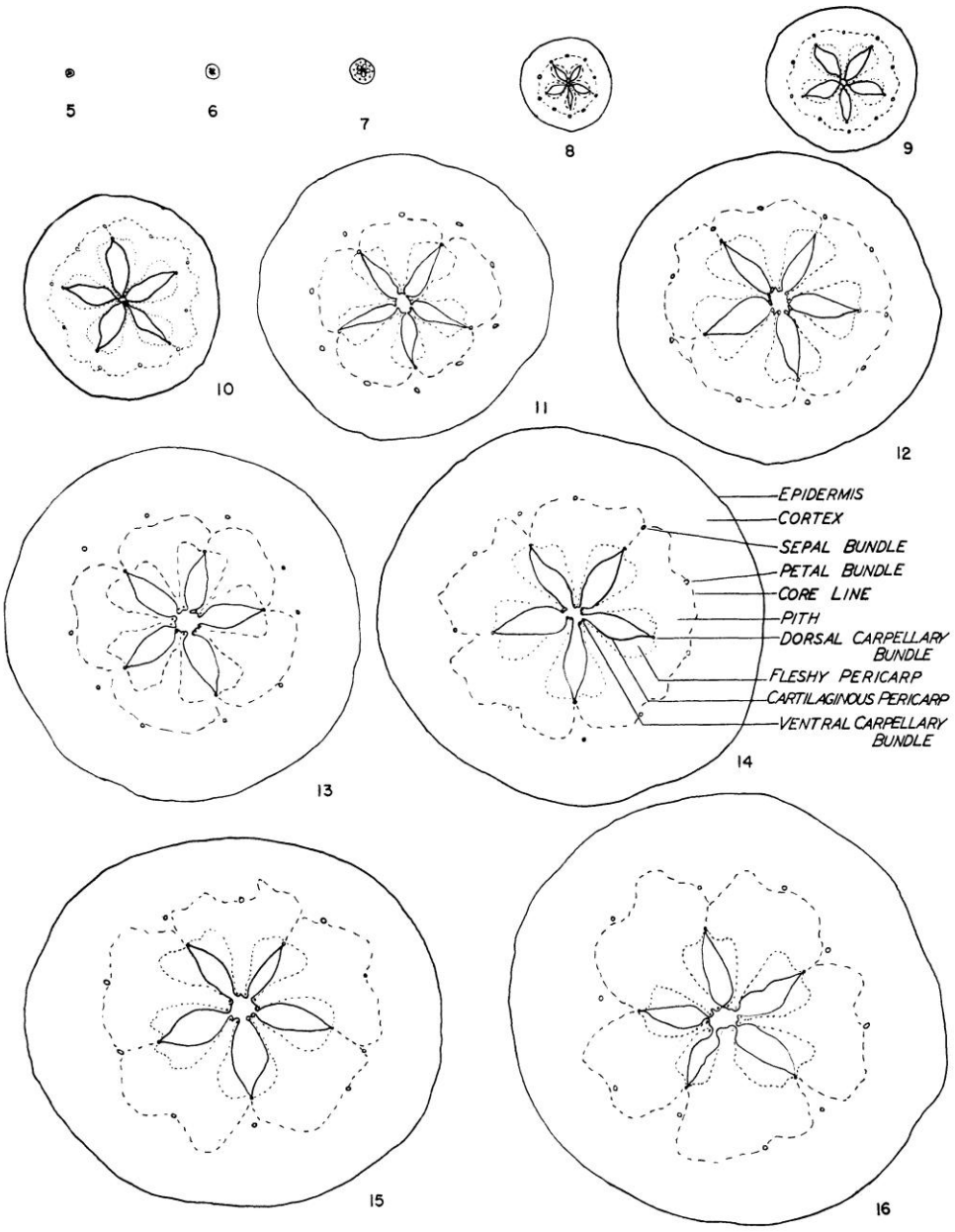

FIGS. 5–16.—Tracings of Twenty Ounce apple in cross-section from 4 weeks before full bloom to fruit ripening: Fig. 5, 4 weeks before full bloom; fig. 6, 2 weeks before full bloom; fig. 7, full bloom; fig. 8, 2 weeks after full bloom; fig. 9, 4 weeks; fig. 10, 6 weeks; fig. 11, 8 weeks; fig. 12, 10 weeks; fig. 13, 12 weeks; fig. 14, 14 weeks; fig. 15, 16 weeks; fig. 16, 18 weeks (ripe).

Figure 3. Characterization of morphology in cultivar 'Twenty Ounce' across entire fruit development from 4 weeks before bloom until ripe. Anatomically distinct tissues named.

2.1.3. Photosynthesis in Apple

There has been much research done on photosynthesis in apple leaves, but primarily in environmental (soil moisture, vapor pressure deficit, light, temperature) response and physiological (source and sink, shading, spur leaf vs. bourse leaf assimilation, carbon allocation) studies (Bhusal et al., 2019; Chun et al., 2002; DeJong, 2022; Fallahi et al., 2001; Grappadelli et al., 1994; Lakso, 1983; Schneider & Childers, 1941; X. Sun et al., 2018; Tartachnyk & Blanke, 2004; Wang et al., 2018). There is relatively little to no study, to the author's knowledge, on differences in the carbon assimilation characteristics of bud sports when crop load has been managed carefully. Since the dawn of portable gas exchange systems, measurements in the field have not only become possible, but also more accurate and reflective of actual commercial growing conditions. In this experiment, we evaluated carbon assimilation on a diurnal basis, meaning that we took leaf measurements throughout the day, starting pre-dawn and ending after sunset. Leaf measurements across an entire day give a more accurate representation of total daily carbon assimilation as opposed to just measuring assimilation at just one time point during the day. With an analysis of daily carbon assimilation, we aimed to uncover any possible correlation between rate of gas exchange in leaf tissue and rate of fruit growth, development, and maturity. If higher carbon assimilation coincided with higher fruit growth rate, for instance, the more rapid fruit development may be enabled by a higher photosynthetic rate or, conversely, the photosynthetic rate might be enhanced by the demands of a higher growth rate. If developmental rate is driven by a higher carbon assimilation in earlier harvesting cultivars, one could look for differences in expression of genes heavily involved in carbon assimilation as a root cause of accelerated development. Alternatively, if no relationship exists between assimilation rates and

maturation date, then perhaps one might logically exclude genes related to photosynthesis as being causal for a shift in maturation date.

2.1.4. Experimental Design and Rationale

For this study, we evaluated bloom date to uncover any differences in full bloom date. If we found differences in full bloom date, the direction of our search would go toward an analysis of flower development or carbohydrates in the beginning of the season. We also evaluated fruit development over the entire growing season until full fruit maturity and compared early and late sports using measures of fruit growth, rate of growth, acceleration of growth, and leaf photosynthesis. For our photosynthesis analysis, we measured carbon assimilation, but other parameters such as stomatal conductance and photosystem II efficiency were also measured. Lastly, we characterized the ripening behavior of each cultivar to determine if there is a pause or slowing in development before ripening of the later cultivars. Characterizing bloom, fruit development, carbon assimilation rates, and ripening among the three different comparisons was intended to narrow the window for our search for candidate genes and genetic events causing early or late maturation in bud sport mutations.

2.2. MATERIALS AND METHODS

2.2.1. Plant Material

The apple trees analyzed in this experiment were located in a research plot at the MSU Clarksville Research Center (42°52’27.3”N 85°16’15.0”W). For each cultivar, three randomized blocks of 8 trees were planted, with tree spacings of 0.9 meters (3-feet) apart within rows, and 3.7 meters (12-feet) between rows with adequate water, nutrition, and pruning provided by the research station. The ‘Fuji’ and ‘Cripps Pink’ trees given by Philip Schwallier were planted in 2019 on ‘Bud-9’ rootstock. The ‘Kidd’s D-8’ and ‘Autumn Gala’ ‘scions were collected from

Catoctin Mountain Orchard (Thurmont, MD) by Dr. Christopher Gottschalk from the original tree from which the mutation in 'Autumn Gala' originated. The 'Gala' trees were grafted into Bud-9 rootstock in 2021. Five trees of each cultivar similar in architecture and tree trunk cross-sectional area were selected for fruit size, leaf photosynthesis, and maturity measurements. Additional trees were selected for DNA leaf tissue and RNA fruit tissue collection.

2.2.2. Bloom

Bloom date was characterized by examining 10 trees randomly throughout the block per cultivar (five of which used for both fruit growth and photosynthesis analyses). 'Full bloom' was determined by visually estimating when 80% of all flowers on the trees were open.

2.2.3. Crop Load Management

Crop load is an essential variable to consider in tree fruit because of its effects on fruit size, tree trunk growth, shoot number, node emergence, and leaf photosynthesis (DeJong, 2022; Palmer et al., 1997). The five trees of each cultivar that were selected for growth measurements were managed to achieve the same final fruit set for the growing season. Tree trunk cross-sectional area (TCA) in cm^2 was measured 30 cm above the graft union of each tree. A multiplier for each variety was used to calculate the total crop load that the tree could handle to obtain maximum growth potential. The calculation is TCA multiplied by 9 for 'Gala', and a factor of 7 for 'Fuji' and 'Cripps Pink'. 'Fuji' and 'Pink Lady' were given lower multipliers due to their biennial bearing nature. After the calculation in 'Gala', the target crop load was halved due to the trees' young age. Immediately after petal fall, fruitlets were initially thinned by hand. Most fruitlets of all varieties were 5-9 mm in diameter at the time of thinning. Fruit was first thinned down to a king fruitlet every other cluster. After this, each tree was further thinned based on 'Equilifruit disc' (National Institute for Agricultural Research, 147 Rue de I'Université 75338 Paris Cedex)

recommendations. The ‘Equilifruit disc’ has notches to estimate the number of fruit that should remain on a branch based on circumference (in mm) of each limb. Each tree was thinned to a fruit number slightly above the crop load target to ensure that enough fruit would remain to achieve target crop load after ‘June drop’, a natural phenomenon when trees shed fruit (Larson & Kon, 2021). Fruit number was re-counted after ‘June drop’ and then thinned to the exact crop load target (7 fruit/tree trunk cross-sectional area (TCA) for ‘Gala’ and ‘Pink Lady’ and 6 fruit/TCA for Fuji) for the remainder of the growing season.

On each tree, five spurs (one king fruit/spur), were selected for fruit diameter measurements during the summer of the year 2023. Clusters that were selected were located on ‘dards’ which are one-year old limbs that are approximately 1-4 inches in length, where the abundance of dards varies based upon vigor, pruning, and cultivar (Boyes, 1923). The selected dards were located on the outer canopy of the tree, having more exposure to sunlight and were the same limbs from which we gathered carbon assimilation data. Measurements were performed twice every week until the rate of growth slowed in the later portion of the season, at which time measurements were taken at least once per week. For the first five weeks post bloom, the apple fruitlet diameter was measured using a standard digital caliper. After about five weeks, measurements were conducted via a produce measuring gauge (Cranston Machinery Co., Oak Grove, Oregon). This gauge has an extendable metal strap that wraps around the fruit equator, giving a more accurate representation of the fruit diameter. The five fruit per tree that were measured for the entire season were harvested and taken to the lab for harvest maturity analysis when comparable fruit suggested fruit ripening had begun (see Fruit Maturity Analysis below). Growth curves as a function of growing degree hours (GDH) were generated using specialized curve-fitting software

(TableCurve 2.0, Jandel Scientific, San Rafael, CA). We used the Weibull (#8088) equation (Eq. 1)

$$y = a + b(1 - \exp(-((x + d * \ln(2)^{\frac{!}{\#}})^{!})) \quad (1)$$

where x=GDH value (Table 1). Variables a, b, c, d, and e all change from one curve fit for a specific fruit to another, but every individual fruit's data was fitted to the generated curve of the same equation with slightly different values for each variable according to small differences in growth behavior of each fruit. Growth rate (1st derivative of growth curve) and acceleration of growth (2nd derivative of growth curve) were manually calculated for each fruit throughout the growing season to identify peak acceleration, peak growth rate, and trough deceleration of fruit growth. These developmental milestones were used as targets for fruit tissue for RNA extraction and analysis (described in Chapter 3). For each date of diameter measurement, a 'Student's T-test' was performed for volume, growth rate, and acceleration of fruit growth. Five trees per cultivar were considered replicates and the 5 fruits measured per tree were considered subsamples. Data for subsamples were averaged and the averages subjected to statistical analysis to compare mutant and standard cultivars.

Table 1: Fitted curve equation for fruit growth of each cultivar showing variables of Weibull equation $y = a + b(1 - \exp(-((x + d * \ln(2)^{\frac{!}{\#}})^{!}))$ *where x=GDH value. These curves are depicted in growth rate and acceleration of growth figures 3-11.*

Variables	a	b	c	d	e	R^2
Kidd's D-8	-14.1656	243.15592	28605.07	167182.7	15.4026	0.9995
Autumn Gala	-14.1674	234.23149	29912.333	366756.62	33.08485	0.9996
September Wonder Fuji	-14.5170	360.12959	30418.000	73339.687	6.063213	0.9997
Aztec Fuji	-5.2252	391.10507	39198.310	53966.135	2.942034	0.9996
Maslin	-3.4059	323.74065	41548.613	52884.155	2.392670	0.9998
Cripps Pink	-25.5178	257.20485	37093.037	222948.29	11.69927	0.9997

2.2.5. Photosynthesis Measurements

Diurnal photosynthesis measurements (i.e., measurements made periodically throughout the day from dawn until dusk) were taken using a portable photosynthesis instrument (LI 6800, LI-COR Biosciences, Lincoln, Nebraska). Carbon assimilation, stomatal conductance, photosystem II operating efficiency, and light intensity were measured. Dates were selected beginning at early fruit growth stage during late cell division, mid-season cell expansion, peak fruit growth rate, and ~2-3 days before and after harvest. The type of leaf that was measured on each tree was the first or second bourse shoot leaf that emerged from a bourse shoot subtending a king fruit. The bourse shoot leaf was selected because bourse shoots proportionately contribute more carbon resources to the fruit than the spur leaves (Wünsche & Lakso, 2000). For the first three time points during the growing season, diurnal measurements for each cultivar were taken on the same day. Diurnal measurements were also taken for each individual cultivar a few days prior and after the respective cultivar's harvest date; these dates differed for each standard and mutant strain. On each date, bourse leaf photosynthesis parameters were measured for all trees within a one-hour period for each of six timepoints. The diurnal measurements were taken pre-dawn, 9 a.m., 12 p.m., 3 p.m., 6 p.m., and post-dusk. The initial and end-of-day measurement times changed as daylength shifted across the season. To select leaves in regions experiencing maximal sun exposure, the leaves were measured on the east side of the tree for the first 3 time points of the day and on the west side for the last 3 time points. We used publicly shared software (R, R Core Team, 2017) for analyses and plots. Total net carbon assimilation of the day was calculated as the area under the curve less the respiratory carbon emitted at night. Net carbon assimilation was fitted to a linear model with cultivars, development, and time of the day as fixed effects

using the ‘lm()’ function. Treatment differences were estimated using ‘emmeans()’ in the ‘emmeans’ package (Lenth et al., 2024).

2.2.6. Fruit Maturity Analysis

During the latter part of the season, apples from each cultivar were evaluated every 3-4 days beginning approximately two weeks before anticipated commercial harvest, at commercial harvest (when the starch index reached 4 and when growers typically harvest for maximum storage and shelf-life quality) and continuing for approximately two weeks after the commercial harvest date. For the before and after harvest timepoints, fruit for maturity analysis came from non-crop load-managed trees. At harvest, the fruit used for tracking growth rate measurements were used for maturity analyses. For all maturity timepoints (excluding the harvest time point when the 25 tracked fruit were analyzed), 10 apples were placed into trays, imaged, and analyzed in the following parameters: weight, DA meter (chlorophyll absorbance), percent redness (subjective), background color (scale 1-5 shades of green to yellow-subjective), internal ethylene, firmness, starch index (scale 1-8-subjective), and titratable acidity.

2.2.7. Fruit Maturity Analysis Methodology

Each apple was placed onto a scale and weight in grams recorded. Chlorophyll (DA) readings were taken from opposing sides of the fruit (red and green) of the apple. Each apple was analyzed by holding the fruit flush to a specialized hand-held reflectance spectrometer (DA Meter, Sintéleia, Turoni, University of Bologna-Department of Agricultural Science, AGRIMAT S.R.L, Bologna, Italy). The DA Meter measures the amount of chlorophyll in the apple by measuring its absorbance and outputting that absorbance as an index. Percent redness as a subjective measure was assessed by holding one’s index finger over and around the stem bowl, and the thumb under and around the calyx end of the apple. Both sides of the apple were

evaluated. Often the bi-colored apples such as ‘Gala’ and ‘Cripps Pink’ were analyzed by first evaluating the reddest side of the apple and then switching to the opposite side of the fruit. The percentage of redness of each side of the apple was estimated in increments of 5% and the average percentage for the two sides recorded. A background color index with 5 shades of green (5=dark green and 1=yellow) according to the ‘Macintosh’ cultivar was used (L.R. Simons, Cornell University Extension-New York State College of Agriculture, Ithaca, New York). The shade of color most accurately representing the background color of each fruit was recorded. A gas chromatograph was used to measure the internal ethylene concentration of each individual apple. A standard of 1 μL L^{-1} ethylene was used (Matheson Tri-Gas, Inc.) and the sample volume was 1 mL. Fruit internal ethylene was measured by withdrawing a 1-mL gas sample from the core of the apple fruit. To do this, a needle, with a clean-out wire inserted to prevent the needle from becoming clogged by apple cortex/juices, was pushed into the calyx end of the fruit, entering the seed cavity of the fruit. The clean-out wire was removed from the needle and a 1-mL plastic syringe was mounted on the needle and 1 mL of the gas sample was extracted. The gas sample was then inserted into a gas chromatograph (Carle AGC series 400, Carle Instruments Company, Fullerton, CA) and the output recorded on a chart recorder (Linear 1200, Barnstead Thermolyne Co. Ramsey, MN, USA). A penetrometer (QA Supplies, FT327) attached to a portable manual drill press was used. A 2-cm dia. disc of peel was removed on opposing sides of the apple equator to expose the cortex. The apple was then held on the press platform and penetrated by the penetrometer to a depth of 1 cm. The penetrometer force was read in pounds and converted to Newtons. For measuring starch index, apples were sliced in half at the equator and one half was dipped into an iodine solution (8.8 grams of potassium iodide dissolved in 30 mL warm water followed by the dissolution of 2.2 grams of iodine into the solution, which was

then brought to 1 L volume). Each stained half was placed into a 20-cell tray and analyzed by comparison to a standardized starch index on a 1-8 scale (Cornell University Starch Index, Blanpied & Silsby, 1992). A hand-held refractometer (ATAGO CO., LTD, Tokyo, Japan) was used to analyze the sugar concentration within the fruit. A drop of juice from the apple was put onto the glass of the refractometer and the plastic cover sealed the juice onto the glass. A digital titratable acidity meter (ATAGO CO., LTD, Tokyo, Japan) was used to calculate the titratable acidity of each fruit. 1-mL of apple juice was placed into a 100-mL beaker. It was then diluted with 49 mL of deionized water and thoroughly mixed. A few drops of the resulting solution were then pipetted onto the digital refractometer/acidity sensor surface and the titratable acidity value was calculated.

2.3. RESULTS

2.3.1. Bloom

There were no differences in bloom between the early and later harvesting cultivars in all three comparisons of the progenitor and sport (Fig. 4, Table 2).

Figure 4: Bloom depicted on May 10, 2023. No visible differences in bloom phenology were observed between maturity sports and standard cultivars.

2.3.2. Fruit Growth, Rate, and Acceleration of Fruit Growth

Throughout the 2023 growing season, fruit diameter was measured at least once per week for all cultivars starting at 14 days after full bloom (DAFB). The R^2 value for curves describing fruit volume as a function of GDH had values above R^2=0.99, with most curves with value R^2 =0.999 or above (Appendix). The fitted variables for the curves using the averages for each cultivar are presented (Table 1).

All cultivars had comparable initial volumes (~0.3-0.5 cm^3). Both the 'Gala' and 'Fuji' mutant/standard comparisons ended in similar final fruit size, but in the 'Pink Lady' comparison, 'Cripps Pink' had less volume at final fruit size than 'Maslin Cripps Pink'. The once-per-week measurement of fruit diameter enabled the collection of highly precise data for curve fitting. This precision enabled a more reliable determination of the first date of divergence in fruit growth between the progenitor and the sport than fruit volume measurements.

In ‘Gala’, the later harvesting bud sport ‘Autumn Gala’ had a smaller volume than its progenitor ‘Kidd’s D-8’ by 17 July, 67 DAFB (Fig. 5). Analysis of fruit growth rate revealed that ‘Autumn Gala’ grew at a significantly lower rate than ‘Kidd’s D-8’ by 15 June, 35 DAFB, which was more than a month before differences were evident in fruit volume (Fig. 6). The fruit growth acceleration of ‘Autumn Gala’ was significantly lower than its progenitor by 1 June, 21 DAFB, which was two weeks prior to the first day of growth rate separation between the cultivars (Fig. 7).

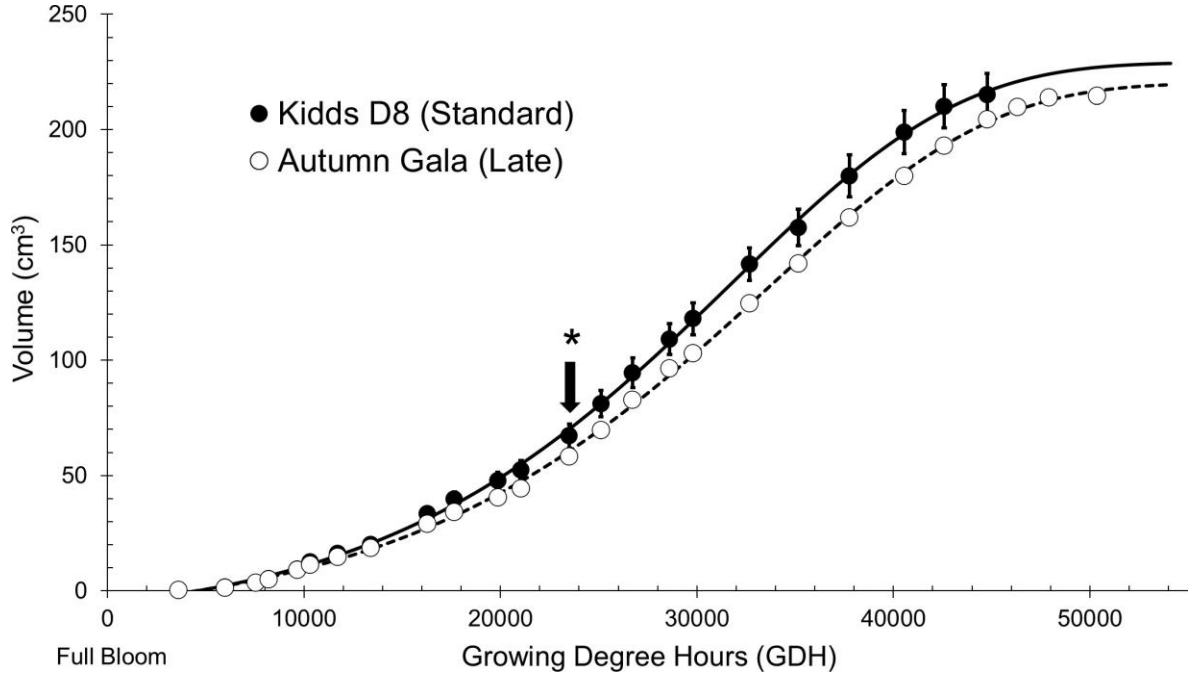

Figure 5: Calculated fruit volume in ‘Gala’ cultivars over the entire season based on measures of fruit diameter or circumference and assuming spherical fruit shape. The fruit volume of late bud sport ‘Autumn Gala’ was less than its progenitor after 17 July, 67 DAFB and 23,509 GDH (arrow; T-test-p=0.039). Each data point represents the average fruit size of 25 fruits from a total of 5 trees (5 fruits per tree). Vertical bars represent standard error of the averages of each tree replicate. ‘Kidd’s D-8’ R^2=0.9994 and ‘Autumn Gala’ R^2=0.9996.

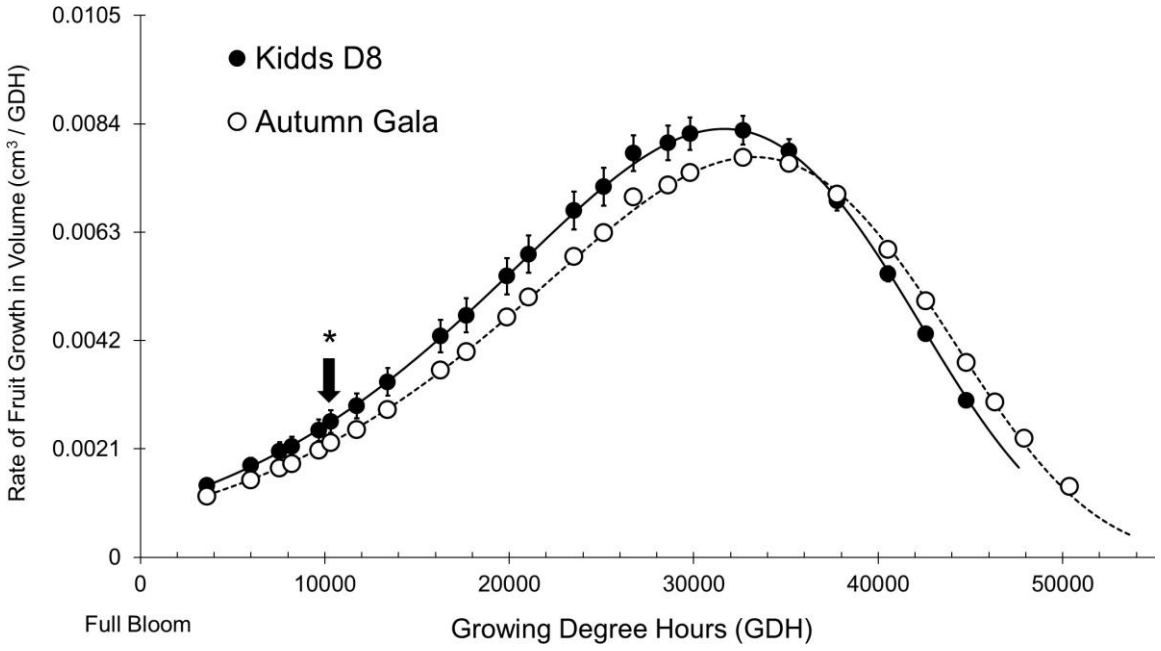

Figure 6: Fruit growth rate in 'Gala' over the growing season. The growth rate in late bud sport 'Autumn Gala' differed initially from its progenitor on 15 June, 35 DAFB and 10,329 GDH (arrow; T-test-p=0.050). Each data point represents the average growth rate of 25 fruits from a total of 5 trees (5 fruits per tree). Vertical bars represent standard error of the averages of each tree replicate.

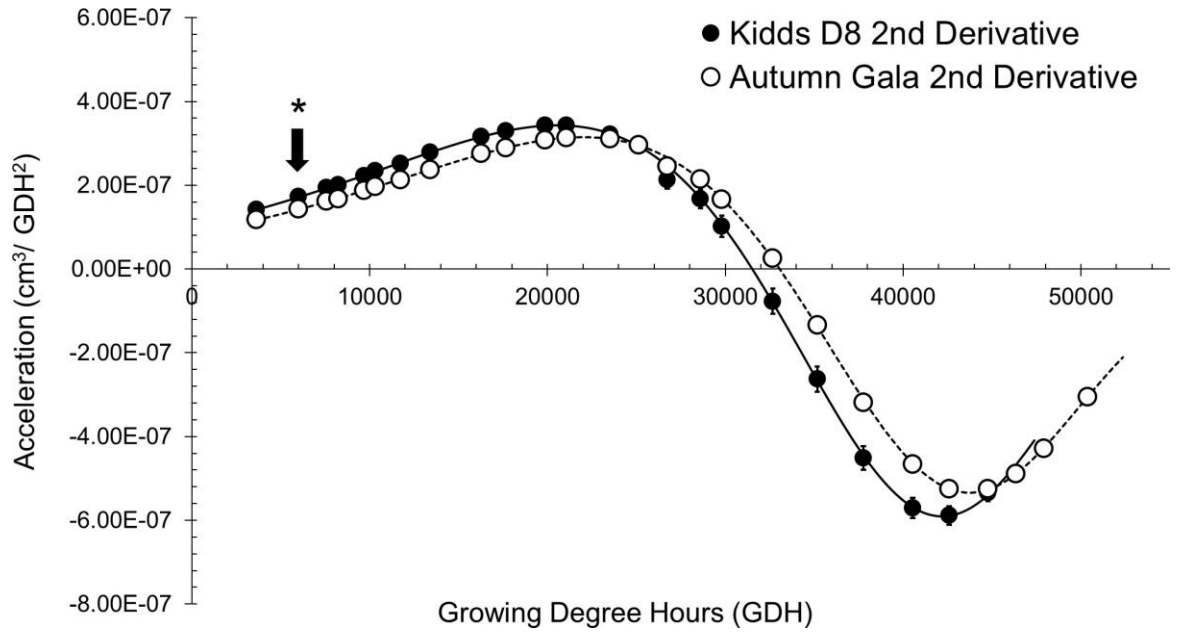

Figure 7: The 2nd derivatives of the data shown in Figure 5. Acceleration of fruit growth was significantly lower in 'Autumn Gala' beginning on 1 June, 21 DAFB and 5,993 GDH (arrow; T-test-p=0.044). Each data point represents the average growth acceleration for 25 fruits from a total of 5 trees (5 fruits per tree) on a date of in-field measurement. Vertical bars represent standard error of the averages of each tree replicate.

In 'Fuji', the early sport 'September Wonder Fuji' had a greater fruit volume than the standard cultivar 'Aztec Fuji' by 8 July, 59 DAFB (Fig. 8). 'September Wonder Fuji' had a higher growth rate than 'Aztec Fuji' by 25 May, 15 DAFB (Fig. 9). 'September Wonder Fuji' had a significantly higher fruit growth acceleration by 25 May, 15 DAFB, compared to 'Aztec Fuji' (Fig. 10). 'September Wonder Fuji' had a higher rate of maximum growth acceleration at ~18,000 GDH, 3 July, than 'Aztec Fuji'. 'September Wonder Fuji' had a faster and earlier deceleration than 'Aztec Fuji', with the maximum rate of deceleration occurring at ~45,000 GDH, 8 September. The maximum rate of deceleration in 'Aztec Fuji' was not as high as 'September Wonder Fuji' and occurred about 10,000 GDH later, on 24 October.

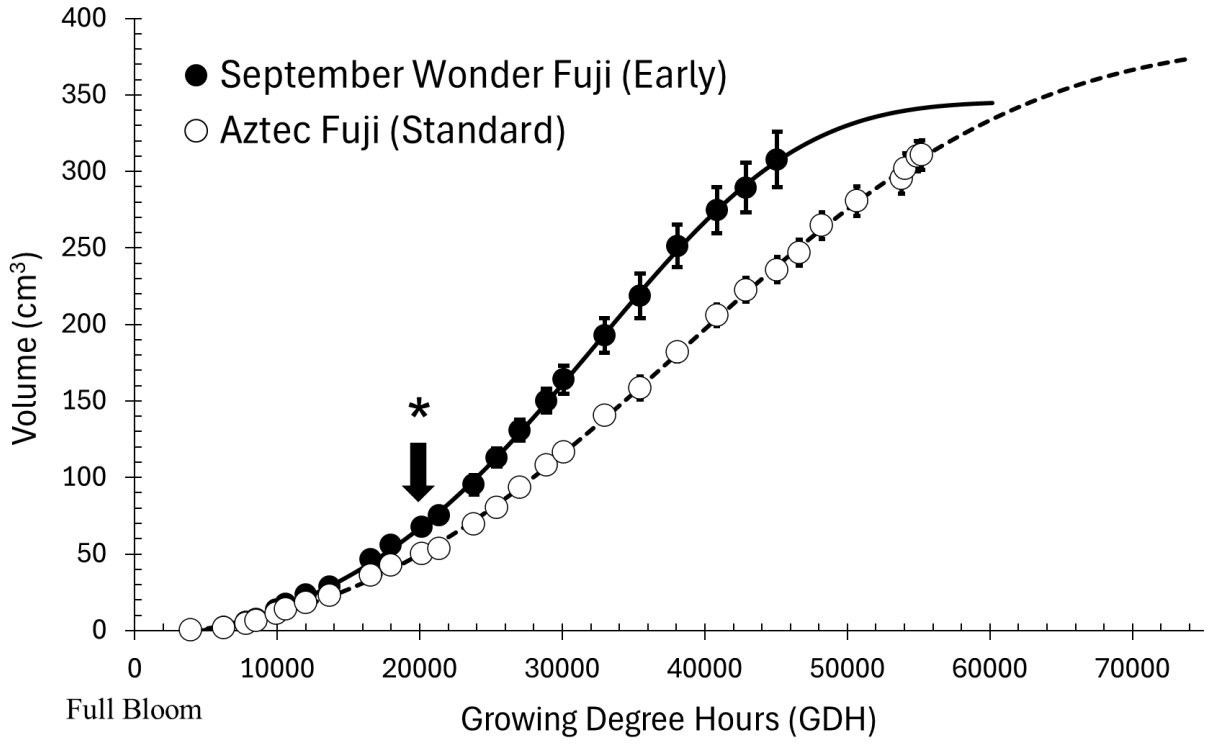

Figure 8: Calculated fruit volume in 'Fuji' cultivars over the entire season based on measures of fruit diameter or circumference and assuming spherical fruit shape. The fruit volume in early bud sport 'September Wonder Fuji' was greater than its standard comparator after 8 July, 59 DAFB and 20,166 GDH (arrow; T-test-p=0.036). Each data point represents the average fruit volume of 25 fruits from a total of 5 trees (5 fruits per tree). Vertical bars represent standard error of the averages of each tree replicate. 'September Wonder Fuji' R^2=0.9997 and 'Aztec Fuji' R^2=0.9996.

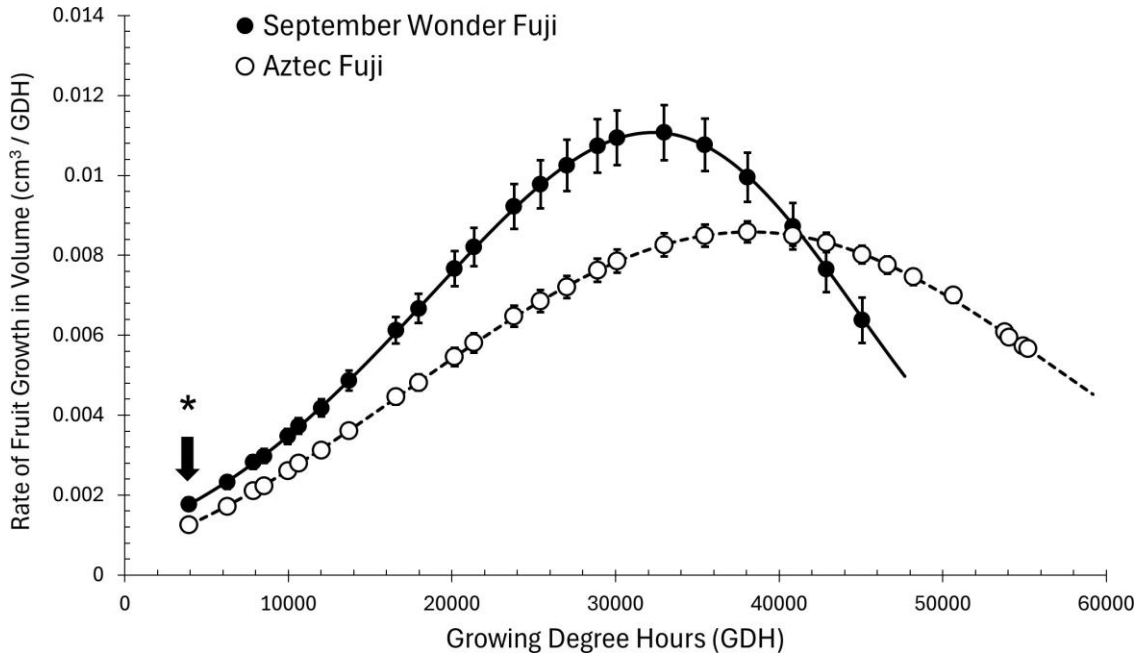

Figure 9: Fruit growth rate in 'Fuji' cultivars over the growing season. The growth rate in early bud sport 'September Wonder Fuji' was higher than its progenitor by 23 May, 13 DAFB and 3,917 GDH (arrow; T-test-p=0.0094). Each data point represents the average growth rate of 25 fruits from a total of 5 trees (5 fruits per tree). Vertical bars represent standard error of the averages of each tree replicate.

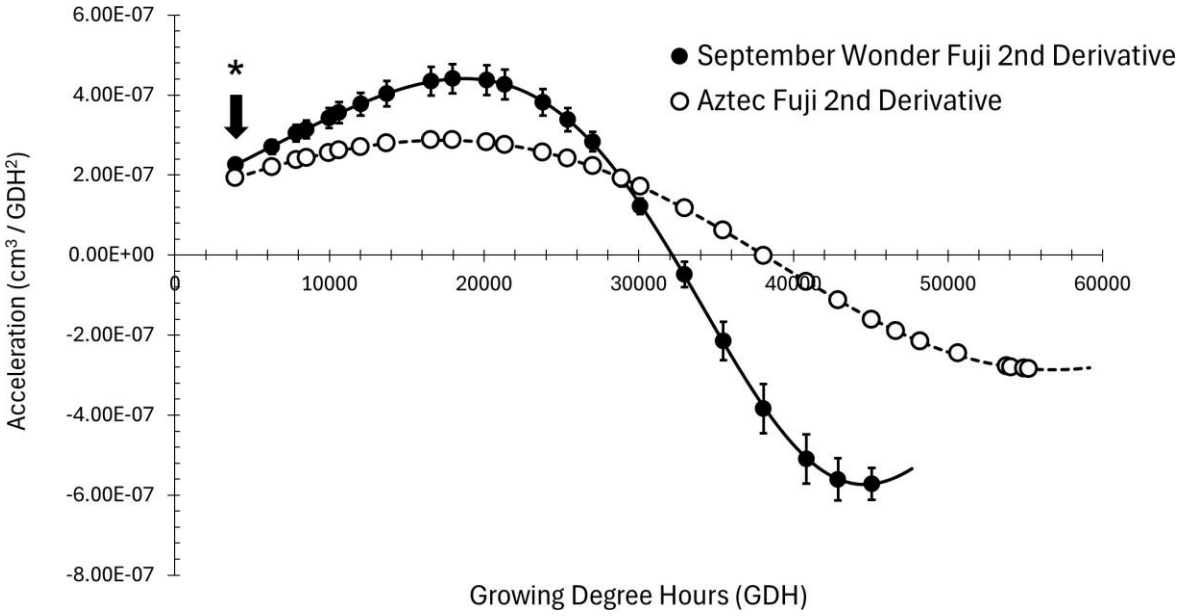

Figure 10: The 2nd derivatives of the data shown in 'Figure 8'. Fruit volume acceleration was initially higher in 'September Wonder Fuji' by 23 May, 13 DAFB and 3,917 GDH (arrow; T-test p=0.041). Each data point represents the average fruit growth acceleration of 25 fruits from a total of 5 trees (5 fruits per tree). Vertical bars represent standard error of the averages of each tree replicate.

In ‘Cripps Pink’, the early harvesting sport ‘Maslin Cripps Pink’ had a greater fruit volume than the standard harvesting cultivar ‘Cripps Pink’ by 29 July, 80 DAFB (Fig. 11). The fruit growth rate of ‘Maslin Cripps Pink’ was significantly higher than ‘Cripps Pink’ by 5 June, 26 DAFB (Fig. 12). Interestingly, the initial growth rate of ‘Cripps Pink’ was higher than ‘Maslin Cripps Pink’, but by 5 June, 26 DAFB, ‘Maslin Cripps Pink’ had already overtaken ‘Cripps Pink’ in growth rate. Acceleration of fruit growth was significantly higher in ‘Maslin Cripps Pink’ by 25 May, 15 DAFB (Fig. 13).

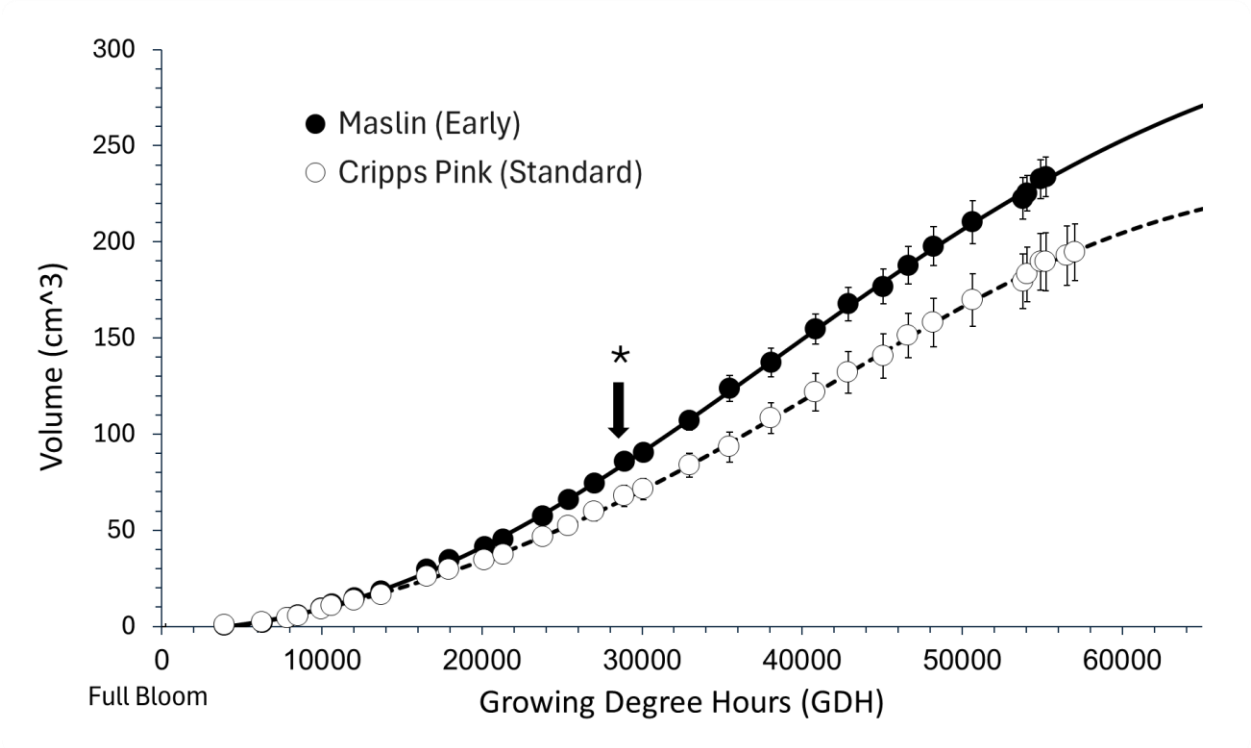

Figure 11: Calculated fruit volume in ‘Pink Lady’ cultivars over the entire season based on measures of fruit diameter or circumference and assuming spherical fruit shape. Significantly higher volume in early bud sport ‘Maslin’ was greater than its progenitor after 29 July, 79 DAFB and 28,897 GDH (arrow; T-test-p=0.031). Each data point represents the average fruit volume of 25 fruits from a total of 5 trees (5 fruits per tree). Vertical bars represent standard error of the averages of each tree replicate. ‘Maslin’ R^2=0.9997 and ‘Cripps Pink R^2=0.9997.

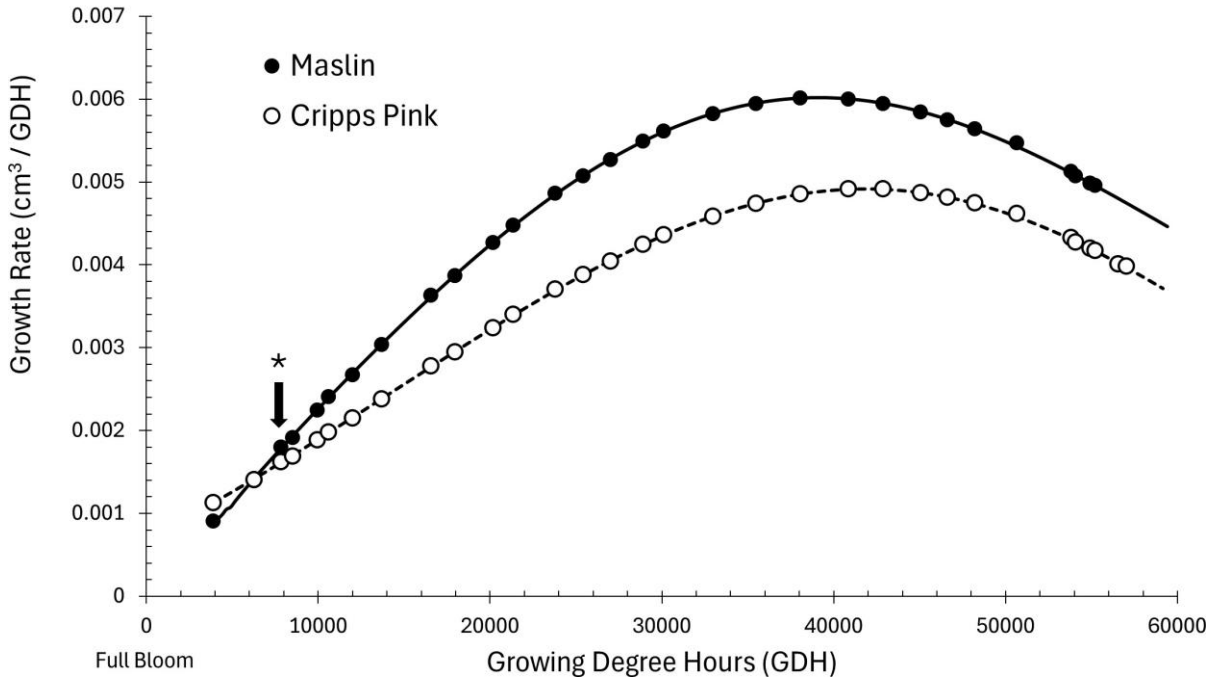

Figure 12: Fruit growth rate in 'Pink Lady' cultivars over the growing season. Significantly higher growth rate in early bud sport 'Maslin' on 5 June, 26 DAFB and 7,848 GDH (arrow; T-test-p=0.0303). Each data point represents the average fruit growth rate of 25 fruits from a total of 5 trees (5 fruits per tree). Vertical bars represent standard error of the averages of each tree replicate.

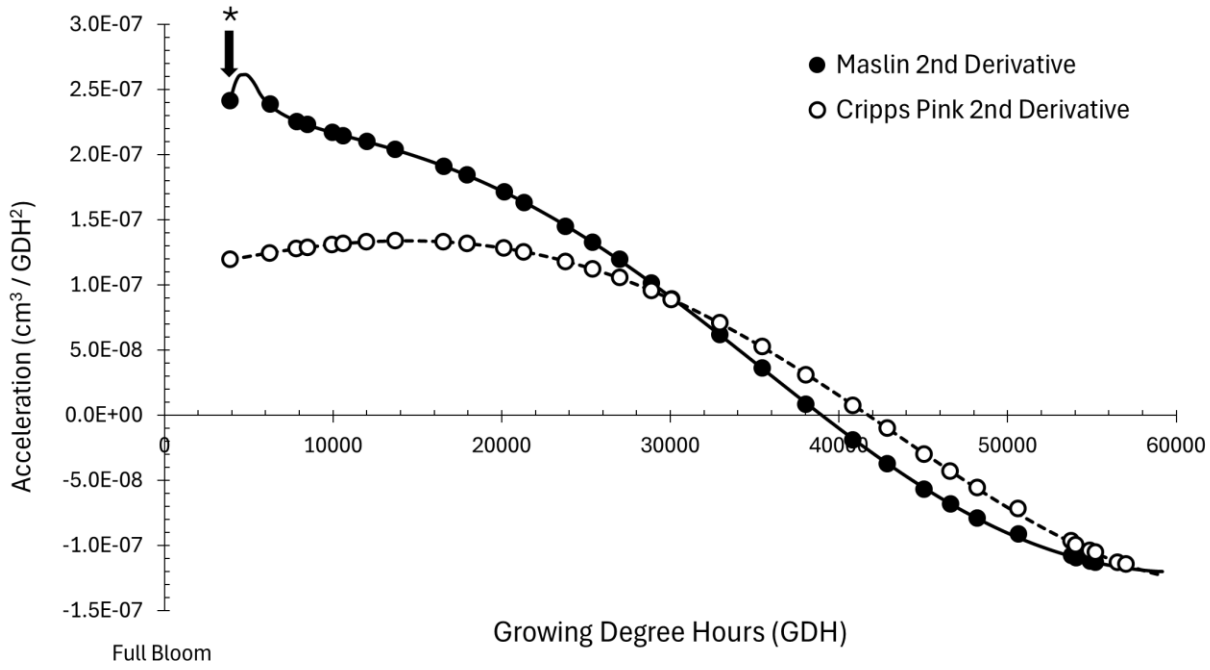

Figure 13: The 2nd derivatives of the data shown in 'Figure 11'. Acceleration of fruit growth significantly higher in 'Maslin' on 23 May, 13 DAFB and 3,917 GDH (arrow; T-test-p=0.0003). Each data point represents the average fruit growth acceleration of 25 fruits from a total of 5 trees (5 fruits per tree). Vertical bars represent standard error of the averages of each tree replicate.

Generally, fruit volume differed between the progenitor and the sport approximately halfway through the growing season. However, when the rate of growth was calculated based on the fitted fruit volume curves, the progenitor and the sport phenotype differed much earlier in development in the exponential phase of the growth curve in each comparison. Differences in fruit growth acceleration was also detected early in each progenitor/sport comparison in the exponential, early phase of volumetric fruit growth. In conclusion, differences in the rate of development can be detected between early and late maturing cultivars at the earliest stages of development and early maturity sports develop at a faster rate than the later maturity sports.

2.3.3. Photosynthesis

Net carbon assimilation for all six cultivars on five days throughout the season was determined by calculating the integral of each diurnal assimilation curve for each leaf measured per cultivar and tree. Generally, the rate of assimilation did not change dramatically between mid-June and mid-August, averaging approximately 0.75 mol m^{-2} d^{-1} for the 'Fuji' strains and 0.6 for the 'Gala' and 'Pink Lady' strains. The ‘Fuji’ and ‘Pink Lady’ cultivars had similar carbon assimilation rates during the growing season until harvest. ‘September Wonder Fuji’, the early sport, matured approximately 27 d before ‘Aztec Fuji’ yet had a lower carbon assimilation rate than ‘Aztec Fuji’ at the developmental preharvest timepoint, 3 days before harvest (Fig. 14). The assimilation rates at harvest declined relative to the mid-season averages due likely to temperature and light decline later in the season (Fig. 15). Significant decreases of CO_2 assimilation after harvest were exhibited by each cultivar except early bud sport ‘September Wonder Fuji’ and standard harvesting ‘Cripps Pink’.

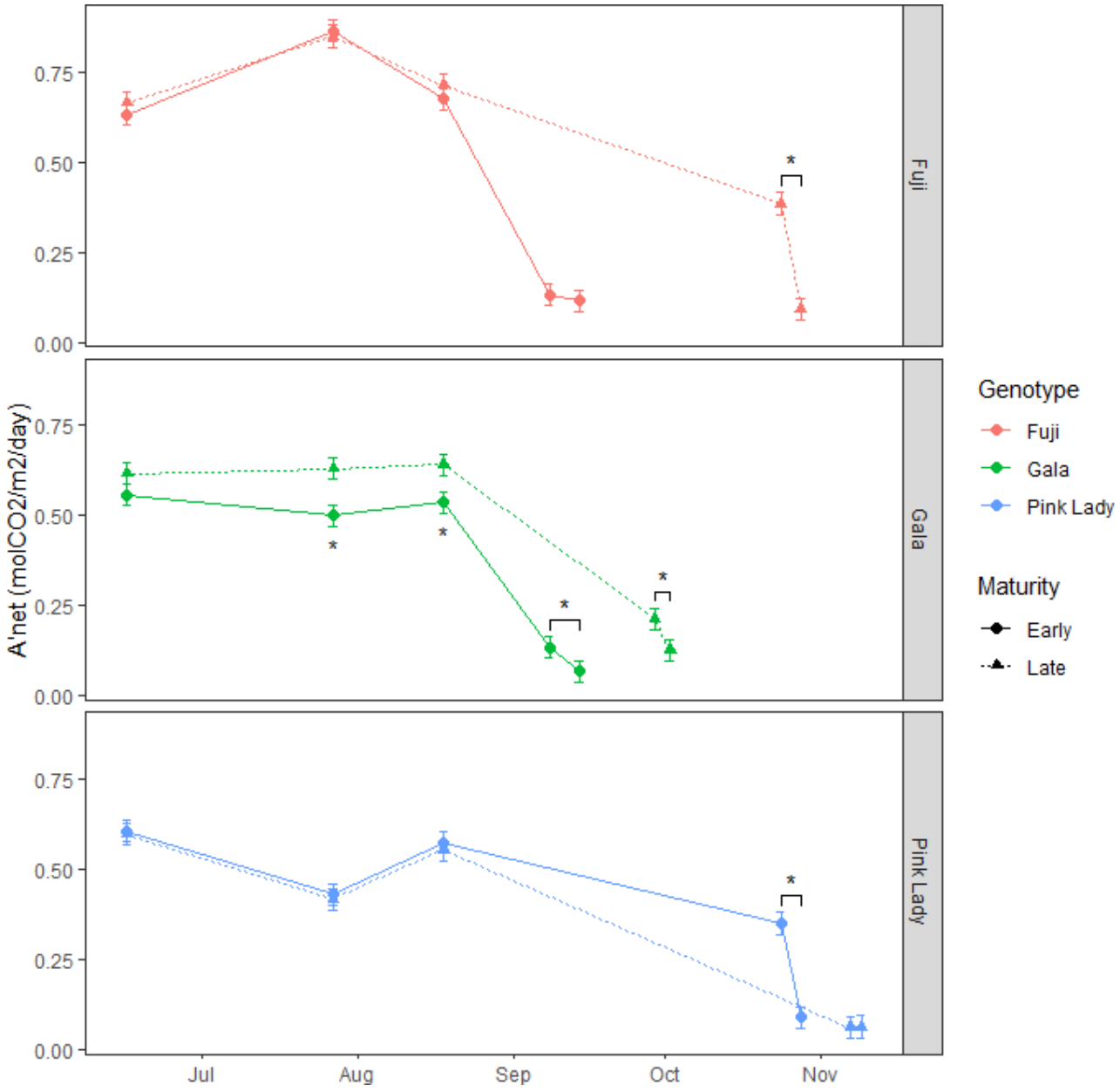

Figure 14: Net carbon assimilation rates for bourse shoot leaves adjacent to apple fruit on 16 June, 27 July, and 18 August and 2 to 5 days pre- and 2 to 5 days post-harvest for the six cultivars evaluated. Total carbon assimilation calculated for each day as the average integral under the curve of each tree containing two subsamples. Pre- and post-harvest measurements were based on the fruit achieving commercial maturity. Each data point represents total carbon assimilated during that day. 2 leaves were measured per tree, 5 trees were measured, and measurements were taken 6 times sequentially throughout the day from dawn until dusk. Vertical bars represent standard deviation. Asterisks indicate significant difference ($p \leq 0.05$).

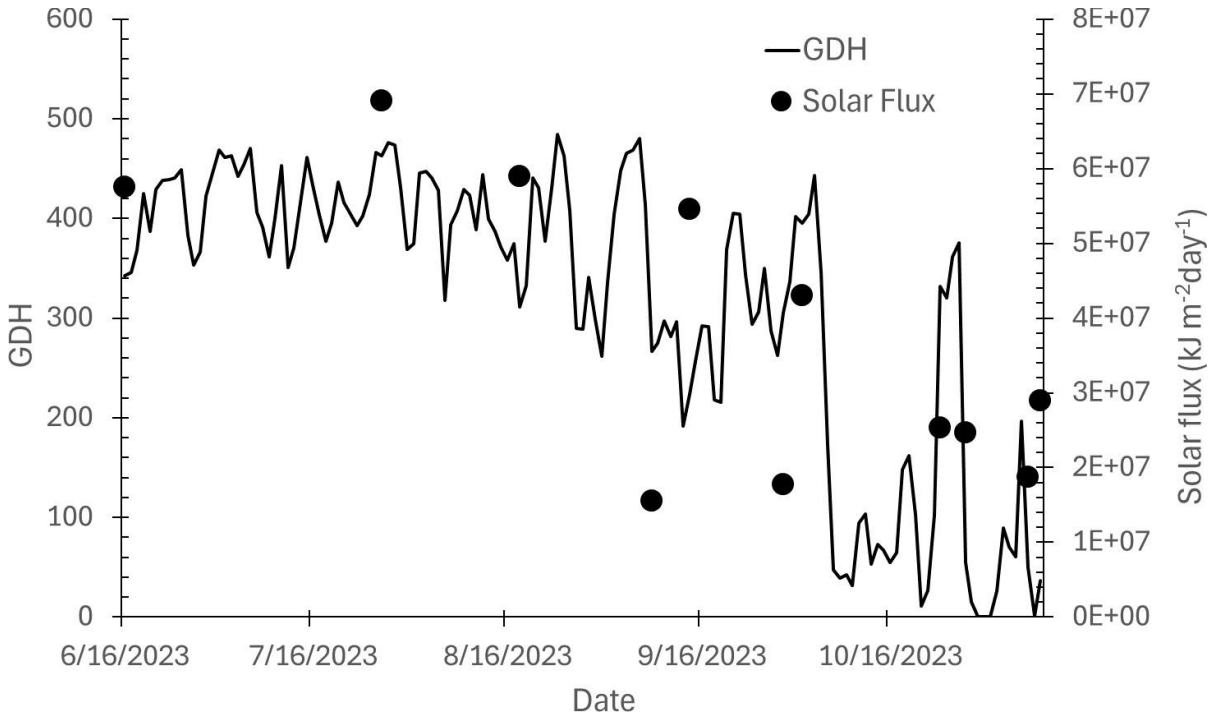

Figure 15: Growing degree hour (GDH) accumulation and solar flux per day according to date from 16 June 2023 through 9 November 2023, spanning all photosynthetic rate assays. Both GDH accumulation and solar flux decrease from 16 June to 9 November. Solar flux was calculated from Clarksville Research Center from 'Langley' units to kJ/m^{-2}s^{-1} for each photosynthetic rate assay date.

2.3.3. Fruit Maturity

There were stark differences in the timing of changes in maturation and ripening indices between different cultivars and between standard/progenitor lines and their respective sport lines. The starch index data inform us that not only is harvest date different, but starch conversion also begins at different dates (Fig. 16). Thus, the delay we see in harvest date is not due to a shortened or prolonged maturation period, but rather due to an advancement or delay in the development of the fruit leading to an advancement or delay in reaching physiological maturity. Data for other indices of maturity and ripening [e.g., weight, internal ethylene content, percent redness, firmness, background color, chlorophyll absorbance, percent sugar (°Brix), and percent malic acid (titratable acid)] (Figs. 17-19) are consistent with the starch conversion data, and further establish the clear difference in time of maturation between the early and late maturing cultivars. Harvest dates were determined by tracking ripening, primarily starch index, approximately 2 weeks before predicted harvest of each cultivar until a few days after each cultivar had an average starch index of 4 (Table 2).

Table 2: Bloom, harvest dates, days from full bloom until harvest (DTH) and growing degree hours (GDH) at harvest. Harvest dates were determined as the date associated with attaining a starch index of 4 according to the Cornell University Starch Index (Blanpied & Silsby, 1992).

Apple Variety	**'Gala'**		**'Fuji'**		**'Pink Lady'**	
Timing	**Standard**	**Late**	**Early**	**Standard**	**Early**	**Standard**
Cultivar	**'Kidd's D-8'**	**'Autumn Gala'**	**'September Wonder'**	**'Aztec Fuji'**	**'Maslin'**	**'Cripps Pink'**
Full Bloom Date	May 11	May 11	May 10	May 10	May 10	May 10
Harvest Date	Sep. 6	Sep. 30	Sep. 6	October 4	October 27	Nov. 5
DTH	118	142	119	147	170	179
GDH	44,002	51,221	44,293	53,120	56,301	56,753

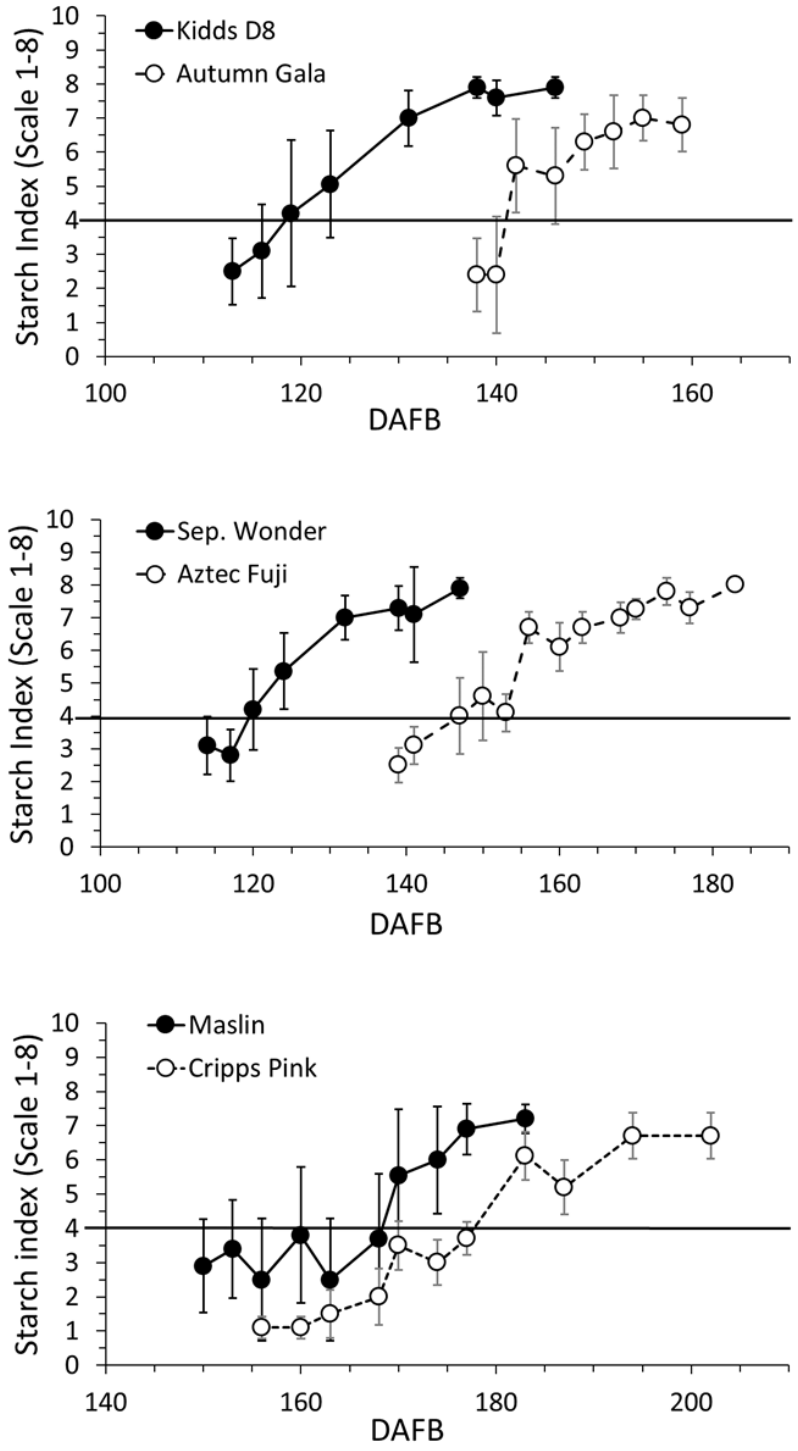

Figure 16: Starch index analysis of all six cultivars. Commercial harvest date for each cultivar was determined by a starch index of 4 according to the Cornell University Starch Index (Blanpied & Silsby, 1992).

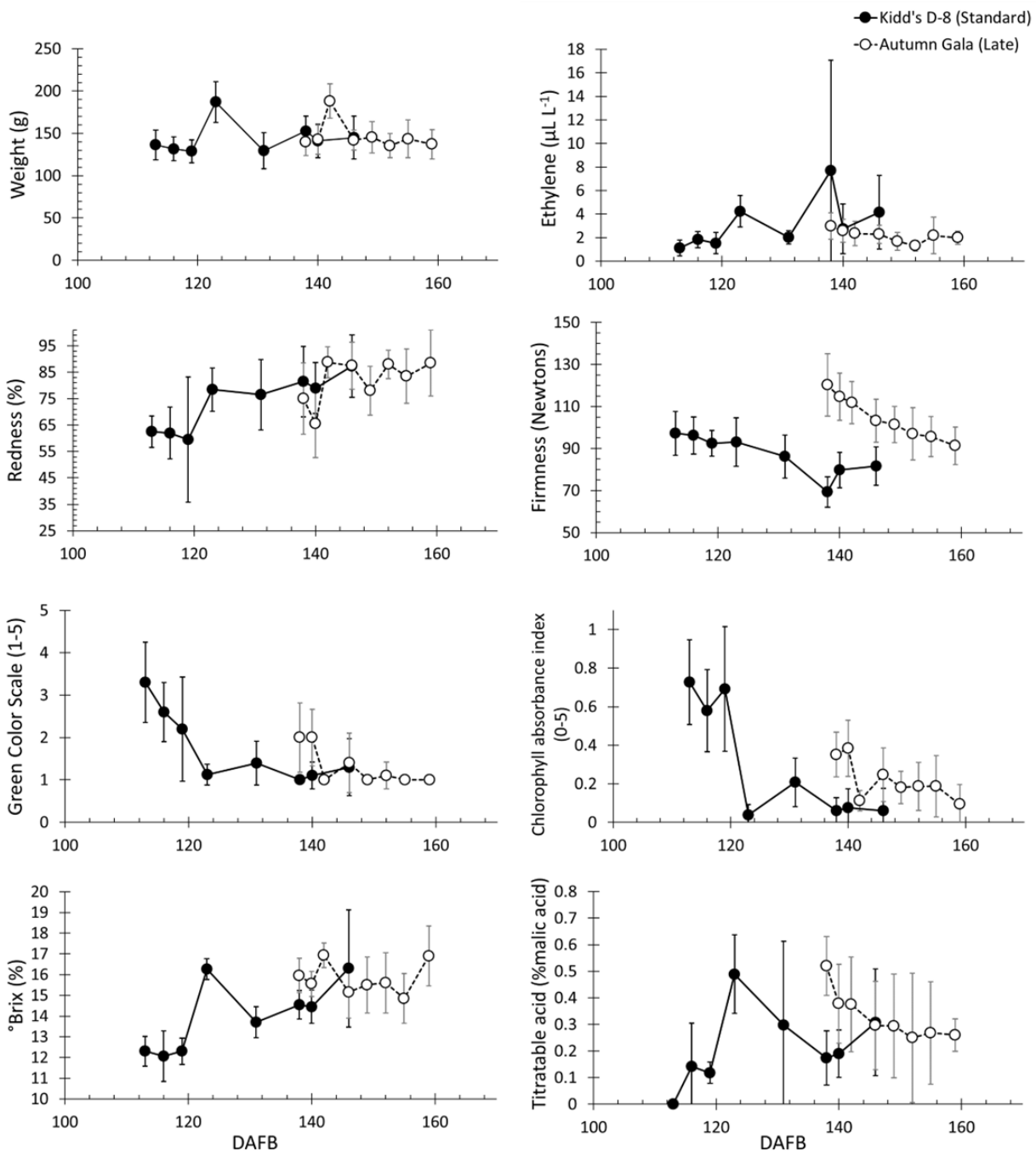

Figure 17: Maturity indices for 'Kidd's D-8' and 'Autumn Gala' fruit from two weeks prior to two weeks after harvest date. Harvest date was 6 September (118 DAFB) for 'Kidd's D-8' and 30 September (142 DAFB) for 'Autumn Gala' based on starch index. Each data point represents an average of 10 fruits randomly selected from 5 similar trees. Vertical lines represent standard deviation.

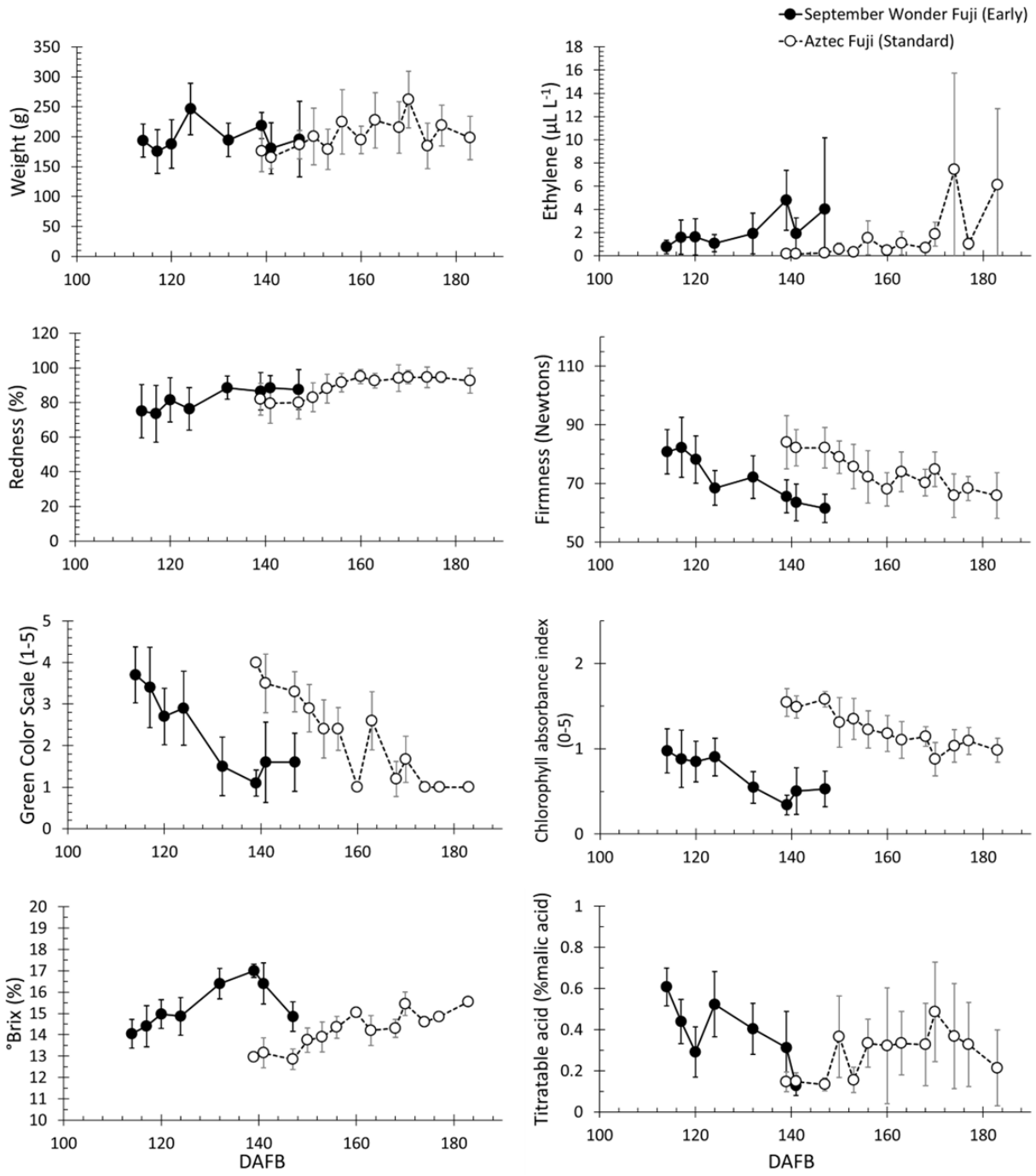

Figure 18: Maturity indices for 'September Wonder Fuji' and 'Aztec Fuji' fruit from two weeks prior to two weeks after harvest date. Harvest date was 6 September (119 DAFB) for 'September Wonder Fuji' and 4 October (147 DAFB) for 'Aztec Fuji'. Each data point represents an average of 10 fruits randomly selected from 5 similar trees. Vertical lines represent standard deviation.

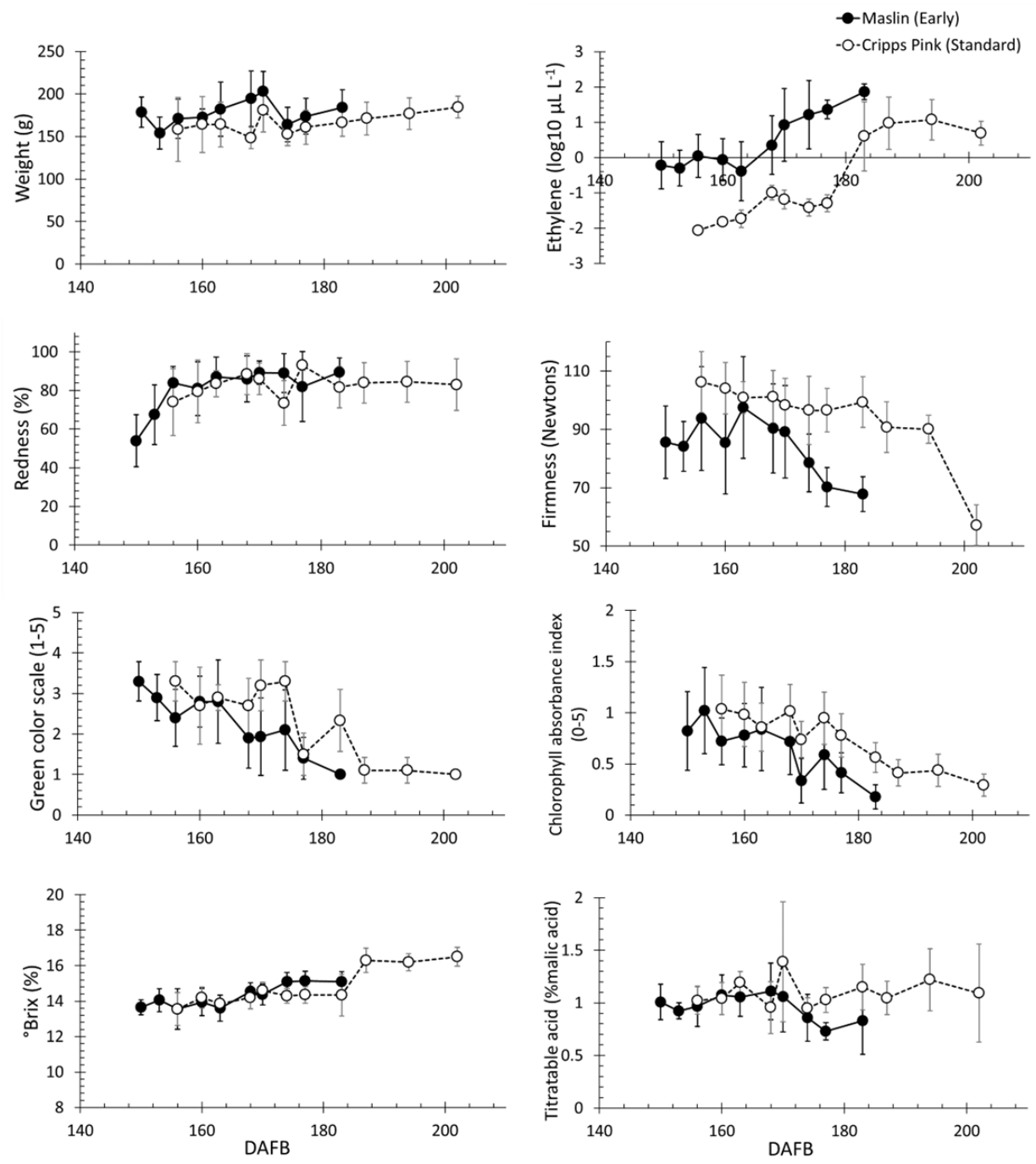

Figure 19: Maturity indices for 'Maslin' and 'Cripps Pink' fruit from two weeks prior to two weeks after harvest date. Harvest date was 27 October (170 DAFB) for 'Maslin' and 5 November (179 DAFB) for 'Cripps Pink'. Each data point represents an average of 10 fruits randomly selected from 5 similar trees. Vertical lines represent standard deviation.

2.4. DISCUSSION

2.4.1. Value of Germplasm Background

The main objective of this study was to identify and characterize differences in fruit development in apple bud sport cultivars that harvest at different dates than the standard or progenitor line. An important variable to consider is that two of the three comparisons were to the bud sport's progenitors. In the case of 'Gala', the comparison is direct, in that the tissue grafted and used in this study was taken directly from the parent tree and its mutant limb that gave rise to the 'Autumn Gala' and differs in this regard from the study done by Ban et al. (2022). The reason that this is relevant is that fruit trees are known to accumulate somatic mutations at a relatively high rate (Sun et al., 2023). Thus, there is the risk that additional genetic alterations may have accumulated in lines that have undergone multiple cloning cycles. In 'Pink Lady', although our comparison is not direct, meaning we don't have the original germplasm of the mutation, the standard harvesting 'Cripps Pink' is still the progenitor of bud sport 'Maslin' and thus a valuable comparison. These direct comparisons are valuable because it is possible that there was very likely only a single mutation responsible for the delay or advancement of maturity in the bud sports. This is not to say that only a single gene is responsible. In the case of deletion events, large portions of chromosomes may be lost or disrupted. Thus, characterizing fruit development differing by strictly one mutation or genetic event may be valuable in further understanding apple fruit development and maturity determination.

2.4.2. Earlier Harvesting Apple Cultivars Exhibit Compressed Developmental Periods

The higher fruit growth rates of earlier harvesting lines relative to the later lines during the exponential phase of volumetric fruit growth suggest genetic differences in the early and late lines is the result if shifts in physiology apparent immediately after flowering and are therefore

likely not related to maturation rate, *per se*. This may result from faster cell division rates, altered hormonal regulation, shifts in the duration of the cell division phase, or a combination of these processes. The data suggest that maturation and ripening rates were similar between early and late cultivars for each of the three varietal lines. The difference between the early and late cultivars regarding maturity was the timing of the onset of maturation and ripening, not the rate of either process. If the early and late cultivars of each comparison had similar dates of full maturation with a difference in ripening rate, the difference in maturity would thus be primarily attributed to a difference in ripening rate and not a compressed development. Since we see a significantly higher rate of fruit growth in all the earlier harvesting cultivars and simultaneously observe earlier harvest dates with no difference in ripening rates, we suggest that the physiological events leading to earlier harvesting cultivars is not due to differences in the physiology associated with ripening, but likely have a compressed developmental period before full maturity. Thus, genetic changes that have occurred in the early and late sports should be a result of gene expression shifts detectable in the early stages of fruit development.

So, while bloom date may not differ (Table 2), future genetic expression analyses should target early stages for signs of differentially expressed genes important in the developmental process causing early/late maturation.

2.4.3. Increase or Decrease in Net Carbon Assimilation Not Responsible for Faster Development in Earlier Harvesting Cultivars

Since the rate of carbon assimilation by bourse leaves was not uniformly higher for the earlier cultivars, data suggest that earlier harvest is likely not driven by a higher carbon assimilation rate during the early and mid-growing season fruit growth. In the ‘Gala’ comparison for example, we would expect that the earlier harvesting cultivar ‘Kidd’s D-8’ would assimilate more carbon

earlier in the season. On the contrary, ‘Kidd’s D-8’ assimilates significantly less carbon. The preharvest carbon assimilation of the early cultivars ‘Kidd’s D-8’ and ‘September Wonder Fuji’ are both lower than the carbon assimilation of their later harvesting progenitor/standard harvest time cultivar. An observation worth mentioning, not relevant to bud sport origin or characterization but rather differences among apple varieties, is that ‘Fuji’ achieved a higher rate of carbon assimilation thank ‘Gala’ or ‘Cripps Pink’ during the growing season, especially on July 27. The final fruit size of both ‘Fuji’ cultivars was also found to be significantly higher than the ‘Gala’ or ‘Pink Lady’ cultivars. A more complete study providing a comprehensive analysis for the full canopy should provide needed details to understand how shifts in the crop's earliness or lateness alter carbon assimilation, flux, and emission.

2.4.4. Relevance of the Study

There has never been comprehensive work done on apple growth rate analysis between apple sports within the same commercial variety, let alone for the purpose of uncovering mechanisms underlying mutated maturity phenotype. Many molecular studies in horticulture lack a robust physiological element in the study. In a recently published paper on a study similar to ours, Ban et al. (2022) found a candidate gene (*MdACT7*) they proposed may cause late maturation in ‘Autumn Gala’ compared to ‘Kidd’s D-8’. They measured apple fruits throughout the season but never mentioned crop load requirements of the trees or did any further analysis of fruit growth rate/acceleration of fruit growth. Dong et al. (2011) evaluated early ripening events in ‘Beni Shogun’ (‘Fuji’) and heavily characterized the earlier ethylene burst in ‘Beni Shogun’ and looked at other ripening characteristics such as volatile production, skin coloration, fruit softening, and starch hydrolysis. In this study, only ripening was extensively evaluated; no preharvest physiological assays were performed. Kim et al. (2023) also evaluated ripening

behavior in early cultivar ‘Beni Shogun’ compared to ‘Fuji’ (Kim et al., 2023). Again, season-long developmental analyses were not performed. Studies focusing on ripening behavior is not surprising, as the phenotype only portrays itself late in development. In analyzing our data, signs of phenotypic differences present themselves very early in apple fruit development. Genomic and transcriptomic analyses are even more powerful when coupled with comprehensive characterization of physiological analyses such as rate of fruit development, rate of carbon assimilation, and ripening behavior. These analyses provide a faster approach to transcriptomic studies due to the narrow window we identified in early development when these cultivars diverged in developmental rate rather than continue to evaluate ripening behavior and gene expression during ripening. Further, given the lack of a consistent relationship between photosynthetic carbon assimilation and earliness or lateness of the cultivar comparisons, the search for the genetic underpinnings controlling maturity timing appear to be less likely to involve genes directly involved in assimilation. We characterized each of the six cultivars, 3 variety pair-comparisons, from bloom until postharvest ripening, and this characterization may lead us and others to a much clearer understanding of the likely complex genetic control of harvest date in apple and maturity bud sport origin.

CHAPTER 3. Genetic underpinnings of early and late maturing apple bud sports

3.1. INTRODUCTION

Apple bud sports are spontaneous mutations in meristematic tissue such that a stable somatic mutation develops through a whole limb, flower, and/or fruit (Foster & Aranzana, 2018). This phenomenon leads to a natural process that humans may take advantage of to produce higher quality fruit. Bud sports that are commercialized into widespread cultivation often contain all desirable attributes of the parent tree, with one, sometimes more, additional quality attributes that justify the high cost of orchard establishment for the genetically novel material. Common bud sport characteristics include change in fruit size, shape, color, spur-bearing behavior, and advanced or delayed harvest.

Harvest date variation is an important concept to the apple industry. Spreading out the harvest window and diversifying apple varieties in the orchard contributes to a growers' productivity. In the case of altered harvest date apple bud sports, hereafter referred to as 'maturity sports', apple fruits may reach their optimal harvest date at an earlier or later date than their progenitor.

Growers often take advantage of early bud sports due to their earlier presence in the market. Later bud sports may be advantageous due to higher fruit firmness and thus storability since higher storability and harvest date are thought to be heavily correlated (Ban et al., 2022; Migicovsky et al., 2016). Later cultivars may also be used to prolong the growing season for higher apple consumption availability later in the season. Although these valuable maturity sports are frequently utilized in the apple industry, the physiological and genetic mechanism behind the phenotype of early or delayed maturation date in maturity sports is currently unknown. Importantly, a proposed genetic link to late fruit maturation in 'Gala' has been

proposed (Ban et al., 2022), but conclusive data on the mechanism of this exciting finding are still lacking.

Molecular studies of bud sports have varied in their approach from observing thousands of genes and several gene groups separated by function, to finding one causal candidate gene responsible for the phenotype of early or late maturity. For example, in apple, Ban et al. (2022) compared the standard harvesting 'Kidd's D-8 Gala' with its late maturing bud sport 'Autumn Gala' (Table 1). They suggested that a dysfunctional ACT7 gene (Mdact7) may be responsible for the alteration in phenotype of the later cultivar. They explored the function of Mdact7 in arabidopsis (*Arabidopsis thaliana*). In arabidopsis, an actin-7-like encoding gene ortholog is responsible for critical roles in plant development due to its effect on plant height and general stunting of the plant. Actin is a crucial protein in plant cells that exists in the form of actin filaments within the cytoskeleton of the cell and participates in multiple essential cellular processes such as cell expansion, cell division, and intracellular transport (Thomas et al., 2009). This *ACT7* gene is the only actin ortholog in Arabidopsis that responds to exogenous hormones and external stimuli such as auxin and light regime and wounding, respectively (McDowell et al., 1996). Transgenic lines that contained the mutated allele *Mdact7 found* in 'Autumn Gala' exhibited stunted growth in arabidopsis. Maturity sports have also been found and studied in other horticultural crops such as citrus (*Citrus sinensis*), pear, (*Pyrus bretschneideri* Rehd.), and grape (*Vitis vinifera* L.). For example, in grape, Wei et al. (2020) found several differentially expressed candidate genes (Table 3) associated with hormone signaling and biosynthesis which may contribute to an early maturation phenotype. Liu et al. (2014) performed a proteomic analysis on the early maturing pear bud sport 'Zaosu' with and found proteins related to cell-wall modification, oxidative stress,

pentose phosphate metabolism, photosynthesis, glycolysis, and vital cellular processes were higher in abundance (Table 3).

The search for mechanisms resulting in altered phenotypes in crops has narrowed from genetic regions to specific genes containing larger structural variants, small insertions, deletions, and single nucleotide polymorphisms (SNPs). Likewise, investigating the underlying mechanisms of bud sports differing in harvest date has, over time, become more refined, resulting in more specific findings (e.g., the identification of single candidate gene candidates that have been proposed or shown to contribute to maturity phenotypes as opposed to lists of genes and proteins that differ in expression). Regarding developmental time required for maturation, breeding efforts may soon be able to focus on generating cultivars for specific growing regions, which require shorter or longer growing seasons, using marker assisted selection. Our physiological work helps narrow marker assisted selection to early on in fruit development by reducing the type of genes to genes heavily involved in fruit development early in the season which will lead to a much clearer understanding of the complex genetic control of harvest date in apple and apple maturity bud sport origin.

Table 3: Summary of studies aimed at identifying causative mutations and molecular mechanisms for maturity sport phenotypes.

Crop	**Sport Cultivar(s)**	**Parent**	**Publication**	**Sport Phenotype**	**Candidate genes**	**Functions of Candidate Genes**
Apple (*Malus domestica*)	'Autumn Gala'	'Kidd's D-8'	Ban et al. 2022	4-week maturation delay	*MdACT7*	Actin homolog involved in cytoskeleton, cell expansion and division, cellular transport
Apple (*Malus domestica*)	'Hirosaki Fuji'	'Fuji'	Wang et al. 2009	40-day earlier maturation	*MdACS1* *MdACO1* *MdETR1* *MdERS1* *MdERS2* *MdPG1* *MdHSP17.5*	Ethylene biosynthesis Ethylene receptor proteins Cell wall degradation Heat shock protein
Apple (*Malus domestica*)	'Beni Shogun'	'Yataka' (early sport of 'Fuji')	Kim and Ban et al. 2023	3-week earlier maturation than Fuji	*MdACO1* *MdARF1* *MdIAA11* *MdNAC3* *MdNAC5* *MdMADS7* *MdMADS8*	Ethylene biosynthesis Auxin regulation Fruit development and ripening transcription factors
Pear *(Pyrus bretschneideri* Rehd.)	*Unnamed early maturing bud sport	'Zaosu'	Liu et al. 2014	Earlier maturation	Several genes (proteomic analysis)	Cell-wall modification Oxidative stress Pentose phosphate metabolism Photosynthesis Glycolysis
Navel Orange *(Citrus sinensis)*	'Fengjiewan-cheng'	'Fengjie 72-1'	Liu et al. 2007	1 month maturation delay	*CitSS1* *CITAI* *CitCS* *CitAC*	Sucrose synthase Acid invertase Mitochondrial citrate synthase Cytosolic aconitase
Table Grape *(Vitis vinifera L.)*	'Tiangong Moyu'	'Summer Black'	Wei et al. 2020	10-day earlier maturation	~45 DEGs	Hormone signaling/biosynthesis Phenolic biosynthesis Flavonoid biosynthesis Anthocyanin biosynthesis Calcium response Plant-pathogen response Sugar accumulation Cell wall (GRIP)

3.2. MATERIALS AND METHODS

3.2.1. Plant Material

The apple trees used for this research were located within a 1.2-acre trellised high-density planting at the Michigan State University Clarksville Research Center (Clarksville, MI 42°52’27.3”N 85°16’15.0”W). For each cultivar, three randomized blocks of 8 trees were planted, with tree spacings of 0.9 meters (3-feet) apart within rows, and 3.7 meters (12-feet) between rows. Budwood for the two ‘Fuji’ and two ‘Pink Lady’ cultivars was provided by Schwallier’s Country Basket (Sparta, Michigan). Budwood for the ‘Gala’ varieties was taken from the original ‘Autumn Gala’ sport branch and branches from progenitor ‘Kidd’s D-8’ tree at Catoctin Mtn Orchards (Thurmont, MD). ‘Fuji’ and ‘Cripps Pink’ budwood was bench grafted onto bareroot Bud-9 rootstock trees in 2019 and planted in the field on 13 May 2019. The ‘Gala’ trees were side-grafted onto two-year old Bud-9 rootstock on 27 April 2021.

3.2.2. Tissue Collections for DNA Sequencing and Future RNA Sequencing

Leaf tissue of each cultivar was collected, flash frozen in liquid nitrogen in the field, and transported on dry ice before being stored in a -80 °C freezer. DNA was extracted from 3-5 leaves per tree for each cultivar. ‘Gala’ tissue collection was of newly emerging leaves from early summer growth on 26 May of 2022. ‘Fuji’ and ‘Pink Lady’ tissues were collected on 24 October of 2022 when there was no actively growing leaf tissue. Leaf tissue for the later cultivars was more aged and more difficult to extract DNA from. Four random trees of each cultivar similar in architecture and tree trunk cross-sectional area were selected randomly throughout the plot for transcriptomic analysis. For each apple variety, at least 10 timepoints were selected to capture important milestones in the developmental periods that included cell division, peak rate of change of fruit growth, peak fruit growth rate, lowest rate of change of fruit

growth, full fruit maturity, and ripening (Fig. 20). Fruit from all cultivars were collected on 23 May, 6, 13, 20 June, 3, 11, 18, 25 July, 1 August, 13 September. Additional collections were made for 'Autumn Gala' on 26 September, 'Aztec Fuji', 'Maslin', and 'Cripps Pink' on 13 and 31 October, and 'Cripps Pink' on 15 November. Of the 4 selected trees per genotype, 3 representative fruit were cut into pieces and put into tubes, then flash-frozen in liquid nitrogen. They were then transported on dry ice to the laboratory and stored in a -80 ℃ freezer until extraction. The first six fruit tissue collections were done slicing the whole fruit into similar sized cubes that would fit into a 50-mL tube. For the 5 later timepoints, tissue was separated between 4 different tissues: peel, cortex, core, and seed. This differentiated tissue was collected with the same methodology as the first 6 timepoints. Extraction of these first 6 timepoints was not complete at the time of assembly of this dissertation.

3.2.3. DNA Sequencing

DNA was extracted from leaf tissue using the Qiagen DNEasy plant mini kit (QIAGEN, Germantown, Maryland). Each sample concentration was ≥ 5 ng μL^{-1}. Illumina Next Generation library preparation and sequencing was performed by the RTSF Genomics Core at Michigan State University (project ID ENG13345). Libraries were prepared using the Roche Kapa HyperPrep DNA Library Kit with Unique Dual Index adapters following manufacturers' recommendations. Completed libraries were quality checked and quantified using a combination of Qubit dsDNA HS and Agilent 4200 TapeStation HS DNA1000 assays. The libraries were pooled in equimolar quantities and this pool quantified using the Invitrogen Collibri Quantification qPCR kit. This pool was loaded onto one lane of an Illumina v1.5 SP flow cell using the Xp Workflow. Sequencing was performed in a '2x150 bp paired end format' using a NovaSeq 6000 v1.5 300 cycle reagent cartridge. Base calling was done by Illumina Real Time

Analysis (RTA) v3.4.4 and output of RTA was demultiplexed and converted to FastQ format with Illumina Bcl2fastq v2.20.0.

3.2.4. Variant Filtering

Sequenced genomes of ‘Kidd’s D-8’, ‘Autumn Gala’, ‘September Wonder Fuji’, ‘Aztec Fuji’, ‘Maslin’, and ‘Cripps Pink’ were mapped to the ‘Gala’ haploid genome (Sun et al., 2020). The ‘Gala’ haploid genome was used primarily for ‘Gala’ due to higher accuracy of calls according to a closer related cultivar compared to other published genomes such as ‘Golden Delicious’ and ‘Honeycrisp’ (Daccord et al., 2017; Khan et al., 2022). After mapping, reads were analyzed for variants. For SNP calling, tools ‘deepvariant’ and ‘freebayes’ were used. For a variant to qualify, it needed to be called in both tools. In structural variant calling, program tools ‘TIDDIT’ and ‘manta’ were used. To narrow candidate variants with higher probability of having deleterious effects, structural variants needed to be at least 30 bp long, called by both tools, and coverage less than 3-4x higher than chromosome average coverage (depending on which tool). Although this filtering process eliminated smaller variants (<30 bp), it should be emphasized that small variants may also cause deleterious effects within the genome. The files for the large (structural variants) and SNP variants were established as follows (using the ‘Gala’ comparison as an example): (1) Same variants in both ‘Kidd’s D-8’ and ‘Autumn Gala’ but different genotype, meaning that where ‘Kidd’s D-8’ was heterozygous for a particular variant, ‘Autumn Gala’ was homozygous. The homozygous variant in ‘Autumn Gala’ refers to, as an example, a deletion occurring in a specific intragenic region on one chromosome of 'Kidd's D-8' and the same deletion occurring on both chromosomes of ‘Autumn Gala’. (2) A unique variant specific to a single cultivar (e.g. structural variant or SNP in ‘Autumn Gala’) that differed from both the

reference genome as well as the early or late cultivar to which the source is being compared. Variants in intragenic regions were selected for further evaluation.

3.3 RESULTS

3.3.1. Genetic Variant Identification

Genomic DNA sequencing reads for all six cultivars were aligned to the annotated 'Gala' haploid genome (Sun et al., 2020). Coverage of haploid genomic data was relatively sufficient for confident analyses, considering 25x as optimal coverage (Table 4). At the time of the analysis annotated genomes for 'Fuji' or 'Pink Lady' cultivars were unavailable.

Table 4: Coverage of each cultivar according to the 'Gala' haploid reference genome (X. Sun et al., 2020).

	Kidd's D-8	**Autumn Gala**	**September Wonder Fuji**	**Aztec Fuji**	**Maslin**	**Cripps Pink**
Haploid	27x	25x	19x	19x	23x	22x

Following alignments, structural variants (e.g., Insertions/Deletions) and SNPs between cultivars and the annotated genomes were identified. Variant calls were then compared between each maturity sport and the corresponding standard maturing cultivar of the same variety. The calls for variants in the tables were called heterozygous and homozygous for standard harvesting cultivars and bud sports, respectively. This means that when a variant was shared between both cultivars in the comparison, the bud sport lost the copy or function of the gene where the variant was called. In the tables containing unique variants, variants were filtered upon two important factors: (1) they were called within an intragenic region which would likely disrupt the coding regions (e.g. missense, frameshift, gain or loss of start or stop codon) and (2) called homozygous by both software programs that we used ('manta' and 'tiddit'). This means that all unique

variants had no alternative allele to call upon for a specific gene where the variant was located. This later filtering method should reveal the most likely candidates for change in maturation.

3.3.2. DNA Variants in 'Kidd's D-8' and 'Autumn Gala' from Haploid Genome Alignments

Variant calling for the 'Gala' cultivars using the haploid mapping identified 15 SNPS and four SVs as potential causative mutations based on our selection criteria (Tables 5, 6, 7, 8, 9, 10). Surprisingly, 11 of the SNPs were in genes in a 2.57 Mb region on chromosome 6 between bases 21,828,353 and 24,402,010 and were all heterozygous in 'Kidd's D-8' and homozygous in 'Autumn Gala', indicating a loss of heterozygosity in the late sport (Table 5). This region also contained two structural variants that were heterozygous in 'Kidd's D-8' and homozygous in 'Autumn Gala' (located in *Mdg_06g010800* starting at base 21,907,728 and *Mdg_06g011660* starting at base 23,072,809) (Table 6). A deletion unique to 'Autumn Gala' was identified in this region as well (starting at base 22,686,399 in *Mdg_06g011460*). These variants span a region of chromosome 6 that maps to the location of the previously reported 2.8 MB deletion (between 24.913 to 27.743 Mb) and the gypsy retrotransposon 10.7 KB insertion associated with the 'Autumn Gala' phenotype (Ban et al., 2022). However, no variant was called for the ortholog of *ACT7* in our variant analysis. Additionally, we found other orthologs of *ACT7* within other regions of the 'Gala' genome (Chr. 14 and 15).

Table 5. SNPs located within genes mapped to the 'Gala' haploid reference genome where, when called heterozygous for 'Kidd's D-8', 'Autumn Gala' SNPs were called homozygous.

Chromosome	Gene	Variant Type	Kidd's D-8 Genotype	Autumn Gala Genotype	Variant location	Gene ortholog	Gene Description
6	Mdg_06g010730	Stop codon gained	Heterozygous	Homozygous	21828353	N/A	Uncharacterized protein
6	Mdg_06g010970	Stop codon gained	Heterozygous	Homozygous	22031482	AT1G64550	ABC transporter F family member 3-like
6	Mdg_06g011060	Splice acceptor variant and intron variant	Heterozygous	Homozygous	22148302	N/A	Uncharacterized protein
6	Mdg_06g011240	Splice donor variant and intron variant	Heterozygous	Homozygous	22382244	AT4G10770	oligopeptide transporter 7
6	Mdg_06g011320	Frameshift variant and synonymous variant	Heterozygous	Homozygous	22436720	AT5G51030	NAD(P)-binding Rossmann-fold superfamily protein
6	Mdg_06g011580	Stop lost and splice region variant	Heterozygous	Homozygous	22958724	AT1G52150	Homeobox-leucine zipper family protein / lipid-binding START domain-containing protein
6	Mdg_06g011670	Frameshift variant	Heterozygous	Homozygous	23079581	N/A	Uncharacterized protein
6	Mdg_06g011710	Frameshift variant	Heterozygous	Homozygous	23140914	AT5G20885	RING/U-box superfamily protein
6	Mdg_06g011710	Frameshift variant	Heterozygous	Homozygous	23143585	AT5G20885	RING/U-box superfamily protein
6	Mdg_06g012310	Splice donor variant and intron variant	Heterozygous	Homozygous	23985531	AT3G23760	transferring glycosyl group transferase
6	Mdg_06g012630	Frameshift variant	Heterozygous	Homozygous	24402010	AT3G48860	coiled-coil protein
13	Mdg_13g005100	Stop codon lost	Heterozygous	Homozygous	3969285	AT2G32230	proteinaceous RNase P 1

Table 6. SNPs located within genes mapped to the 'Gala' haploid reference genome where all variants are unique to 'Kidd's D-8' compared to both the reference genome and 'Autumn Gala'.

Chromosome	Gene	Variant Type	Variant location	Gene ortholog	Gene Description
1	Mdg_01g018420	Frameshift	29044966	AT3G21790	UDP-Glycosyltransferase superfamily protein
10	Mdg_10g003900	Frameshift and start codon lost	4978943	AT4G15760	monooxygenase 1

Table 7. SNPs located within genes mapped to the 'Gala' haploid reference genome where all variants are unique to 'Autumn Gala' compared to both the reference genome and 'Kidd's D-8'.

Chromosome	Gene	Variant Type	Variant location	Gene ortholog	Gene Description
1	Mdg_01g008670	Stop codon gained and conservative in-frame insertion	19075786	AT1G31280	Argonaute family protein

Table 8. Structural variants located within genes mapped to the 'Gala' haploid reference genome where, when called heterozygous for 'Kidd's D-8', 'Autumn Gala' SNPs were called homozygous.

Chromosome	Gene	Variant Type	Kidd's D-8 Genotype	Autumn Gala Genotype	Variant location	Variant length	Gene ortholog	Gene Description
6	Mdg_06g010800	Deletion	Heterozygous	Homozygous	21907728-21912511	4783	At1G64510	Translation elongation factor EF1B/ribosomal protein S6 family protein
6	Mdg_06g011660	Deletion	Heterozygous	Homozygous	23072809-23072911	102	At1G32928	Avr9/Cf-9 rapidly elicited protein

Table 9. Structural variants located within genes mapped to the 'Gala' haploid reference genome where all variants are unique to 'Kidd's D-8' compared to both the reference genome and 'Autumn Gala'.

Chromosome	Gene	Variant Type	Variant location	Variant length	Gene ortholog	Gene Description
1	Mdg_01g020600	Deletion	30865375-30865454	79	AT5G16750	Transducin family protein / WD-40 repeat family protein

Table 10: Structural variants located within genes mapped to the 'Gala' haploid reference genome where all variants are unique to 'Autumn Gala' compared to both the reference genome and 'Kidd's D-8'.

Chromosome	Gene	Variant Type	Variant location	Variant length	Gene ortholog	Gene Description
6	Mdg_06g011460	Deletion	22686399-22686629	230	AT4G00870	protein dimerization activity

3.3.3. DNA Variants in ‘September Wonder Fuji’ and ‘Aztec Fuji’ from Haploid Gene Alignments

Variant calling for the ‘Fuji’ cultivars according to the ‘Gala’ haploid genome identified several candidate genes potentially responsible for the difference in development and maturity (Tables 11, 12, 13, 14, 15). There were 5 SNPs called heterozygous in ‘September Wonder Fuji’ and homozygous in ‘Aztec Fuji’ while 12 SNPs were called the converse: homozygous in ‘September Wonder Fuji’ and heterozygous and ‘Aztec Fuji’. 13 SNPs were called unique to ‘September Wonder Fuji’, while 8 unique SNPs were called for ‘Aztec Fuji’. There were no structural variants shared between ‘September Wonder Fuji’ and ‘Aztec Fuji’ near a gene. 28 structural variants were unique to ‘September Wonder Fuji’ and 54 structural variants unique to ‘Aztec Fuji’ were identified.

Table 11. SNPs located within genes mapped to the 'Gala' haploid reference genome where, when called homozygous for 'September Wonder Fuji', 'Aztec Fuji' SNPs were called heterozygous, and vice versa.

Chromosome	Gene	Variant Type	September Wonder Fuji Genotype	Aztec Fuji Genotype	Variant location	Gene ortholog	Gene Description
1	Mdg_01g004110	Frameshift	Homozygous	Heterozygous	11555142	AT2G13600	Pentatricopeptide repeat (PPR) superfamily protein
2	Mdg_02g006630	Stop codon gained	Homozygous	Heterozygous	5194646	AT2G19540	Transducin family protein / WD-40 repeat family protein
2	Mdg_02g023100	Stop codon lost and splice region variant	Homozygous	Heterozygous	32196900	AT3G12490	cystatin B
2	Mdg_02g023350	Frameshift and splice region variant	Homozygous	Heterozygous	32565350	AT3G14470	NB-ARC domain-containing disease resistance protein
3	Mdg_03g000920	Frameshift and start codon lost	Homozygous	Heterozygous	799574	AT1G69770	chromomethylase 3
3	Mdg_03g005160	Stop codon gained	Heterozygous	Homozygous	4675007	AT1G06930	TPRXL
5	Mdg_05g002820	Stop codon gained	Homozygous	Heterozygous	4691984	N/A	Uncharacterized protein
5	Mdg_05g014460	Stop codon gained	Heterozygous	Homozygous	26958605	AT5G17680	disease resistance protein (TIR-NBS-LRR class)
6	Mdg_06g005500	Frameshift	Heterozygous	Homozygous	7569463	AT4G02570	cullin 1
8	Mdg_08g011080	Splice donor, region, and intron variant	Homozygous	Heterozygous	10412779	AT5G25610	BURP domain-containing protein
9	Mdg_09g016940	Splice donor and intron variant	Homozygous	Heterozygous	16394615	AT1G17720	Protein phosphatase 2A%2C regulatory subunit PR55
-	Mdg_scaffold227g000070	Frameshift	Heterozygous	Homozygous	66088	N/A	Uncharacterized protein
-	Mdg_scaffold333g000030	Frameshift	Homozygous	Heterozygous	31840	AT3G07110	Ribosomal protein L13 family protein
-	Mdg_scaffold644g000020	Stop codon gained	Homozygous	Heterozygous	3048	AT1G69550	disease resistance protein (TIR-NBS-LRR class)
10	Mdg_10g003610	Frameshift	Homozygous	Heterozygous	4594552	AT1G22730	MA3 domain-containing protein
10	Mdg_10g007370	Stop codon gained	Homozygous	Heterozygous	9385826	AT2G21580	Ribosomal protein S25 family protein
10	Mdg_10g010190	Stop codon lost and splice region variant	Heterozygous	Homozygous	17068441	ATMG00860	DNA/RNA polymerases superfamily protein

Table 11 (cont'd)

10	Mdg_10g012560	Stop codon lost and splice region variant	Heterozygous	Homozygous	21409000	AT5G23590	DNAJ heat shock N-terminal domain-containing protein
10	Mdg_10g014210	Stop codon lost and splice region variant	Heterozygous	Homozygous	23858541	AT1G43760	DNAse I-like superfamily protein
10	Mdg_10g021190	Frameshift	Heterozygous	Homozygous	33158308	N/A	protein FAR1-RELATED SEQUENCE 5-like [Prunus avium]
11	Mdg_11g008880	Frameshift	Homozygous	Heterozygous	8134959	AT1G06740	MuDR family transposase
11	Mdg_11g009770	Stop codon lost and splice region variant	Homozygous	Heterozygous	9051436	N/A	PREDICTED: metallothionein-like protein type 2 [Malus domestica]
11	Mdg_11g010200	Stop codon gained	Homozygous	Heterozygous	9536837	AT1G40087	Plant transposase (Ptta/En/Spm family)
11	Mdg_11g015780	Splice acceptor and intron variant	Heterozygous	Homozygous	19147535	N/A	Uncharacterized protein
11	Mdg_11g024440	Frameshift	Heterozygous	Homozygous	36321824	N/A	Uncharacterized protein
12	Mdg_12g017710	Splice donor and intron variant	Heterozygous	Homozygous	26630528	AT4G11150	vacuolar ATP synthase subunit E1
13	Mdg_13g001910	Stop codon gained	Heterozygous	Homozygous	1443149	AT1G23200	Plant invertase/pectin methylesterase inhibitor superfamily
14	Mdg_14g001740	Stop codon gained	Homozygous	Heterozygous	1721359	AT5G39340	histidine-containing phosphotransmitter 3
14	Mdg_14g003090	Stop codon gained	Heterozygous	Homozygous	2992565	AT2G19130	S-locus lectin protein kinase family protein
14	Mdg_14g004670	Stop codon gained	Homozygous	Heterozygous	5126589	AT3G12010	C18orf8
14	Mdg_14g005920	Splice acceptor and intron variant	Heterozygous	Homozygous	6548252	N/A	Uncharacterized protein
14	Mdg_14g012840	Stop codon gained	Heterozygous	Homozygous	19579529	AT2G34320	Polynucleotidyl transferase%2C ribonuclease H-like superfamily protein
15	Mdg_15g028330	Splice acceptor, splice region, and intron variant	Homozygous	Heterozygous	31241492	N/A	Uncharacterized protein

Table 11 (cont'd)

15	Mdg_15g031110	Frameshift	Homozygous	Heterozygous	40781377	ATMG00310	RNA-directed DNA polymerase (reverse transcriptase)-related family protein
15	Mdg_15g033100	Frameshift	Homozygous	Heterozygous	44562688	N/A	Uncharacterized protein
15	Mdg_15g033790	Frameshift	Heterozygous	Homozygous	46091054	AT5G36930	Disease resistance protein (TIR-NBS-LRR class) family
17	Mdg_17g021670	Stop codon gained	Homozygous	Heterozygous	28156959	AT2G38995	O-acyltransferase (WSD1-like) family protein

Table 12. SNPs located within genes mapped to the 'Gala' haploid reference genome where all variants are unique to 'September Wonder Fuji' compared to both the reference genome and 'Aztec Fuji'.

Chromosome	Gene	Variant Type	Variant location	Gene ortholog	Gene Description
2	Mdg_02g013000	Stop codon gained	11079927	AT2G18570	UDP-Glycosyltransferase superfamily protein
2	Mdg_02g025220	Frameshift	34710788	AT5G19440	NAD(P)-binding Rossmann-fold superfamily protein
3	Mdg_03g010260	Stop codon gained	10017807	N/A	Uncharacterized protein
3	Mdg_03g016050	Splice acceptor, region, missense, and intron variant	23950438	N/A	Uncharacterized protein
7	Mdg_07g001700	Frameshift and missense	1802896	AT3G21640	FKBP-type peptidyl-prolyl cis-trans isomerase family protein
-	Mdg_scaffold422g000040	Frameshift	22202	AT3G14470	NB-ARC domain-containing disease resistance protein
-	Mdg_scaffold676g000050	Stop codon gained	22334	AT2G18280	tubby like protein 2
11	Mdg_11g008910	Stop codon gained	8152436	N/A	Uncharacterized protein
11	Mdg_11g020960	Frameshift	31148937	AT1G47490	RNA-binding protein 47C
12	Mdg_12g011930	Frameshift	18821575	AT3G54400	Eukaryotic aspartyl protease family protein
14	Mdg_14g017480	Frameshift	25768540	AT1G63500	kinase with tetratricopeptide repeat domain-containing protein
16	Mdg_16g019850	Frameshift	21911304	AT4G29090	Ribonuclease H-like superfamily protein
17	Mdg_17g024890	Frameshift	33085205	AT2G47300	ribonuclease Ps

Table 13. SNPs located within genes mapped to the 'Gala' haploid reference genome where all variants are unique to 'Aztec Fuji' compared to both the reference genome and 'September Wonder Fuji'.

Chromosome	Gene	Variant Type	Variant location	Gene ortholog	Gene Description
2	Mdg_02g017670	Stop codon gained	19960266	N/A	Uncharacterized protein
4	Mdg_04g017200	Frameshift	27362300	AT5G57580	Calmodulin-binding protein
8	Mdg_08g020420	Frameshift	28155987 28156026	N/A	PREDICTED: mediator of RNA polymerase II transcription subunit 30 [Malus domestica]
9	Mdg_09g014140	Frameshift and splice region variant	12285390	N/A	PREDICTED: replication protein A 70 kDa DNA-binding subunit B-like [Pyrus x bretschneideri]
-	Mdg_scaffold395g000010	Splice acceptor and intron variant	3583	N/A	PREDICTED: Regulator of rDNA transcription protein 15 [Capsicum baccatum]
-	Mdg_scaffold824g000060	Splice acceptor, region, and intron variant	39547	AT4G08850	Leucine-rich repeat receptor-like protein kinase family protein
11	Mdg_11g025170	Splice acceptor and intron variant	37256975	N/A	Uncharacterized protein
17	Mdg_17g019270	Frameshift	24704155	AT1G32900	UDP-Glycosyltransferase superfamily protein

Table 14. Structural variants located within genes mapped to the 'Gala' haploid reference genome where all variants are unique to 'September Wonder Fuji' compared to both the reference genome and 'Aztec Fuji'.

Chromosome	Gene	Variant Type	Variant location	Variant length	Gene ortholog	Gene Description
1	Mdg_01g020600	Deletion	30865375- 30865454	79	AT5G16750	Transducin family protein / WD-40 repeat family protein
2	Mdg_02g004740	Translocation	3683286- 2294687	0	AT4G13360	ATP-dependent caseinolytic (Clp) protease/crotonase family protein
2	Mdg_02g004740	Deletion	3679515- 3679842	327	AT4G13360	ATP-dependent caseinolytic (Clp) protease/crotonase family protein
2	Mdg_02g019670	Deletion	27419843- 27419991	148	AT1G66920	Protein kinase superfamily protein
2	Mdg_02g019980	Deletion	28010781- 28011216	435	AT3G22690	LOW protein: PPR containing-like protein
2	Mdg_02g021650	Deletion	30385003- 30385403	400	AT4G12330	cytochrome P450%2C family 706%2C subfamily A%2C polypeptide 7
2	Mdg_02g024180	Deletion	33601979- 33602889	910	AT5G59100	Subtilisin-like serine endopeptidase family protein
3	Mdg_03g006990	Deletion	6573562- 6573667	105	AT1G61190	LRR and NB-ARC domains-containing disease resistance protein
3	Mdg_03g010230	Deletion	9876470- 9878074	1604	AT3G09740	syntaxin of plants 71
9	Mdg_09g001350	Deletion	846075- 850886	4811	AT2G03050	Mitochondrial transcription termination factor family protein
9	Mdg_09g004960	Deletion	3480511- 3481288	777	AT2G03340	WRKY DNA-binding protein 3
9	Mdg_09g017070	Deletion	16643045- 16644019	974	AT1G73040	Mannose-binding lectin superfamily protein
9	Mdg_09g017220	Deletion	16940019- 16940282	263	AT1G51850	Leucine-rich repeat protein kinase family protein
9	Mdg_09g019280	Deletion	22653283- 22663204	9921	N/A	Uncharacterized protein
10	Mdg_10g026700	Duplication	38749505- 38749588	83	N/A	PREDICTED: polyphenol oxidase I, chloroplastic-like [Malus domestica]
10	Mdg_10g000300	Deletion	529946- 533651	3705	AT1G56070	Ribosomal protein S5/Elongation factor G/III/V family protein
10	Mdg_10g008880	Deletion	12364570- 12364622	52	AT2G25970	KH domain-containing protein
10	Mdg_10g009130	Deletion	12828553- 12828700	147	AT1G49590	C2H2 and C2HC zinc fingers superfamily protein
10	Mdg_10g013060	Deletion	22287395- 22290799	3404	N/A	Uncharacterized protein

Table 14 (cont'd)

10	Mdg_10g023800	Deletion	36081008- 36081229	221	AT5G46250	RNA-binding protein
11	Mdg_11g000460 Mdg_11g000470	Deletion	381246- 384184	2938	N/A	PREDICTED: F-box/kelch-repeat protein At3g06240-like [Prunus mume]
11	Mdg_11g015610 Mdg_11g015620 Mdg_11g015630	Inversion	18524249- 18689300	165051	AT1G05750 AT2G01820 AT1G08440	Tetratricopeptide repeat (TPR)-like superfamily protein Leucine-rich repeat protein kinase family protein Aluminum activated malate transporter family protein
13	Mdg_13g004400	Deletion	3370842- 3371477	635	AT5G51700	cysteine and histidine-rich domain-containing protein RAR1
14	Mdg_14g013400	Deletion	20742477- 20744226	1749	AT1G13320	protein phosphatase 2A subunit A3
15	Mdg_15g028520	Deletion	32006359- 32011367	5008	AT4G38180	FAR1-related sequence 5
16	Mdg_16g014140	Deletion	12033369- 12034152	783	AT5G49360	beta-xylosidase 1
16	Mdg_16g015340	Deletion	13850067- 13850220	153	AT5G18640	alpha/beta-Hydrolases superfamily protein
17	Mdg_17g004250	Deletion	3098599- 3098656	57	AT3G28460	Methyltransferase

Table 15. Structural variants located within genes mapped to the 'Gala' haploid reference genome where all variants are unique to 'Aztec Fuji' compared to both the reference genome and 'September Wonder Fuji'.

Chromosome	Gene	Variant Type	Variant location	Variant length	Gene ortholog	Gene Description
1	Mdg_01g014680	Deletion	25632047- 25632573	526	N/A	Uncharacterized protein
1	Mdg_01g017670	Deletion	28411734-28411789	55	AT5G23850	O-glucosyltransferase rumi-like protein (DUF821)
1	Mdg_01g017860	Deletion	28594343-28594557	214	AT1G64940	cytochrome P450%2C family 87%2C subfamily A%2C polypeptide 6
1	Mdg_01g019640	Deletion	30141518-30141733	215	AT5G53130	cyclic nucleotide gated channel 1
2	Mdg_02g005240	Deletion	4080234-4080296	199	AT2G25770	Polyketide cyclase/dehydrase and lipid transport superfamily protein
2	Mdg_02g009940	Deletion	7976438-7976601	163	AT4G03500	Ankyrin repeat family protein
2	Mdg_02g020250	Deletion	28512421-28512581	160	AT3G52990	Pyruvate kinase family protein
2	Mdg_02g026650	Deletion	36559368-36559426	58	N/A	Uncharacterized protein
2	Mdg_02g026700	Deletion	36617991-36618103	112	AT1G05590	beta-hexosaminidase 2
3	Mdg_03g010410	Deletion	10277516-10277616	100	AT2G28450	zinc finger (CCCH-type) family protein
3	Mdg_03g012370	Deletion	14331372-14343997	12625	N/A	Uncharacterized protein
4	Mdg_04g004750	Deletion	5081867-5081918	51	AT3G52050	5'-3' exonuclease family protein
4	Mdg_04g005340	Deletion	5786040-5786131	91	AT5G47090	coiled-coil protein
4	Mdg_04g020430	Deletion	30274880-30275765	885	N/A	PREDICTED: Ubiquitin-like domain-containing protein
5	Mdg_05g016670	Deletion	29705370-29711520	6150	AT4G29035	Plant self-incompatibility protein S1 family
5	Mdg_05g017420	Deletion	30528837	299	N/A	Uncharacterized protein
5	Mdg_05g023310	Deletion	38382749-38391092	8343	AT5G45160	Root hair defective 3 GTP-binding protein (RHD3)
5	Mdg_05g030220	Deletion	44860570-44861560	990	N/A	PREDICTED: G-type lectin S-receptor-like serine/threonine-protein kinase At1g11410 isoform X5 [Pyrus x bretschneideri]
5	Mdg_05g030280	Deletion	44906222-44911226	5004	AT1G11410	S-locus lectin protein kinase family protein
5	Mdg_05g032370	Deletion	46450774-46450871	97	AT5G47540	Mo25 family protein
6	Mdg_06g010730	Translocation	21831333-39066986	0	N/A	Uncharacterized protein

Table 15 (cont'd)

6	Mdg_06g010950	Deletion	22018714-22021699	2985	AT2G39020	Acyl-CoA N-acyltransferases (NAT) superfamily protein
8	Mdg_08g006030	Deletion	5046920-5048082	1162	AT5G26180	S-adenosyl-L-methionine-dependent methyltransferases superfamily protein
8	Mdg_08g006120 Mdg_08g006130	Deletion	5107082-5117560	10478	AT3G54920 AT5G12020	Pectin lyase-like superfamily protein 17.6 kDa class II heat shock protein
9	Mdg_09g012280	Translocation	9996582-19761301	0	AT3G22170	far-red elongated hypocotyls 3
9	Mdg_09g006020	Deletion	4303090-4303090	100	AT3G29635	HXXXD-type acyl-transferase family protein
10	Mdg_10g011550	Translocation	19649141-29189379	0	AT3G07940	Calcium-dependent ARF-type GTPase activating protein family
10	Mdg_10g006820	Deletion	8591448-8591622	174	AT5G60670	Ribosomal protein L11 family protein
10	Mdg_10g013840	Deletion	23459141-23459484	343	AT2G17250	CCAAT-binding factor
10	Mdg_10g016100	Deletion	26450192-26450371	179	AT5G48740	Leucine-rich repeat protein kinase family protein
11	Mdg_11g020100	Translocation	29954863-35074315	0	AT4G08850	Leucine-rich repeat receptor-like protein kinase family protein
11	Mdg_11g011870	Deletion	11516225-11528837	12786	N/A	Uncharacterized protein
11	Mdg_11g025090	Deletion	37165867-37173784	7917	AT3G63270	Nuclease
12	Mdg_12g012240	Deletion	19214211-19215426	1215	N/A	Uncharacterized protein
12	Mdg_12g012250	Deletion	19219111-19238373	19262	N/A	Uncharacterized protein
12	Mdg_12g016070	Deletion	24495858-24503183	7325	AT3G27070	translocase outer membrane 20-1
13	Mdg_13g012930	Deletion	10869601-10869986	385	AT5G49930	zinc knuckle (CCHC-type) family protein
13	Mdg_13g014810	Deletion	13193422-13208669	15411	N/A	Uncharacterized protein
13	Mdg_13g019160	Deletion	20442610-20442716	106	AT3G23920	beta-amylase 1
13	Mdg_13g019830	Deletion	21599467-21599532	65	N/A	PREDICTED: replication protein A 70 kDa DNA-binding subunit B [Prunus persica]
14	Mdg_14g012510	Translocation	19087046-37282952	0	AT5G42050	DCD (Development and Cell Death) domain protein
14	Mdg_14g018770	Translocation	26890519-23727181	0	N/A	PREDICTED: cyclic dof factor 5-like [Malus domestica]
14	Mdg_14g002660	Deletion	2470299-2470512	213	AT5G06140	sorting nexin 1
14	Mdg_14g018140	Deletion	26394672-26402408	7736	N/A	Uncharacterized protein
15	Mdg_15g001620	Deletion	1102955-1103055	100	AT4G16310	LSD1-like 3

Table 15 (cont'd)

15	Mdg_15g025060	Deletion	24292486-24296967	4481	AT4G39950	cytochrome P450%2C family 79%2C subfamily B%2C polypeptide 2
15	Mdg_15g029100	Deletion	33545360-33545696	336	AT1G68470	Exostosin family protein
15	Mdg_15g033320	Deletion	44992873-44993050	177	AT1G22275	Myosin heavy chain-related protein
15	Mdg_15g033690	Deletion	45819172-45827385	8213	AT1G11870	Seryl-tRNA synthetase
15	Mdg_15g039310	Deletion	54042100-54042164	64	AT1G59740	Major facilitator superfamily protein
16	Mdg_16g019230 Mdg_16g019240	Deletion	20885340-20887554	2214	AT4G29090	Ribonuclease H-like superfamily protein
17	Mdg_17g001370	Deletion	926481-927185	704	AT2G34930	disease resistance family protein / LRR family protein
17	Mdg_17g002720	Deletion	1838393-1839478	1085	AT5G04700	Ankyrin repeat family protein
17	Mdg_17g019520	Deletion	25028238-25033213	4975	AT5G20230	blue-copper-binding protein

3.3.4. DNA Variants in 'Maslin' and 'Cripps Pink' from Haploid Genome Alignments

Variant calling of 'Pink Lady' cultivars mapped to the 'Gala' diploid reference genome resulted in many different candidate genes potentially causing faster development and earlier maturation in 'Maslin' than 'Cripps Pink' (Tables 16, 17, 18, 19, 20). Of the SNPs shared between both cultivars, 12 SNPs were called homozygous and heterozygous in 'Maslin' and 'Cripps Pink', respectively. 6 SNPs unique to 'Maslin' and 10 SNPs unique to 'Cripps Pink' were identified. A single structural variant was called that is shared by both cultivars, heterozygous in 'Maslin' and homozygous in 'Cripps Pink'. We identified 34 structural variants unique to 'Maslin', and 12 structural variants unique to 'Cripps Pink'.

Table 16. SNPs located within genes mapped to the 'Gala' haploid reference genome where, when called homozygous for 'Maslin', 'Cripps Pink' SNPs were called heterozygous.

Chromosome	Gene	Variant Type	Maslin Genotype	Cripps Pink Genotype	Variant location	Gene ortholog	Gene Description
2	Mdg_02g008760	Frameshift	Homozygous	Heterozygous	6923933	AT5G17880	disease resistance protein (TIR-NBS-LRR class)
2	Mdg_02g013760	Frameshift	Homozygous	Heterozygous	12406291	AT5G66900	Disease resistance protein (CC-NBS-LRR class) family
2	Mdg_02g021330	Splice acceptor, splice region, and intron variant	Homozygous	Heterozygous	29949183	AT3G14470	NB-ARC domain-containing disease resistance protein
3	Mdg_03g006990	Frameshift	Homozygous	Heterozygous	6574422	AT1G61190	LRR and NB-ARC domains-containing disease resistance protein
4	Mdg_04g012150	Frameshift	Homozygous	Heterozygous	21218517	N/A	Uncharacterized protein
5	Mdg_05g002920	Stop codon gained	Homozygous	Heterozygous	4792319	AT5G58430	exocyst subunit exo70 family protein B1
9	Mdg_09g002180	Splice donor and intron variant	Homozygous	Heterozygous	1402559	AT5G40510	Sucrase/ferredoxin-like family protein
10	Mdg_10g014740	Stop codon gained	Homozygous	Heterozygous	24617859	N/A	PREDICTED: CDT1-like protein a, chloroplastic [Pyrus x bretschneideri]
13	Mdg_13g015550	Stop codon gained	Homozygous	Heterozygous	14141799	AT3G10310	P-loop nucleoside triphosphate hydrolases superfamily protein with CH (Calponin Homology) domain-containing protein
13	Mdg_13g017980	Frameshift	Homozygous	Heterozygous	18344552	AT5G43580	Serine protease inhibitor%2C potato inhibitor I-type family protein
13	Mdg_13g018970	Stop codon gained	Homozygous	Heterozygous	20225335	AT1G10000	Ribonuclease H-like superfamily protein
17	Mdg_17g005610	Stop codon gained	Homozygous	Heterozygous	4277370	N/A	Uncharacterized protein

Table 17. SNPs located within genes mapped to the 'Gala' haploid reference genome where all variants are unique to 'Maslin' compared to both the reference genome and 'Cripps Pink'.

Chromosome	Gene	Variant Type	Variant location	Gene ortholog	Gene Description
2	Mdg_02g010040	Frameshift	8088886	N/A	PREDICTED: ubiquitin domain-containing protein DSK2b-like isoform X1 [Prunus mume]
8	Mdg_08g016540	Stop codon gained and splice region variant	22299333	AT4G38180	FAR1-related sequence 5
10	Mdg_10g015210	Frameshift	25228705	N/A	Uncharacterized protein
12	Mdg_12g015750	Splice donor and intron variant	24192220	AT3G51830	SAC domain-containing protein 8
17	Mdg_17g002760	Stop codon lost and splice region variant	1866004	AT5G04700	Ankyrin repeat family protein
-	Mdg_scaffold713g000010	Frameshift	11768	AT5G05800	Myb/SANT-like DNA-binding domain protein

Table 18. SNPs located within genes mapped to the 'Gala' haploid reference genome where all variants are unique to 'Cripps Pink' compared to both the reference genome and 'Maslin'.

Chromosome	Gene	Variant Type	Variant location	Gene ortholog	Gene Description
2	Mdg_02g020820	Frameshift and missense	29381235	AT5G38260	Protein kinase superfamily protein
5	Mdg_05g023530	Frameshift	38623658	N/A	Uncharacterized protein
7	Mdg_07g004890	Stop codon gained	5246684	AT3G14470	NB-ARC domain-containing disease resistance protein
8	Mdg_08g016450	Frameshift	22182455	N/A	Uncharacterized protein
10	Mdg_10g012140	Start codon lost	20724755	AT2G02650	Ribonuclease H-like superfamily protein
10	Mdg_10g027910	Frameshift	40265746	N/A	PREDICTED: RINT1-like protein MAG2 [Malus domestica]
12	Mdg_12g002000	Stop codon gained	2212591	AT1G50830	Aminotransferase-like%2C plant mobile domain family protein
12	Mdg_12g015590	Stop codon gained and splice region variant	23985583	N/A	Uncharacterized protein
14	Mdg_14g013960	Frameshift	21590378	AT4G23160	cysteine-rich RECEPTOR-like kinase
-	Mdg_scaffold197g000010	Stop codon lost and aplice region variant	6145	N/A	Uncharacterized protein

Table 19. Structural variants located within genes mapped to the 'Gala' haploid reference genome where, when called homozygous for 'Maslin', 'Cripps Pink' SNPs were called heterozygous and vice versa.

Chromosome	Gene	Variant Type	Maslin Genotype	Cripps Pink Genotype	Variant location	Variant length	Gene ortholog	Gene Description
17	Mdg_17g007020	Deletion	Heterozygous	Homozygous	5411012-5411211	199	AT5G15680	ARM repeat superfamily protein

Table 20. Structural variants located within genes mapped to the 'Gala' haploid reference genome where all variants are unique to 'Maslin' compared to both the reference genome and 'Cripps Pink'.

Chromosome	Gene	Variant Type	Variant location	Variant length	Gene ortholog	Gene Description
2	Mdg_02g003910	Deletion	2942895-2943260	365	AT5G36930	Disease resistance protein (TIR-NBS-LRR class) family
2	Mdg_02g004330	Deletion	3238270-3238737	467	AT3G24503	aldehyde dehydrogenase 2C4
2	Mdg_02g006520	Deletion	5139871-5140431	560	AT5G11800	K+ efflux antiporter 6
2	Mdg_02g017160	Deletion	18570329-18576272	5943	AT1G01950	armadillo repeat kinesin 2
3	Mdg_03g013050	Deletion	16134306-16136604	2298	AT3G05850	MuDR family transposase
5	Mdg_05g000290	Deletion	870334-878413	8079	AT4G10300	RmlC-like cupins superfamily protein
5	Mdg_05g031220	Deletion	45612762-45633696	20934	AT1G66250	O-Glycosyl hydrolases family 17 protein
6	Mdg_06g019700	Deletion	31681850-31692400	10550	AT1G67000	Protein kinase superfamily protein
6	Mdg_06g020940	Deletion	32910050-32923020	12970	AT1G21280	Copia-like polyprotein/retrotransposon
9	Mdg_09g007580	Deletion	5802137-5802532	395	AT3G18670	Ankyrin repeat family protein
9	Mdg_09g007720	Deletion	5924767-5924924	157	AT1G03620	ELMO/CED-12 family protein
9	Mdg_09g013250	Deletion	11054344-11055262	918	AT1G06520	glycerol-3-phosphate acyltransferase 1
9	Mdg_09g017070	Deletion	16643049-16644019	970	AT1G73040	Mannose-binding lectin superfamily protein
10	Mdg_10g013060	Deletion	22286696-22291159	4463	N/A	Uncharacterized protein
10	Mdg_10g015720	Deletion	25960991-25961245	254	AT4G13780	methionine-tRNA ligase%2C putative / methionyl-tRNA synthetase%2C putative / MetRS
10	Mdg_10g024300	Deletion	36503422-36503579	157	AT4G18040	eukaryotic translation initiation factor 4E
10	Mdg_10g027920	Deletion	40282120-40285495	3375	AT4G23180	cysteine-rich RLK (RECEPTOR-like protein kinase) 10
11	Mdg_11g008630	Translocation	7856923	0	AT2G29040	Exostosin family protein
11	Mdg_11g002210	Deletion	1994363-2000908	6545	AT4G23160	cysteine-rich RECEPTOR-like kinase
11	Mdg_11g002400	Deletion	2157189-2158297	1108	AT5G60900	receptor-like protein kinase 1
11	Mdg_11g002950	Deletion	2693145-2693209	64	AT5G55850	RPM1-interacting protein 4 (RIN4) family protein
12	Mdg_12g001820	Deletion	1999892-2000850	958	N/A	Uncharacterized protein
12	Mdg_12g002650	Deletion	2862700-2863349	649	AT3G18830	polyol/monosaccharide transporter 5
12	Mdg_12g007620	Deletion	9098264-9098585	321	AT1G67810	sulfur E2
12	Mdg_12g008920	Deletion	11202669-11205088	2419	N/A	Uncharacterized protein
12	Mdg_12g013300	Deletion	20963025-20963078	53	AT2G17080	hypothetical protein (DUF241)
12	Mdg_12g015080	Deletion	23455300-23456238	938	AT5G23960	terpene synthase 21
13	Mdg_13g017160	Deletion	16852131-16852345	214	AT5G43860	chlorophyllase 2
13	Mdg_13g020580	Deletion	23404689-23404821	132	AT5G58430	exocyst subunit exo70 family protein B1
14	Mdg_14g011280	Deletion	16784501-16793536	9035	AT1G64040	type one serine/threonine protein phosphatase 3

Table 20 (cont'd)

15	Mdg_15g011940	Deletion	9287941-9288435	494	AT4G31980	PPPDE thiol peptidase family protein
15	Mdg_15g025510	Deletion	25067107-25068788	1681	AT4G37030	membrane protein
15	Mdg_15g038710	Deletion	53365293-53365878	585	AT2G40890	cytochrome P450%2C family 98%2C subfamily A%2C polypeptide 3
15	Mdg_15g039130	Deletion	53856135-53856209	74	AT5G42260	beta glucosidase 12

Table 21. Structural variants located within genes mapped to the 'Gala' haploid reference genome where all variants are unique to 'Cripps Pink' compared to both the reference genome and 'Maslin'.

Chromosome	Gene	Variant Type	Variant location	Variant length	Gene ortholog	Gene Description
4	Mdg_04g003020	Deletion	3394853-3395994	1141	AT1G05785	Got1/Sft2-like vescicle transport protein family
5	Mdg_05g013960	Deletion	26255452-26255558	106	AT2G17350	beta-mannosyltransferase-like protein
5	Mdg_05g023470 Mdg_05g023480	Deletion	38568224-38574419	6195	AT1G56130 AT4G02550	Leucine-rich repeat transmembrane protein kinase Myb/SANT-like DNA-binding domain protein
8	Mdg_08g010660 Mdg_08g010670	Inversion	9857204-9876445	19241	AT3G63520	carotenoid cleavage dioxygenase 1
9	Mdg_09g013060 Mdg_09g013070	Deletion	10859222-10861376	2154	AT1G55000	peptidoglycan-binding LysM domain-containing protein
9	Mdg_09g015190	Deletion	13751408-13755530	4122	AT4G37030	membrane protein
11	Mdg_11g002670	Deletion	2380774-2380844	70	AT3G20870	ZIP metal ion transporter family
12	Mdg_12g012270	Deletion	19263940-19267692	3752	AT3G10180	P-loop containing nucleoside triphosphate hydrolases superfamily protein
14	Mdg_14g005750	Deletion	6381972-6382893	921	AT3G10300	Calcium-binding EF-hand family protein
14	Mdg_14g020930	Deletion	28736671-28742421	5750	AT3G18290	zinc finger protein-like protein
15	Mdg_15g015240	Deletion	12281144-12281195	51	AT5G35080	ER lectin-like protein
17	Mdg_17g020190	Deletion	26196912-26197057	145	AT5G36110	cytochrome P450%2C family 716%2C subfamily A%2C polypeptide 1

3.3.4. Preparation for Transcriptomic Study

A comprehensive transcriptome study was designed to complement our DNA variant analyses. Fruit tissue from all six cultivars was collected throughout the 2023 growing season between May 23 and harvest date of each cultivar. Collections from May 23 to July 11 were of whole fruit, while July 18 – harvest date, hand dissections were done to isolate peel, cortex, core, and seed tissues. Table 22 indicates collection details for timing and type of collection of tissue. Our analysis of fruit growth between sport and standard maturity cultivars, as described in chapter 2, suggests that fruit in early maturing lines for all three varieties increased size at a

faster rate early in development than the late-maturing lines. This suggests that the causative mutation(s) for the altered maturity time for each of our varieties likely impacts a gene involved in early fruit development, or carpel development preceding it. For this reason, upcoming transcriptome studies should be done using RNA extracted from fruit harvested at these dates between 23 May and 26 September 2023 (Table 22; and the Fig. 21 below).

Table 22. Tissue collections for RNA extraction and sequencing, including date, days after full bloom (DAFB), and type of tissue.

Date	**DAFB**	**Julian Date**	**Tissue**
5/23/2023	14	143	Whole fruit, cut in half
6/6/2023	28	157	Whole fruit, cut in quarters
6/13/2023	35	164	Whole fruit, cut in quarters
6/20/2023	42	171	Whole fruit, cut in 1/16's
7/3/2023	55	184	Whole fruit, cut many pieces
7/11/2023	63	192	Whole fruit, cut many pieces
7/18/2023	70	199	Peel, cortex, seed
7/25/2023	77	206	Peel, cortex, core, seed
8/1/2023	84	213	Peel, cortex, core, seed
9/13/2023	127	256	Peel, cortex, core, seed

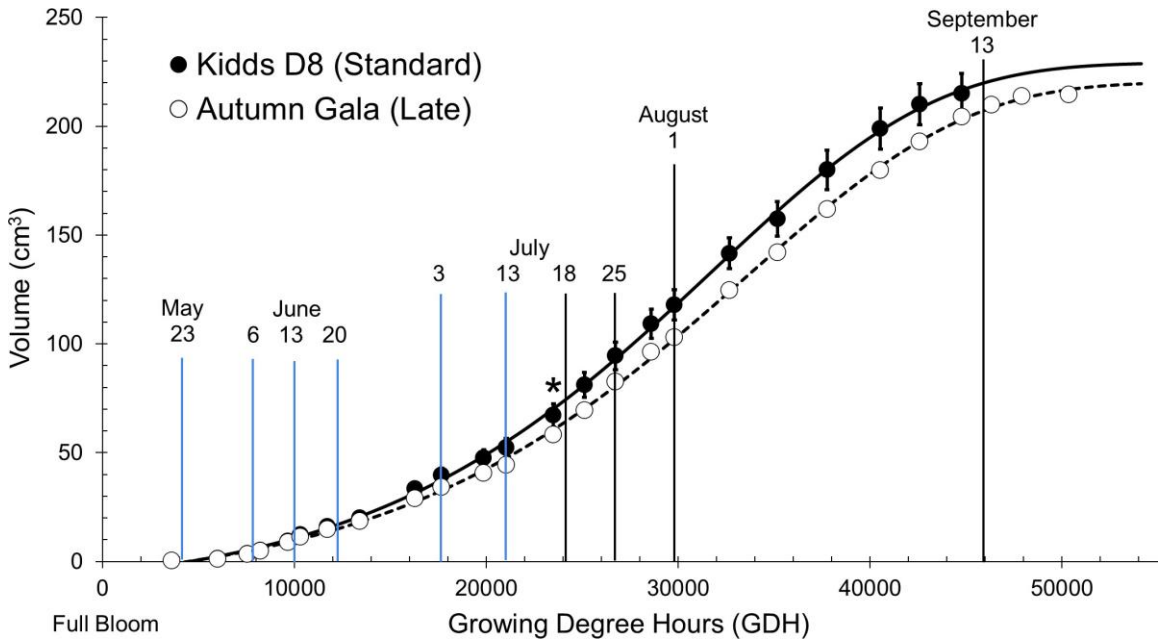

Figure 20. Volumetric growth curve of standard harvesting 'Kidd's D-8' and its late-harvesting sport, 'Autumn Gala' according to growing degree hours (GDH). The 6 first blue lines indicate dates (Table 22) when whole fruit tissue was collected for RNA extraction and sequencing. These dates refer to fruit at the cell division (23 May), cell division and cell expansion overlap (6, 13, 20 June), and cell expansion stages of development. The last 4 black lines indicate dates (Table 22) when dissected fruit tissue was collected for RNA extraction and sequencing (Fig. 21).

Figure 21. Example of fruit tissue dissections that were collected 25 July 2023 and later.

3.4. DISCUSSION

3.4.1. Preliminary Genomic Analysis

Our preliminary genomic results indicate many mechanisms that need to be assessed for causation of early or late maturation. Our phenotypical data (chapter 2) suggests that the genetic differences between a maturity sport and its progenitor, or a standard maturity cultivar of the same variety, may relate to genes that are associated with early fruit development. Therefore, variants in genes associated with cell division would be strong candidates for causative mutations for the maturity phenotypes, unlike one of the few genes listed above potentially related to photosynthesis (Table 20). In ‘Gala’, we find the least number of variants. This is

likely due to the close relation to the reference genome ‘Gala Haploid’, which was derived from budwood from the original 'Gala' accession a.k.a. 'Kidd's D-8 Gala' (Sun et al., 2020). Even if there are other homologs in the genome encoding proteins that maintain the same or similar functions as gene ‘*Mdg_04A010840’* (which encodes a motor family protein), such genetic events may cause a reduction of total expression of the other genes and may result in lower rates of, as an example, cell division early in fruit development. Slower cell division early in fruit development may result in a ‘compound interest’ effect where slower cell division early in fruit development may significantly impact the rest of the fruit’s development. In ‘Fuji’ and ‘Pink Lady’ comparisons, we find many variants of genes encoding important proteins. These proteins are part of large families, and the causal genes regulating fruit maturation may be a result of many genes in a particular locus in the genome being differentially expressed. Transcriptomic analyses may provide more insight into the mechanisms behind final fruit maturation date by closing in on specific genes that have specific functions involved in contributing to the early or late maturity phenotype. Analysis of differential gene expression at different timepoints could also prove useful. Finding unexpressed genes that are in our variant lists may also assist in filtering out candidate genes, while also evaluating the pathways in which those genes are involved.

Although we were not able to directly detect a large deletion of 2.8 Mb in ‘Autumn Gala’ with our short-read sequencing, our haploid results of 11 homozygous SNPs and 2 homozygous deletions within a 2.8 Mb region in the ‘Gala’ haploid genome agree with the 2.8 Mb deletion found in ‘Autumn Gala’ by Ban et al. (2022). Since all ‘Autumn Gala’ SNP variants are homozygous in the matching 2.8 Mb region, we can infer that we are likely also seeing a 2.8 Mb deletion in ‘Autumn Gala’. It is unclear from our results, however, if the candidate Mdact7 gene

‘*MD06G1127300’* that Ban et al. (2022) proposed as the primary candidate for the delayed maturation in ‘Autumn Gala’. What we did find was other homologs of gene *‘MD06G1127300’* [from the ‘Golden Delicious’ genome (Daccord et al., 2017)] in the ‘Gala’ diploid and haploid genomes (X. Sun et al., 2020) responsible for actin-7 production. Plants often have multiple genes encoding for similar proteins critical to plant processes. It is possible that removing functionality of one single gene may not necessarily turn a plant process off, but rather delay the process. In the case of early maturing bud sports, there may be transcription factors enabled by mutation that promote more genetic expression of basic molecular processes, leading to the advancement of maturity.

The phenotype of change in maturation could be due to a mechanism such as a mutational change in a particular protein encoded by one gene that is similar amongst all apple cultivars. Since harvest date is potentially such a complex trait, there may be many possible mechanisms that contribute to early- or late-maturation of an apple bud sport. It is possible that a slight manipulation of a particular gene involved in basic cell activity such as division early in fruit development could create a compound interest effect for the rest of the season, not just in size, but in developmental rate. Based on our findings in all 3 apple variety comparisons, since each earlier harvesting cultivar shows almost an immediate increase in rate of development after flowering, mechanisms that result in shifting harvest date in these three varieties commence early in fruit development. In the case of the non-functional actin-7 encoding gene proposed to confer late a maturity date by Ban et al. (2022), the suggestion is that a mutation in a gene providing basic cellular functions such as suppressed actin production may lead to a delay in maturity. It is unclear, however, how such a loss in gene function would not also result in a change in the canopy of the sport tree.

CHAPTER 4. Conclusions and Future Direction

4.1. INTRODUCTION

In early apple fruit development, there are many mechanisms underlying crucial processes integrating the effects of both the whole tree as an organism and its environment. Fortunately, gene expression during early fruit development has been studied since the early 2000's (Eccher et al., 2014). Eccher et al. (2014) noted in their concluding statements the knowledge gap in the study and knowledge of apple early fruit development and singled out possible interactions between the seeds and the cortex as an example. However, apple fruit are often seedless and no shift in maturation of seedless fruit to seeded fruit has, to our knowledge, been described. They also note the lack of information regarding controls, modulators, and molecular mechanisms that determine maturation rate and timing. They ask questions such as: "What kind of "molecular" competences does the apple fruit acquire during the maturation phase?", "Which are the modulators of this process?", and "Can this process be tuned by exogenous treatments?". They mention how much work needs to be done and specifically note the need for "omics" work combined with classical physiological approaches that actually evaluate the tree in the orchard (Eccher et al., 2014). Thus, the complexity of fruit development and its interaction with fruit maturation remains to be further explored. Comprehensive analyses of mechanisms responsible for early or delayed maturation remain to be confirmed. The loss-of-function actin allele in the Ban et al. (2022) study remains to be expressed in apple tissue. The closer we as researchers come to uncovering these mechanisms, the better we may understand the complexities of the relationship between fruit development and fruit maturation.

4.2. DISCUSSION AND FUTURE DIRECTION

4.2.1. Discussion and Future Direction

What our current findings suggest is that early fruit development and fruit maturation are interconnected, meaning that fruit size, harvest date, and harvest traits such as firmness, sugars, flavor, and internal ethylene production are, to an extent, predetermined or influenced by events early on in fruit development (Chapter 2 Results). The exciting benefit of our physiological data is that we now have a much more targeted approach to interrogate the genome and transcriptome. We have also improved *how* we look. The transcriptomic data may show gene expression differences that aren't detectable by genomic analysis. The absence in variants of orthologs of the *ACT7* gene in 'Gala' may be further revealed by gene expression differences between the two cultivars. The early emergence of phenotypic differences in growth rate between the bud sport and the control lines suggests the physiological processes leading to an early or late harvest date may also emerge very early in fruit development. If so, the early or delayed maturation date is very likely not strictly a function of ripening-related processes, but rather is derived from a season-long shift in metabolic activity. We now believe that we can look at transcriptomic events very early in development and link those to maturation rate/harvest date.

Future endeavors should involve comprehensive physiological and molecular characterization of fruit tissue during cell differentiation, division, and expansion periods, as well as the rate at which these processes occur. This includes evaluating floral development, with a focus on late-stage ovary development, as well as investigating anatomical and molecular changes happening right after fertilization. Another analysis that should be performed is an evaluation of anatomical differences (e.g. cell size and number) as well as molecular differences in expanding the transcriptomic studies to flowers and flower buds *before* fertilization. Our preliminary results of

filtered variants in our ‘Gala’ comparison may show promise, but much work needs to be done to determine if one or more of the candidate genes causes the early or late maturity phenotype in apple bud sports.

4.2.2. Advantages of the Study

An advantage of our study is that our ‘Gala’ comparison used the original germplasm. We were graciously given scions from the original ‘Autumn Gala’ limb sport, as well as the original progenitor tree. Over time, apples accumulate mutations and may slightly alter their expression of certain fruit phenotypes such as color and size, so this approach minimizes that risk. This original germplasm partially eliminates much of that variability. In our ‘Fuji’ comparison, we have the bud sport ‘September Wonder Fuji’, from the early ‘Fuji’ bud sport ‘Yataka Fuji’. We are comparing this early sport to a quite unrelated (relative to direct sport mutations) cultivar ‘Aztec Fuji’, for which there is no patent to the author’s knowledge. The separation in genetics of these two sports may give unique perspective to our study, especially if we find a similar mechanism in this ‘Fuji’ comparison as we may find in our ‘Gala’ or ‘Cripps Pink’ analyses. Our ‘Cripps Pink’ analysis between ‘Maslin Cripps Pink’ and its progenitor ‘Cripps Pink’ is also unique in that although ‘Maslin’ is a direct sport of ‘Cripps Pink’, we do not have the original germplasm from the original sport limb and progenitor tree. Through several generations of grafting, possible mutational change may have accumulated and could complicate the filtering process in finding a single region in which a candidate gene has been manipulated. Variation in somatic mutations even across individual branches of a single tree elaborated by Sun et al. (2023) underlies the importance of utilizing original tissue of progenitor and mutant. This may also be a reason why there are so few variants in our ‘Gala’ filtered variant results compared to the ‘Fuji’ and ‘Cripps Pink’ lines. It is certainly valuable to study these three separate

comparisons concurrently because of replication of maturity sport studies in apple, as well as the fact that these three commercial varieties are widely cultivated across the globe. Understanding these mechanisms will inevitably lead to greater advances in breeding efforts to establish unique cultivars with better and more desirable traits better tailored to growing method and region.

LITERATURE CITED

AgroFresh. (n.d.). *Harvista™ near-harvest treatment from AgroFresh*. AgroFresh. Retrieved November 27, 2023, from https://www.agrofresh.com/solutions/harvista/

Argenta, L. C., Wood, R. M., De Angelis Monteiro Terra, F., & Neuwald, D. A. (2022). Effect of preharvest ethylene inhibitor application on 'Fuji' apple on-tree maturation and quality after storage. *Acta Horticulturae*, *1344*, 219–226. https://doi.org/10.17660/ActaHortic.2022.1344.32

Ban, S., El-Sharkawy, I., Zhao, J., Fei, Z., & Xu, K. (2022). An apple somatic mutation of delayed fruit maturation date is primarily caused by a retrotransposon insertion-associated large deletion. *The Plant Journal*, *111*(6), 1609–1625. https://doi.org/10.1111/tpj.15911

Bergh, O. (1990). Effect of temperature during the first 42 days following full bloom on apple fruit growth and size at harvest. *South African Journal of Plant and Soil*, *7*(1), 11–18. https://doi.org/10.1080/02571862.1990.10634530

Bhusal, N., Han, S.-G., & Yoon, T.-M. (2019). Impact of drought stress on photosynthetic response, leaf water potential, and stem sap flow in two cultivars of bi-leader apple trees (*Malus × domestica* Borkh.). *Scientia Horticulturae*, *246*, 535–543. https://doi.org/10.1016/j.scienta.2018.11.021

Biale, J. B. (1964). Growth, Maturation, and Senescence in Fruits. *Science*, *146*(3646), 880–888.

Blanpied, G. D., & Silsby, K. J. (1992). *Predicting Harvest Date Windows for Apples*. Cornell Cooperative Extension. https://hdl.handle.net/1813/3299

Bramlage, W. J., Greene, D. W., Autio, W. R., & McLaughlin, J. M. (1980). Effects of Aminoethoxyvinylglycine on Internal Ethylene Concentrations and Storage of Apples1. *Journal of the American Society for Horticultural Science*, *105*(6), 847–851. https://doi.org/10.21273/JASHS.105.6.847

Brookfield, P., Murphy, P., Harker, R., & MacRae, E. (1997). Starch degradation and starch pattern indices; interpretation and relationship to maturity. *Postharvest Biology and Technology*, *11*(1), 23–30. https://doi.org/10.1016/S0925-5214(97)01416-6

Chagné, D., Dayatilake, D., Diack, R., Oliver, M., Ireland, H., Watson, A., Gardiner, S. E., Johnston, J. W., Schaffer, R. J., & Tustin, S. (2014). Genetic and environmental control of fruit maturation, dry matter and firmness in apple (Malus × domestica Borkh.). *Horticulture Research*, *1*, 14046. https://doi.org/10.1038/hortres.2014.46

Chassagne-Berces, S., Poirier, C., Devaux, M.-F., Fonseca, F., Lahaye, M., Pigorini, G., Girault, C., Marin, M., & Guillon, F. (2009). Changes in texture, cellular structure and cell wall composition in apple tissue as a result of freezing. *Food Research International*, *42*(7), 788–797. https://doi.org/10.1016/j.foodres.2009.03.001

Cho, H. J., Kim, G. H., & Choi, C. (2020). Differential gene expression and epigenetic

analyses between striped and blushed skinned sports of 'Fuji' apple. *Scientia Horticulturae*, *261*, 108944. https://doi.org/10.1016/j.scienta.2019.108944

Chun, I.-J., Fallahi, E., Shafii, B., Tripepi, R. R., & Colt, W. M. (2002). Influence of rootstocks and microsprinkler fertigation on photosynthesis of "Fuji" apple trees. *Journal of the American Pomological Society*, *56*, 23–29.

Contreras, C., Alsmairat, N., & Beaudry, R. (2014). Prestorage Conditioning and Diphenylamine Improve Resistance to Controlled-atmosphere-related Injury in 'Honeycrisp' Apples. *HortScience*, *49*(1), 76–81. https://doi.org/10.21273/HORTSCI.49.1.76

Daccord, N., Celton, J.-M., Linsmith, G., Becker, C., Choisne, N., Schijlen, E., van de Geest, H., Bianco, L., Micheletti, D., Velasco, R., Di Pierro, E. A., Gouzy, J., Rees, D. J. G., Guérif, P., Muranty, H., Durel, C.-E., Laurens, F., Lespinasse, Y., Gaillard, S., … Bucher, E. (2017). High- quality de novo assembly of the apple genome and methylome dynamics of early fruit development. *Nature Genetics*, *49*(7), Article 7. https://doi.org/10.1038/ng.3886

Darwin, C. (1868). *The Variation of Animals and Plants Under Domestication*. J. Murray.

DeJong, T. (2022). *Concepts for understanding fruit trees*. https://www.cabidigitallibrary.org/doi/epdf/10.1079/9781800620865.0000

Dong, Q. L., Yan, Z. Y., Liu, Z., & Yao, Y. X. (2011). Early ripening events caused by bud mutation in Beni Shogun apple. *Russian Journal of Plant Physiology*, *58*(3), 439–447. https://doi.org/10.1134/S1021443711030034

Eccher, G., Ferrero, S., Populin, F., Colombo, L., & Botton, A. (2014). Apple (Malus domestica L. Borkh) as an emerging model for fruit development. *Plant Biosystems - An International Journal Dealing with All Aspects of Plant Biology*, *148*(1), 157–168. https://doi.org/10.1080/11263504.2013.870254

Engelsma, J., & Ott, E. (2024). *Cost of PGR's in Michigan Apple Industry* (A. Engelsma, Interviewer) [Personal communication].

Fallahi, E., Chun, I.-J., Neilsen, G. H., & Colt, W. M. (2001). Effects of Three Rootstocks on Photosynthesis, Leaf Mineral Nutrition, and Vegetative Growth of "Bc-2 Fuji" Apple Trees. *Journal of Plant Nutrition*, *24*(6), 827–834. https://doi.org/10.1081/PLN-100103776

Flore, J. A., & Lakso, A. N. (1989). Environmental and Physiological Regulation of Photosynthesis in Fruit Crops. In *Horticultural Reviews* (pp. 111–157). John Wiley & Sons, Ltd. https://doi.org/10.1002/9781118060841.ch4

Foster, T. M., & Aranzana, M. J. (2018). Attention sports fans! The far-reaching contributions of bud sport mutants to horticulture and plant biology. *Horticulture Research*, *5*(1), 44. https://doi.org/10.1038/s41438-018-0062-x

Fujii, J., & Kennedy, R. (1984). Seasonal Changes in the Photosynthetic Rate in Apple Trees: A comparison between Fruiting and Nonfruiting Trees. *American Society of Plant Biologists*,

78(3), 519–524.

Giné-Bordonaba, J., Echeverria, G., Duaigües, E., Bobo, G., & Larrigaudière, C. (2019). A comprehensive study on the main physiological and biochemical changes occurring during growth and on-tree ripening of two apple varieties with different postharvest behaviour. *Plant Physiology and Biochemistry*, *135*, 601–610. https://doi.org/10.1016/j.plaphy.2018.10.035

Goffinet, M. C., Robinson, T. L., & Lakso, A. N. (1995). A comparison of 'Empire' apple fruit size and anatomy in unthinned and hand-thinned trees. *Journal of Horticultural Science*. https://www.tandfonline.com/doi/abs/10.1080/14620316.1995.11515307

Grappadelli, L. C., Lakso, A. N., & Flore, J. A. (1994). Early Season Patterns of Carbohydrate Partitioning in Exposed and Shaded Apple Branches. *Journal of the American Society for Horticultural Science*, *119*(3), 596–603. https://doi.org/10.21273/JASHS.119.3.596

Griffith, C. (2022). *Effects of Plant Growth Regulators and Weather on Bitter Pit Incidence in 'Honeycrisp' Apple* [M.S., Michigan State University]. https://www.proquest.com/docview/2708306894/abstract/29EB20B06AAB4112PQ/1

Gussman, C. D., Goffreda, J. C., & Gianfagna, T. J. (1993). Ethylene Production and Fruit-softening Rates in Several Apple Fruit Ripening Variants. *HortScience*, *28*(2), 135–137. https://doi.org/10.21273/HORTSCI.28.2.135

Harker, F. R., Kupferman, E. M., Marin, A. B., Gunson, F. A., & Triggs, C. M. (2008). Eating quality standards for apples based on consumer preferences. *Postharvest Biology and Technology*, *50*(1), 70–78. https://doi.org/10.1016/j.postharvbio.2008.03.020

Iglesias, I., Echeverría, G., & Lopez, M. L. (2012). Fruit color development, anthocyanin content, standard quality, volatile compound emissions and consumer acceptability of several 'Fuji' apple strains. *Scientia Horticulturae*, *137*, 138–147. https://doi.org/10.1016/j.scienta.2012.01.029

Isard, S., & Schaetz, R. (1998). EFFECTS OF WINTER WEATHER CONDITIONS ON SOIL FREEZING IN SOUTHERN MICHIGAN. *Physical Geography*, *19*(1), 71–94.

Kappel, F., & Flore, J. A. (1983). Effect of Shade on Photosynthesis, Specific Leaf Weight, Leaf Chlorophyll Content, and Morphology of Young Peach Trees. *Journal of the American Society for Horticultural Science*, *108*(4), 541–544. https://doi.org/10.21273/JASHS.108.4.541

Khan, A., Carey, S. B., Serrano, A., Zhang, H., Hargarten, H., Hale, H., Harkess, A., Honaas, L., Carey, S. B., Serrano, A., Zhang, H., Hargarten, H., Hale, H., Harkess, A., & Honaas, L. (2022). A phased, chromosome-scale genome of 'Honeycrisp' apple (Malus domestica). *Gigabyte*, *2022*, 1–15. https://doi.org/10.46471/gigabyte.69

Kim, Y. J., Ban, S., Cho, H. J., Han, A. R., & Choi, C. (2023). Comparative Analysis of Gene Expression between Early Maturation Mutant 'Beni Shogun' and 'Fuji' Cultivars during FruitDevelopment and Ripening. *Horticulturae*, *9*(4), Article 4. https://doi.org/10.3390/horticulturae9040430

Kunihisa, M., Moriya, S., Abe, K., Okada, K., Haji, T., Hayashi, T., Kim, H., Nishitani, C., Terakami, S., & Yamamoto, T. (2014). Identification of QTLs for fruit quality traits in Japanese apples: QTLs for early ripening are tightly related to preharvest fruit drop. *Breeding Science*, *64*(3), 240–251. https://doi.org/10.1270/jsbbs.64.240

Lakso, A., & Goffinet, M. (2017). Advances in understanding apple fruit development. In *Achieving sustainable cultivation of apples*. Burleigh Dodds Science Publishing Limited.

Lakso, A. N. (1979). Seasonal Changes in Stomatal Response to Leaf Water Potential in Apple1. *Journal of the American Society for Horticultural Science*, *104*(1), 58–60. https://doi.org/10.21273/JASHS.104.1.58

Lakso, A. N. (1983). Morphological and Physiological Adaptations for Maintaining Photosynthesis under Water Stress in Apple Trees. In R. Marcelle, H. Clijsters, & M. van Poucke (Eds.), *Effects of Stress on Photosynthesis: Proceedings of a conference held at the 'Limburgs Universitair Centrum' Diepenbeek, Belgium, 22–27 August 1982* (pp. 85–93). Springer Netherlands. https://doi.org/10.1007/978-94-009-6813-4_8

Lakso, A. N. (2011). EARLY FRUIT GROWTH AND DROP - THE ROLE OF CARBON BALANCE IN THE APPLE TREE. *Acta Horticulturae*, *903*, 733–742. https://doi.org/10.17660/ActaHortic.2011.903.102

Lakso, A. N. (2022). Challenges to interpreting internal and external factors limiting apple fruit growth, set and abscission. *Acta Horticulturae*, *1342*, 317–328. https://doi.org/10.17660/ActaHortic.2022.1342.45

Lakso, A. N., White, M. D., & Tustin, D. S. (2001). SIMULATION MODELING OF THE EFFECTS OF SHORT AND LONG-TERM CLIMATIC VARIATIONS ON CARBON BALANCE OF APPLE TREES. *Acta Horticulturae*, *557*, 473–480. https://doi.org/10.17660/ActaHortic.2001.557.63

Larson, J., & Kon, T. (2021). Apple Fruitlet Abscission Mechanisms. *Horticultural Reviews*, *49*, 243–274.

Lenth, R. V., Bolker, B., Buerkner, P., Giné-Vázquez, I., Herve, M., Jung, M., Love, J., Miguez, F., Piaskowski, J., Riebl, H., & Singmann, H. (2024). *emmeans: Estimated Marginal Means, aka Least-Squares Means* (1.10.2) [Computer software]. https://cran.r-project.org/web/packages/emmeans/index.html

Linné, C. von, Linné, C. von, Smith, J. E., Baillie, M., & London, R. C. of P. of. (1821). *A selection of the correspondence of Linnaeus and other naturalists, from the original manuscripts: Vol. v.1* (pp. 1–640). Longman, Hurst, Rees, Orme, and Brown. https://doi.org/10.5962/bhl.title.141275

Liu, X., Zhai, R., Feng, W., Zhang, S., Wang, Z., Qiu, Z., Zhang, J., Ma, F., & Xu, L. (2014). Proteomic analysis of 'Zaosu' pear (*Pyrus bretschneideri* Rehd.) and its early-maturing bud sport. *Plant Science*, *224*, 120–135. https://doi.org/10.1016/j.plantsci.2014.04.012

Liu, Y., Gao, X., Tong, L., Liu, M., Zhou, X., Tahir, M. M., Xing, L., Ma, J., An, N., Zhao, C., Yao, J.-L., & Zhang, D. (2022). Multi-omics analyses reveal MdMYB10 hypermethylation being responsible for a bud sport of apple fruit color. *Horticulture Research*, *9*, uhac179. https://doi.org/10.1093/hr/uhac179

Liu, Y., Liu, Q., Xiong, J., & Deng, X. (2007). Difference of a citrus late-ripening mutant (Citrus sinensis) from its parental line in sugar and acid metabolism at the fruit ripening stage. *Science in China Series C: Life Sciences*, *50*(4), 511–517. https://doi.org/10.1007/s11427-007-0063-8

Migicovsky, Z., Gardner, K. M., Money, D., Sawler, J., Bloom, J. S., Moffett, P., Chao, C. T., Schwaninger, H., Fazio, G., Zhong, G.-Y., & Myles, S. (2016). Genome to Phenome Mapping in Apple Using Historical Data. *The Plant Genome*, *9*(2), plantgenome2015.11.0113. https://doi.org/10.3835/plantgenome2015.11.0113

Morimoto, T., Hiramatsu, Y., & Banno, K. (2013). A Major QTL Controlling Earliness of Fruit Maturity Linked to the Red leaf/Red flesh Trait in Apple cv. 'Maypole.' *Journal of the Japanese Society for Horticultural Science*, *82*(2), 97–105. https://doi.org/10.2503/jjshs1.82.97

MSUE. (2014). *Growth Stages*. Apples. https://www.canr.msu.edu/apples/horticulture/growth-stages

Palmer, J. W., Giuliani, R., & Adams, H. M. (1997). Effect of crop load on fruiting and leaf photosynthesis of 'Braeburn'/M.26 apple trees. *Tree Physiology*, *17*(11), 741–746. https://doi.org/10.1093/treephys/17.11.741

Pratt, H. K., & Goeschl, J. D. (1969). Physiological Roles of Ethylene in Plants. *Annual Review of Plant Physiology*, *20*(1), 541–584. https://doi.org/10.1146/annurev.pp.20.060169.002545

Schneider, G. W., & Childers, N. F. (1941). Influence of Soil Moisture on Photosynthesis, Respiration, and Transpiration of Apple Leaves1. *Plant Physiology*, *16*(3), 565–583. https://doi.org/10.1104/pp.16.3.565

SHAMEL, A. D., & POMEROY, C. S. (1936). BUD MUTATIONS IN HORTICULTURAL CROPS. *Journal of Heredity*, *27*(12), 487–494. https://doi.org/10.1093/oxfordjournals.jhered.a104171

Shane, B., & Lavely, E. (2023). *2023 Predicted Apple Harvest Dates – Grand Rapids Area*. Michigan State University Extension. https://www.canr.msu.edu/resources/predicted-apple-harvest-dates-grand-rapids-area

Shane, B., Lavely, E., Plotkowski, D., Rothwell, N., Lauwers, E., & Brown, L. (2023, August 9). *Michigan apple harvest prediction dates for 2023*. Apples. https://www.canr.msu.edu/news/michigan-apple-harvest-prediction-dates-2023

Singh, V., Weksler, A., & Friedman, H. (2017). Different Preclimacteric Events in Apple Cultivars with Modified Ripening Physiology. *Frontiers in Plant Science*, *8*. https://www.frontiersin.org/articles/10.3389/fpls.2017.01502

Song, J., Deng, W., Beaudry, R. M., & Armstrong, P. R. (1997). Changes in Chlorophyll Fluorescence of Apple Fruit during Maturation, Ripening, and Senescence. *HortScience*, *32*(5), 891–896. https://doi.org/10.21273/HORTSCI.32.5.891

Sun, H., Abeli, P., Campoy, J. A., Rütjes, T., Krause, K., Jiao, W.-B., Korff, M. von, Beaudry, R., & Schneeberger, K. (2023). *The identification and analysis of meristematic mutations within the apple tree that developed the RubyMac sport mutation* (p. 2023.01.10.523380). bioRxiv. https://doi.org/10.1101/2023.01.10.523380

Sun, X., Jiao, C., Schwaninger, H., Chao, C. T., Ma, Y., Duan, N., Khan, A., Ban, S., Xu, K., Cheng, L., Zhong, G.-Y., & Fei, Z. (2020). Phased diploid genome assemblies and pan-genomes provide insights into the genetic history of apple domestication. *Nature Genetics*, *52*(12), Article 12. https://doi.org/10.1038/s41588-020-00723-9

Sun, X., Wang, P., Jia, X., Huo, L., Che, R., & Ma, F. (2018). Improvement of drought tolerance by overexpressing MdATG18a is mediated by modified antioxidant system and activated autophagy in transgenic apple. *Plant Biotechnology Journal*, *16*(2), 545–557. https://doi.org/10.1111/pbi.12794

Tartachnyk, I. I., & Blanke, M. M. (2004). Effect of delayed fruit harvest on photosynthesis, transpiration and nutrient remobilization of apple leaves. *New Phytologist*, *164*(3), 441–450. https://doi.org/10.1111/j.1469-8137.2004.01197.x

Telias, A., Lin-Wang, K., Stevenson, D. E., Cooney, J. M., Hellens, R. P., Allan, A. C., Hoover,

E. E., & Bradeen, J. M. (2011). Apple skin patterning is associated with differential expression of MYB10. *BMC Plant Biology*, *11*(1), 93. https://doi.org/10.1186/1471-2229-11-93

Thammawong, M., & Arakawa, O. (2007). Starch Degradation of Detached Apple Fruit in Relation to Ripening and Ethylene. *Journal of the Japanese Society for Horticultural Science*, *76*(4), 345–350. https://doi.org/10.2503/jjshs.76.345

Thomas, C., Tholl, S., Moes, D., Dieterle, M., Papuga, J., Moreau, F., & Steinmetz, A. (2009). Actin bundling in plants. *Cell Motility*, *66*(11), 940–957. https://doi.org/10.1002/cm.20389

Tian, Y., Thrimawithana, A., Ding, T., Guo, J., Gleave, A., Chagné, D., Ampomah-Dwamena, C., Ireland, H. S., Schaffer, R. J., Luo, Z., Wang, M., An, X., Wang, D., Gao, Y., Wang, K., Zhang, H., Zhang, R., Zhou, Z., Yan, Z., … Yao, J.-L. (2022). Transposon insertions regulate genome-wide allele-specific expression and underpin flower colour variations in apple (Malus spp.). *Plant Biotechnology Journal*, *20*(7), 1285–1297. https://doi.org/10.1111/pbi.13806

Tong, C., Krueger, D., Vickers, Z., Bedford, D., Luby, J., El-Shiekh, A., Shackel, K., & Ahmadi, H. (1999). Comparison of Softening-related Changes during Storage of `Honeycrisp' Apple, Its Parents, and `Delicious'. *Journal of the American Society for Horticultural Science*, *124*(4), 407–415. https://doi.org/10.21273/JASHS.124.4.407

Trimble, S. (2020, October 14). How to Analyze Photosynthesis in Plants: Methods and Tools. *CID Bio-Science*. https://cid-inc.com/blog/how-to-analyze-photosynthesis-in-plants-methods-

and-tools/

Tukey, H. B., & Young, J. O. (1942). Gross Morphology and Histology of Developing Fruit of the Apple. *Botanical Gazette*. https://doi.org/10.1086/335103

USDA ERS - Food Availability and Consumption. (2023). https://www.ers.usda.gov/data-products/ag-and-food-statistics-charting-the-essentials/food-availability-and-consumption/

Wang, A., Tan, D., Tatsuki, M., Kasai, A., Li, T., Saito, H., & Harada, T. (2009). Molecular mechanism of distinct ripening profiles in 'Fuji' apple fruit and its early maturing sports. *Postharvest Biology and Technology*, *52*(1), 38–43. https://doi.org/10.1016/j.postharvbio.2008.09.001

Wang, Z., Li, G., Sun, H., Ma, L., Guo, Y., Zhao, Z., Gao, H., & Mei, L. (2018). Effects of drought stress on photosynthesis and photosynthetic electron transport chain in young apple tree leaves. *Biology Open*, *7*(11), bio035279. https://doi.org/10.1242/bio.035279

Wei, L., Cao, Y., Cheng, J., Xiang, J., Shen, B., & Wu, J. (2020). Comparative transcriptome analyses of a table grape 'Summer Black' and its early-ripening mutant 'Tiangong Moyu' identify candidate genes potentially involved in berry development and ripening. *Journal of Plant Interactions*, *15*(1), 213–222. https://doi.org/10.1080/17429145.2020.1760367

Wu, Y., Fu, T., Wang, Z., Jiao, C., Yang, Z., Ali, B., & Zhou, W. (2015). Differential gene expression analysis of early-ripening mutants of grape (*Vitis vinifera* L.). *Scientia Horticulturae*, *194*, 7–17. https://doi.org/10.1016/j.scienta.2015.07.022

Wünsche, J., & Lakso, A. (2000). *Apple tree physiology—Implications for orchard and tree management*. https://www.semanticscholar.org/paper/Apple-tree-physiology-implications-for-orchard-and-W%C3%BCnsche-Lakso/f72a3de510269c5f3b726bf2c881a2f5b02f03e8

Zotta, L. (2015). *200 Year and Growing: The Story of Stark Bro's Nurseries & Orchards Co.* (First). Stark Bro's Nurseries & Orchards Co.

APPENDIX

*Table 1A: Table containing variables fitting 'Kidd's D-8' individual fruits with Weibull equation "y=a+b(1-exp(-((x+d*ln(2)^(1/e)/d)^e))" where x=GDH.*

FruitID#	Eq'n variables	R8P5T33	R8P5T36	R8P5T40	R4P7T52	R4P7T54
1	a	-14.7786	-20.2625	n/a	-16.0925	-9.81037
1	b	243.2489	269.3274	n/a	278.4696	235.3808
1	c	29192.05	27387.42	n/a	28819.61	30126.13
1	d	200089.7	276027.1	n/a	113178.7	158352.7
1	e	18.14616	25.17357	n/a	9.833075	15.45435
1	r^2	0.99949	0.999473	n/a	0.999408	0.999462
2	a	-5.54555	-4.20008	-12.7617	-19.738	-18.1269
2	b	183.761	237.5556	246.1911	262.4043	290.3277
2	c	30501.12	30039.02	29896.13	27380.27	29501.82
2	d	92120.54	40640.32	84197.78	4002470	12166900
2	e	8.942774	2.82606	6.800462	371.6084	1149.293
2	r^2	0.999343	0.999666	0.999665	0.999209	0.999039
3	a	n/a	-23.0221	-20.274	-13.7894	-16.3933
3	b	n/a	333.8096	297.2722	212.7947	271.6507
3	c	n/a	27173.04	27726.81	28709.52	29037.17
3	d	n/a	124123.2	14450900	3897740	468555
3	e	n/a	11.0133	1430.081	369.2073	43.69957
3	r^2	n/a	0.999423	0.999282	0.999291	0.999399
4	a	-9.15377	-9.11297	-16.3655	-14.3757	-14.4708
4	b	219.2494	241.0538	244.309	234.4832	221.3806
4	c	29562.83	27371.7	28529.96	28331.84	28811.46
4	d	143134.7	64766.32	358775.2	345939.7	157295.3
4	e	14.31445	6.238303	32.94056	32.69629	13.50557
4	r^2	0.999132	0.999079	0.999419	0.99962	0.999325
5	a	-4.242	-16.586	-16.6445	-12.4736	-13.8515
5	b	172.8713	265.9863	240.6024	230.035	235.5481
5	c	30843.54	28007.02	27500.45	27666.63	28104.12
5	d	82070.28	216000.9	1187640	84235.23	221189.1

Table 1A (cont'd)

5	e	8.031553	20.27853	116.1411	7.104348	21.35506
5	r^2	0.999211	0.99949	0.999425	0.999072	0.999515

*Table 2A: Table containing variables fitting 'Autumn Gala' individual fruits with Weibull equation "y=a+b(1-exp(-((x+d*ln(2)^(1/e)/d)^e))" where x=GDH.*

FruitID#	Eq'n variables	R9P10T77	R9P10T80	R6P6T42	R6P6T44	R6P6T48
1	a	-12.8614	-14.1475	-15.0931	-15.1211	-9.1989
1	b	232.6125	263.115	239.0808	228.8246	189.6441
1	c	29143.22	30117.17	29290.24	29622.25	29926.87
1	d	3.06E+14	279278.5	606937.7	2760980	169138.1
1	e	3E+10	25.19976	57.45338	250.2667	15.50311
1	r^2	0.999184	0.999312	0.999502	0.999388	0.999314
2	a	-7.78923	-12.0583	-12.8888	-11.0496	-11.8443
2	b	261.8401	250.0777	226.4592	239.5882	273.217
2	c	32633.49	31215.53	30443.92	30497.87	31142.94
2	d	77376.89	166419	321037.7	114836.3	114929
2	e	6.190056	14.56693	29.22473	9.832361	10.0197
2	r^2	0.999572	0.999383	0.999494	0.999388	0.999615
3	a	-17.5212	-12.6148	-10.5394	-8.58099	-12.163
3	b	239.494	221.3435	216.9841	263.4307	260.5754
3	c	28512.28	29331.4	30193.9	31942.03	30774.21
3	d	4234720	452144.1	102369.7	70251.74	132533.5
3	e	386.1333	41.87417	8.928548	5.353924	11.49471
3	r^2	0.999083	0.999318	0.999447	0.999093	0.999342
4	a	n/a	-8.03232	-12.5872	-12.0979	-9.36054
4	b	n/a	185.9505	228.0075	227.573	181.8399
4	c	n/a	29809.46	29853.82	29420.52	29922.99
4	d	n/a	94156.63	266305.1	357934	1462850
4	e	n/a	8.006715	24.19293	34.3791	145.3677
4	r^2	n/a	0.999066	0.99955	0.999479	0.99927
5	a	-11.6483	-9.66838	-2.70397	-15.4767	-10.4614
5	b	210.3919	265.0208	196.6732	260.1989	241.3664
5	c	29106.24	30742.31	30272.79	30786.03	29346.59
5	d	373556.4	89796.92	49294.65	660264.4	4640250
5	e	36.26616	7.660358	4.303254	58.41564	493.9297
5	r^2	0.999373	0.999452	0.99889	0.999138	0.999282

*Table 3A: Table containing variables fitting 'September Wonder Fuji' individual fruits with Weibull equation "y=a+b(1-exp(-((x+d*ln(2)^(1/e)/d)^e))" where x=GDH.*

Fruit ID	variables	R9P3T19	R2P10T74	R4P4T27	R4P4T28	R4P4T31
1	a	-8.3302	-37.613	-11.0884	-9.95104	-10.3801
1	b	308.3109	289.8988	356.6878	255.6673	411.6456
1	c	29214.52	26815.58	34335.18	31439.69	31439.76
1	d	71157.84	1189000	58501.54	86628.8	59028.07
1	e	6.970579	81.02593	3.691376	7.422976	4.886517
1	r^2	0.998677	0.99798	0.999474	0.999678	0.999503
2	a	-22.6952	-35.8326	-10.8807	-13.1166	-13.6269
2	b	374.6911	416.7749	272.6775	354.4169	457.9507
2	c	28141.88	28932.44	30873.87	31561.11	32134.48
2	d	268466.2	157212.3	67050.02	57254.07	61755.47
2	e	26.26278	11.89085	5.181052	4.028458	4.847512
2	r^2	0.999744	0.999233	0.999547	0.999659	0.999251
3	a	-6.51645	-11.1426	-9.96459	-5.86727	-7.5745
3	b	339.6552	350.2616	390.4459	332.1468	497.7085
3	c	29093.4	30252	31686.65	32505.12	34607.71
3	d	51487.68	59110.07	52855.43	48456.22	48412.21
3	e	4.751867	4.802036	4.102293	3.611961	3.30096
3	r^2	0.99755	0.999769	0.999683	0.999493	0.999684
4	a	-0.03457	-9.76093	-6.60575	-10.9771	-18.6124
4	b	526.6187	333.4435	347.3878	368.839	492.5191
4	c	33697.98	30942.34	33579.3	30957.96	29579.18
4	d	37642.41	53821.54	47431.99	78415.41	55954.07
4	e	2.405745	3.938487	3.050267	7.053881	4.424552
4	r^2	0.999174	0.999763	0.999726	0.999346	0.99973
5	a	-13.3363	-31.7364	-18.8093	-10.8147	-12.3349
5	b	284.09	393.493	362.8681	430.752	400.9978
5	c	29342.37	28532.51	29670.44	32561.48	31164.36
5	d	120356.1	140480.3	96315.37	57721.01	66826.44
5	e	11.46549	11.43237	8.142745	4.406268	5.683702
5	r^2	0.99936	0.999338	0.999563	0.999593	0.999651

*Table 4A: Table containing variables fitting 'Aztec Fuji' individual fruits with Weibull equation "y=a+b(1-exp(-((x+d*ln(2)^(1/e)/d)^e))" where x=GDH.*

Fruit ID#	variables	R6P5T33	R6P5T34	R3P1T2	R3P1T3	R3P1T5
1	a	2.933954	-9.11068	-2.75461	-11.0014	-4.06264
1	b	355.2165	294.9136	253.1499	417.6879	400.546
1	c	39444.97	38386.95	39148.94	38145.64	39519.12
1	d	41154.23	79750.99	54424.13	73610.79	51074.45
1	e	1.767552	5.043896	3.157899	4.886753	2.725295
1	r^2	0.996218	0.99943	0.998435	0.999748	0.999488
2	a	-4.73901	-20.8374	-0.76954	-8.24091	-4.31885
2	b	307.5253	417.5925	480.5034	342.5184	534.5191
2	c	38523.05	37710.07	45281.81	37399.1	40523.84
2	d	54806.45	117528.1	53094.32	66307.71	51145.34
2	e	3.071899	7.533184	2.12136	4.160884	2.491646
2	r^2	0.999741	0.99952	0.998982	0.99963	0.999386
3	a	-7.10844	-1.7473	-5.1872	-3.90094	-1.13526
3	b	410.8042	583.5026	304.0852	295.6473	456.1313
3	c	37142.33	40981.3	36823.43	38570.9	38381.94
3	d	53461.62	48425.92	59782.02	55110.88	45196.64
3	e	3.049857	2.329276	3.812866	3.086562	2.487479
3	r^2	0.999158	0.999402	0.999223	0.999058	0.999188
4	a	-8.71883	-8.89516	-4.80469	-2.14058	-1.46562
4	b	388.629	354.6148	388.2507	498.2038	393.4741
4	c	36880.17	38994.03	37773.68	39497.02	37715.84
4	d	57114.61	63423.12	53450.56	48673.18	46581.25
4	e	3.457651	3.578128	3.203993	2.555593	2.693918
4	r^2	0.999493	0.999589	0.999143	0.99939	0.998497
5	a	-11.4999	-8.99066	-9.81694	-3.58516	-7.67437
5	b	484.6034	329.3124	407.1651	357.0502	363.879
5	c	38111.47	37173.17	39688.63	41918.71	37612.85
5	d	59840.24	60031.99	60660.4	56512.83	57329.49
5	e	3.383604	3.459768	3.034833	2.84947	3.317622
5	r^2	0.999556	0.999422	0.998856	0.999038	0.999478

*Table 5A: Table containing variables fitting 'Maslin' individual fruits with Weibull equation "y=a+b(1-exp(-((x+d*ln(2)^(1/e)/d)^e))" where x=GDH.*

Fruit ID	Fruit Variables	R6P8T61	R6P8T62	R6P8T63	R3P9T69	R3P9T70
1	a	0.06866	-1.16861	-4.50129	-0.99457	-1.48408
1	b	1323.415	448.2086	253.3919	417.0138	309.6818
1	c	142904.5	55133.52	38629.48	39680.29	38875.98
1	d	177124	65002.54	54400.88	47081.22	47776.58
1	e	1.474805	1.915038	2.68527	2.344374	2.51705
1	r^2	0.999596	0.999693	0.999277	0.999464	0.999521
2	a	-0.33123	n/a	0.790002	-2.4533	0.350288
2	b	513.9362	n/a	320.0965	438.2541	514.0266
2	c	51550.89	n/a	44479.65	40611.47	56737.21
2	d	59978.71	n/a	52309.13	49554.04	65820.79
2	e	1.692566	n/a	2.001848	2.355074	1.737849
2	r^2	0.999664	n/a	0.999548	0.99957	0.999152
3	a	n/a	0.380962	-2.61855	-5.98574	-8.50168
3	b	n/a	578.7336	314.8147	277.1088	309.896
3	c	n/a	65338.22	42439.71	40119.53	39721.1
3	d	n/a	76448.87	52748.1	64078.91	62349.57
3	e	n/a	1.646007	2.286415	3.616752	3.245363
3	r^2	n/a	0.999501	0.999235	0.999341	0.999017
4	a	-8.08906	0.527276	n/a	-6.15839	-3.53778
4	b	311.5888	394.991	n/a	587.928	302.807
4	c	47507.99	45238.44	n/a	63060.04	37674.11
4	d	69891.68	51316.31	n/a	81015.87	50734.34
4	e	2.621621	1.86293	n/a	2.116428	2.831615
4	r^2	0.999594	0.999269	n/a	0.999598	0.999577
5	a	-2.77432	0.73366	-2.75421	-7.21217	-8.80547
5	b	454.9381	443.3501	306.202	302.0484	306.7224
5	c	67291.35	47091.75	40625.5	37494.76	37050.62
5	d	83847.33	52378.81	51217.11	58371.82	61136.91
5	e	1.839799	1.825036	2.382964	3.333166	3.464483
5	r^2	0.999278	0.999535	0.999759	0.999514	0.999573

*Table 6A: Table containing variables fitting 'Cripps Pink' individual fruits with Weibull equation "y=a+b(1-exp(-((x+d*ln(2)^(1/e)/d)^e))" where x=GDH.*

Fruit ID	Fruit Variables	R5P7T52	R5P7 T54	R6P10T77	R6P10T78	R6P10T79
1	a	-5.62069	-7.74034	-8.04981	-8.27267	-19.3067
1	b	304.4466	373.0066	290.805	245.2403	228.2765
1	c	39273.99	41497.07	45606.86	43694.44	40484.64
1	d	59154.74	60237.17	65557.75	70401.57	204434.6
1	e	3.141581	2.977606	2.412422	2.927474	10.056
1	r^2	0.99967	0.999734	0.999596	0.99959	0.999579
2	a	-6.63533	-12.486	-8.27004	n/a	-21.3761
2	b	349.2691	304.038	314.2441	n/a	228.7415
2	c	44976.79	40612.97	48797.97	n/a	36069.79
2	d	63589.6	69587.51	72925.42	n/a	441884
2	e	2.625894	3.133108	2.614779	n/a	25.51886
2	r^2	0.99988	0.999691	0.999579	n/a	0.999617
3	a	-1.36917	n/a	-1.5162	-6.58313	-9.28882
3	b	416.1578	n/a	271.8481	292.1664	187.23
3	c	47083.6	n/a	51465.99	44745.92	38319.77
3	d	57474.72	n/a	62871.29	64170	88361.75
3	e	2.129991	n/a	1.834832	2.646137	4.920321
3	r^2	0.999451	n/a	0.999396	0.99948	0.999283
4	a	-3.55025	n/a	-8.90982	-24.333	-3.16585
4	b	301.5525	n/a	214.0246	264.8133	332.5045
4	c	40550.15	n/a	40843.82	39448.53	50694.27
4	d	52798.24	n/a	75268.05	205574.4	63286.11
4	e	2.512841	n/a	3.581775	9.980935	1.977023
4	r^2	0.99965	n/a	0.999595	0.999536	0.999135
5	a	-23.6679	-0.00865	-12.6905	-14.0427	-24.7252
5	b	318.3164	349.8363	226.6002	215.1272	241.9423
5	c	43014.81	49971.74	40560.02	40250.17	37859.51
5	d	123743.5	57025.96	102154.4	108264.7	329208.6
5	e	5.383155	1.946425	5.079653	5.217302	16.8965
5	r^2	0.999523	0.999703	0.999505	0.99955	0.999676

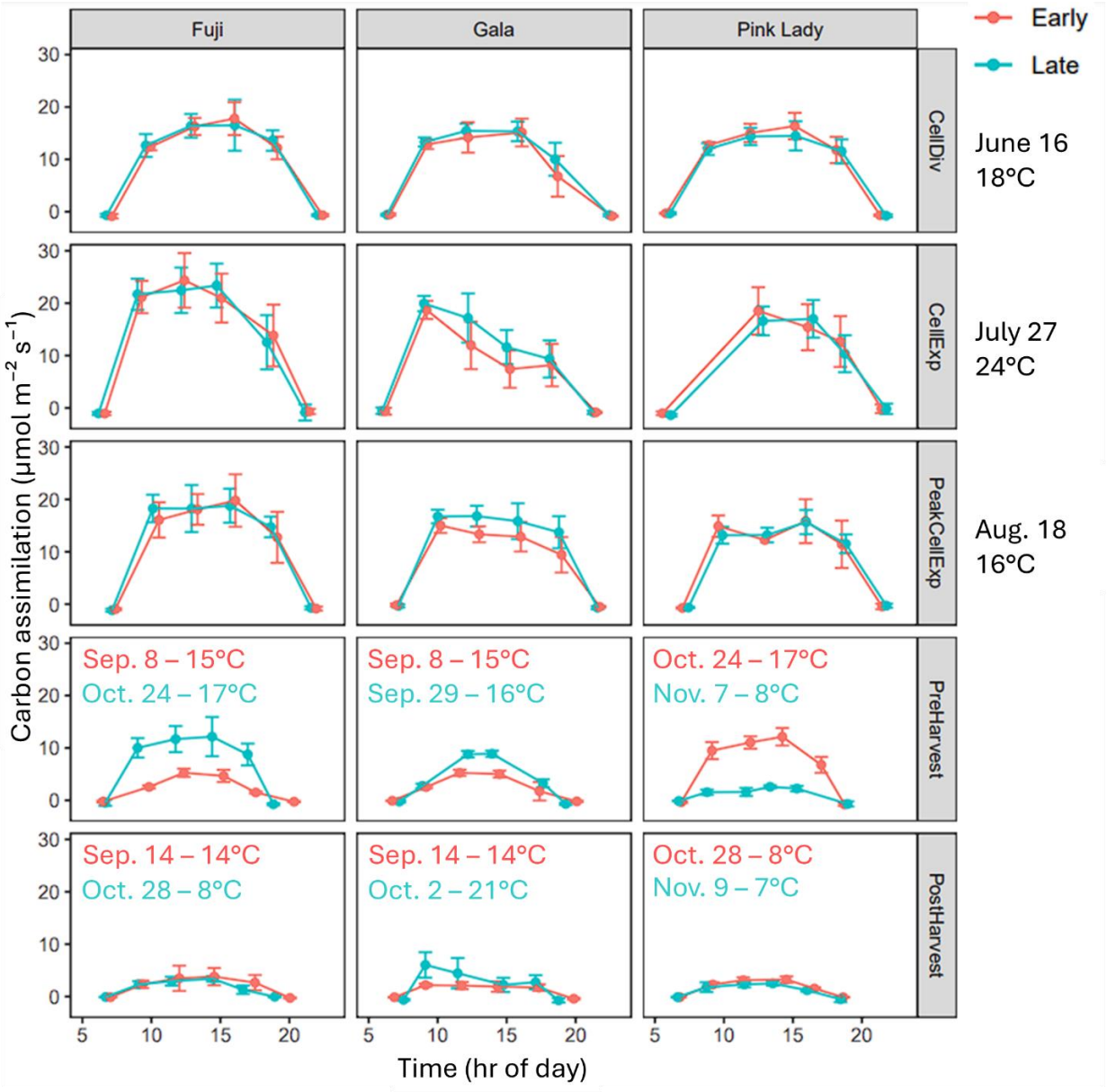

Figure 1A: Carbon assimilation shown for each cultivar. Each point represents the average of 2 leaves per tree, five trees in total. Data was analyzed via ANOVA in R software (R Core Team, 2017). Temperature data collected from Clarksville weather station. Results of carbon assimilation comparisons between early and late cultivars are mixed.

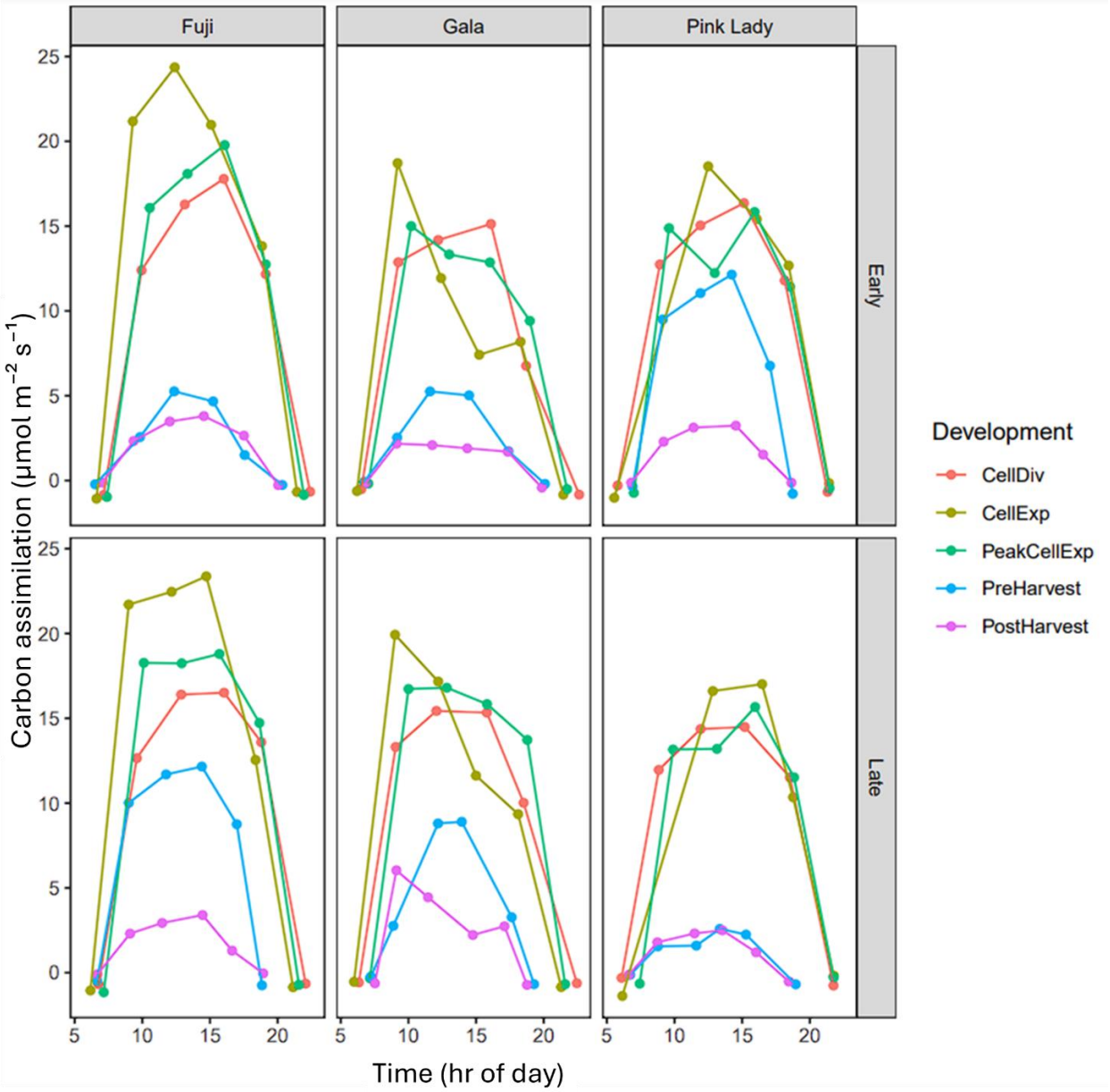

Figure 2A: Carbon assimilation shown for each cultivar, capturing differences in carbon assimilation throughout the season according to developmental stage and maturity (earlier or later harvesting cultivar). Each different color represents a different date when the data was collected: red=June 16, brown=July 27, green=18 August, and pre/postharvest dates are unique to cultivar and shown in Fig. 1A above within the appendix. Each data point represents an average of 2 leafs per 5 trees. Each complete area under the diurnal curve represents total carbon assimilated for that particular date/developmental timepoint.